AD/A-005 631

INVESTIGATION OF DF LASER PROPAGATION

Robert E. Meredith, et al

Science Applications, Incorporated

Prepared for:

Army Electronics Command

December 1974

DISTRIBUTED BY:

NTIS

National Technical Information Service
U. S. DEPARTMENT OF COMMERCE

065181

AD A005631

AD

Reports Control Symbol
OSD-1366

RESEARCH AND DEVELOPMENT TECHNICAL REPORT
ECOM--74-4

INVESTIGATION OF DF LASER PROPAGATION

By

Robert E. Meredith

Thomas W. Tuer

Douglas R. Woods

Science Applications, Inc.
15 Research Drive
Ann Arbor, Michigan 48103

Prepared for

Atmospheric Sciences Laboratory
US Army Electronics Command
White Sands Missile Range, New Mexico 88002

December 1974

Approved for public release; distribution unlimited.

DDC
RECEIVED
FEB 27 1975
D

ECOM

UNITED STATES ARMY ELECTRONICS COMMAND - FORT MONMOUTH, NEW JERSEY 0

Reproduced by
NATIONAL TECHNICAL
INFORMATION SERVICE
U S Department of Commerce
Springfield VA 22151

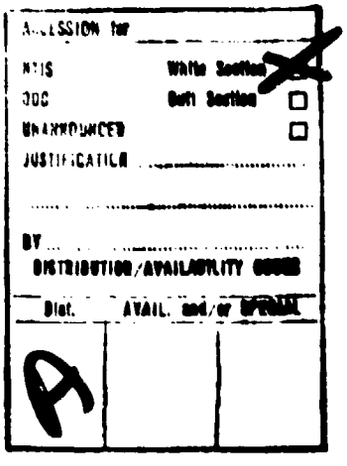

NOTICES

Disclaimers

The findings in this report are not to be construed as an official Department of the Army position, unless so designated by other authorized documents.

The citation of trade names and names of manufacturers in this report is not to be construed as Official Government indorsement or approval of commercial products or services referenced herein.

Disposition

Destroy this report when it is no longer needed. Do not return it to the originator.

UNCLASSIFIED

SECURITY CLASSIFICATION OF THIS PAGE (When Data Entered)

REPORT DOCUMENTATION PAGE		READ INSTRUCTIONS BEFORE COMPLETING FORM
1. REPORT NUMBER ECOM 74-4	2. GOVT ACCESSION NO.	3. RECIPIENT'S CATALOG NUMBER
4. TITLE (and Subtitle) INVESTIGATION OF DF LASER PROPAGATION		5. TYPE OF REPORT & PERIOD COVERED Final Report - Contract
		6. PERFORMING ORG. REPORT NUMBER SAI-74-001-AA
7. AUTHOR(s) Robert E. Meredith Thomas W. Tuer Douglas R. Woods		8. CONTRACT OR GRANT NUMBER(s) DAEA18-73-A-0127/ Order No. BN-01
9. PERFORMING ORGANIZATION NAME AND ADDRESS Science Applications, Inc. 15 Research Drive Ann Arbor, MI 48103		10. PROGRAM ELEMENT, PROJECT, TASK AREA & WORK UNIT NUMBERS
11. CONTROLLING OFFICE NAME AND ADDRESS Atmospheric Sciences Laboratory U. S. Army Electronics Command White Sands Missile Range, NM 88002		12. REPORT DATE December 1974 13. NUMBER OF PAGES 133
14. MONITORING AGENCY NAME & ADDRESS(if different from Controlling Office)		15. SECURITY CLASS. (of this report) Unclassified 15a. DECLASSIFICATION/DOWNGRADING SCHEDULE

16. DISTRIBUTION STATEMENT (of this Report)

Approved for public release; distribution unlimited.

17. DISTRIBUTION STATEMENT (of the abstract entered in Block 20, if different from Report)

DDC
RECEIVED
FEB 27 1975
D

18. SUPPLEMENTARY NOTES

19. KEY WORDS (Continue on reverse side if necessary and identify by block number)

DF Laser, Atmospheric Transmittance, Molecular Absorption.

20. ABSTRACT (Continue on reverse side if necessary and identify by block number)

Molecular absorption coefficients are calculated in the region of 27 important DF laser wavelengths for typical sea level conditions. The important absorption mechanisms for this region are discussed and improved modeling procedures are suggested. A series of graphs and tables clearly show the importance of individual molecular absorption lines and continua

DD FORM 1 JAN 73 1473 EDITION OF 1 NOV 65 IS OBSOLETE

UNCLASSIFIED

SECURITY CLASSIFICATION OF THIS PAGE (When Data Entered)

PRICES SUBJECT TO CHANGE

20. Abstract (Continued)

for each important DF line. Calculations and recommendations are given for White cell measurements of absorption coefficients for the H_2O and N_2 continuum, and HDO, N_2O, CH_4 and H_2O line absorption at DF wavelengths.

CONTENTS

FIGURES

FIGURES

FIGURES

TABLES

TABLES

TABLES

1. INTRODUCTION AND BACKGROUND

One of the more important problems of high energy laser technology is the determination of intensity loss at target caused by atmospheric effects. Aerosol and particulate scattering, molecular absorption and turbulence all contribute significantly to propagation losses. The molecular absorption at low or moderate altitudes is of particular importance to the Army mission since it leads to severe thermal blooming losses in addition to the linear absorption loss.

The deuterium fluoride (DF) laser operates in a wavelength region at which the atmosphere is generally less absorbing than at most other infrared wavelengths. Molecular absorption processes are of a complicated nature, however, and many of them are very wavelength dependent. Consequently, atmospheric absorption at the precise DF laser frequencies cannot be predicted with desired confidence at this time. The present investigation was undertaken to supply quantitative predictions of atmospheric molecular absorption at sea level at the more important DF frequencies to define the important questions that exist, and to suggest a measurements approach to solve these questions. In addition, the absorption mechanisms responsible for atmospheric molecular absorption are discussed, and a modeling procedure more sophisticated than used to date is suggested.

Preceding page blank

2. NATURE OF ABSORPTION AT DF WAVELENGTHS

General Considerations

Atmospheric molecular absorption at a particular wavelength is a composit of separate contributions from many different molecular species and their isotopes, weighted by their abundance in the atmosphere. In general, each molecular absorber's contribution will arise from many lines, some centered at or near the laser frequency, and some centered tens or hundreds of cm^{-1} from the laser frequency. Each individual line is expected to have the same functional frequency dependence (shape), but each line invariably has a unique set of shape parameters. Thus, one might be tempted to conclude that a precise calculation of absorption coefficients for open air laser propagation may not be feasible. However, molecular physics and spectroscopy are very well developed subjects, and consequently it is possible to perform such calculations at some wavelengths with a high degree of accuracy, using simple molecular absorption models, if an adequate data base is available. The region of DF laser emission (3.6 - 4.0μm) appears to be one region where the absorption processes are well amenable to such modeling techniques (see Section 4) although the data base in this region is not sufficient at this time. The remainder of this section will discuss the general approach to modeling the molecular absorption process, and to defining the relevant theoretical concepts.

Molecular Absorption Modeling Procedure

Two characteristic types of molecular absorption exist at DF wavelengths: continuum absorption and line absorption. Continuum absorption is caused either by higher order pressure effects on molecules which do not normally absorb, or by absorption in the distant wings of lines located far from the laser line center. Continuum absorption by definition varies slowly with wavelength in the general vicinity of laser frequencies. The line (or line core) absorption occurs

very near one or more absorption centers. Consequently, it may vary rapidly with wavelength in the vicinity of a laser frequency. In the following discussion, transmittance will be written in terms of an absorption coefficient, in units $(\text{length})^{-1}$ and absorbing path length, as follows,

$$\tau = \exp [-kL].$$

Current practice is to write the total absorption coefficient as the sum of a line and a continuum contribution:

$$k(\nu) = k_{line}(\nu) + k_c(\nu)$$

Both k_{line} and k_c are the sum of absorption coefficients from all molecular constituents which contribute at the particular wavelength:

$$k_{line}(\nu) = \sum_i k^i_{line}(\nu)$$

$$k_c = \sum_j k^j_c$$

The distinction between line and continuum absorption is natural since different measurements techniques are usually required for each, and their physical mechanisms are not necessarily the same. The altitude, temperature, pressure and concentration dependence of line and continuum absorption may be quite different, but each obeys principles characteristic of itself, regardless of the particular molecules involved. It is therefore natural to separate the two effects both in analytical and in measurements studies.

The line absorption coefficient is expressed more generally as the product of the absorption strength and a shape factor $f(\nu-\nu_0)$:

$$k_{line}(\nu) = Sf(\nu-\nu_0)$$

The proper shape $f(\nu-\nu_0)$ for a given absorption line is determined by the physical mechanism which causes the spectral spread of the absorption about the center frequency ν_0. If the spread is caused by collisions (the so-called pressure broadening) the shape factor has the Lorentz form:

$$f(\nu-\nu_0)_{lor} = \frac{\gamma}{\pi[(\nu-\nu_0)^2+\gamma^2]}$$

The factor π in the denominator is a normalization factor inserted to maintain S as the strength, or integrated absorption coefficient, of the transition. If the absorption spread is caused by The Doppler effect, $f(\nu-\nu_0)$ is as follows:

$$f(\nu-\nu_0) = \frac{1}{\gamma_D}\sqrt{\frac{\log_e 2}{\pi}}\ \exp\left[-\left(\frac{\nu-\nu_0}{\gamma_D}\right)^2 \log_e 2\right]$$

Often the combination Doppler-Lorentz (or Voigt) profile is used to represent a line shape for which Doppler and collision broadening is competitive. This should be done cautiously since a third effect, collisional narrowing, may significantly reduce the Doppler width, and thus the Voigt profile. Since the narrowing effects can reduce the Doppler width to insignificance, often it is best to include both effects, or to include neither. Although each case must be treated individually, between 1 and 15 microns, and at altitudes below 10 km, the Doppler width is reduced by the narrowing effect. However, the impact under these conditions is minimal since the Doppler width is usually small correction on the dominant collision broadening.

Significant collision broadening which is not necessarily described by the Lorentz shape may occur. These vary slowly with frequency, and they usually occur far from line center. It is these contributions which are modeled as the constant or monotonically varying contributions k_c. Molecular absorbers at a given laser wavelength are few. In the DF region for example, H_2O, HDO, N_2O and CH_4 are known to be significant line contributors, and at a given laser wavelength, only two or three of these dominate. With regard to k_c, only H_2O and N_2 are known to be significant at DF wavelengths.

The distinction drawn here between line and continuum absorption is not precise, since the exact distance from line center at which the ideal shapes may deviate significantly is not well known, and it may differ for each absorber-collision partner combination. We prefer, in general, to refer to line absorption as consisting of a line "core" contribution and a "near wing"

contribution which describes the region where significant deviations from the ideal shape begin to occur. In this context, continuum caused by infrared active molecules is essentially a "far wing" absorption:

$$k(\nu) = k_{line}(\nu) + k_{nw}(\nu) + k_c$$

For sea level conditions, i.e., P ~ 1 atm. pressure, each line absorption coefficient at DF wavelengths will be assumed to have the Lorentz shape:

$$k_{line} = k_{lor}(\nu) = \frac{S\gamma}{\pi\left|(\nu-\nu_0)^2 + \gamma^2\right|}$$

The superscript and the individual line designations have been deleted for clarity of notation. The three parameters of importance are S, γ and ν_0, the strength, width, and line center position. At absorption line center, $\nu = \nu_0$, the peak value of $k(\nu)$ is as follows,

$$k(\nu_0) = k^P = \frac{S}{\gamma\pi}$$

It can be seen that $k(\nu = \gamma) = \frac{1}{2}k^P$. Consequently, γ has the interpretation of half of the width of $k(\nu)$ at half its peak value. Near line center, k varies as $\frac{S}{\gamma}$, but well beyond $\nu = \nu_0 + \gamma$, $k \sim S\gamma$. Prediction of laser absorption coefficients $k(\nu_L) \equiv k_L$ is sensitive to possible error in the location of ν_L or of the absorption center ν_0. For example, for the Lorentz shape,

$$k_{lor}(\nu_L) = \frac{S\gamma}{\pi\left|(\nu_L-\nu_0)^2 + \gamma^2\right|}$$

Thus, core absorption at ν_L is very sensitive to S, γ, and $\delta\nu = (\nu_L - \nu_0)$. It can be seen that the form of $k(\nu)$ is such that such errors in S or γ, coupled with errors in $\delta\nu$ of order γ or 2γ can give incorrect predictions which cannot be identified unambiguously by a single wavelength monochromatic measurement alone.

The near wing of the line is defined as the location on $k(\nu)$ at which $|\nu-\nu_0| >> \gamma$. Thus, for a Lorentz line,

$$k_{nw} \simeq \frac{S\gamma}{\pi(\nu-\nu_0)^2}$$

It is precisely this region where deviations from the Lorentz shape are expected. Consequently, more precise modeling may require a non-Lorentz expression for k_{nw}. For example, the following form, which depends on a single parameter, has been used [1, 2] for the frequency range beyond Lorentz cutoff frequency ν_c.

$$k_{nw} = \frac{\Gamma S\gamma}{\pi\nu_c^{2-\eta}[(\nu-\nu_0)^\eta + \gamma^\eta]} \qquad \nu > \nu_c$$

where Γ is a normalization constant. In the above, $\eta > 2$ implies sub-Lorentz absorption, and $\eta < 2$ implies super-Lorentz behavior. For $\nu < \nu_c$, the Lorentz form is assumed. Other expressions have also been used to describe non-Lorentz behavior not too far from line center [3, 4].

In the DF region, the near wings of absorption lines appear to contribute much less than line core absorption. Therefore, the less sophisticated approach which ignores shape considerations is adopted here. This is essentially the approach taken in the recent AFCRL line-by-line computations [5, 6, 7]. Each laser region must be considered individually, however, since the near wings and other effects such as dimer absorption may be important. This appears to be the case at CO laser wavelengths, and at CO_2 wavelengths, respectively. At these wavelengths, the more sophisticated modeling of the core, near wing, far wing and continuum contributions is suggested.

Nature of the S, γ and ν_0 Parameters

The line center parameter ν_0 depends on the intramolecular forces of the molecule. They are therefore not variable for normal conditions of

pressure and temperature. The S and γ parameters do vary in complex ways for each transition of each molecule, and for different pressure conditions. Therefore, a brief description of the variability of S and γ will be given.

The basic quantity upon which the strength S depends is the Einstein coefficient for induced absorption B(f←i).

$$S \propto B(f \leftarrow i)$$

B(f←i) is a function of only the molecular species and the initial and final states. It is independent of the temperature, pressure, or concentration. Thus B(f←i) is the most fundamental quantity normally used to obtain line strengths. The temperature and concentration dependence of the line strength S come in through well understood processes. Thus once one has measured the strength at single temperature and concentration (and thus the Einstein coefficient B) the strength at all temperatures and concentrations can generally be determined with great confidence and accuracy. If T_1 and T_2 are two arbitrary temperatures, then S at T_2 may be obtained from S at T_1 as follows [5]:

$$S(T_2) = S(T_1) \frac{Q_v(T_1)Q_r(T_1)}{Q_v(T_2)Q_r(T_2)} \exp\left[\frac{1.439\,E\,(T_2-T_1)}{T_1T_2}\right]$$

where the Q are vibrational and rotational partition functions and E is the energy of the initial level.

For the general case of a polyatomic molecule,

$$B(\alpha_j', v', J' \leftarrow \alpha, v, J) \propto |\langle \alpha_j', v', J'|\vec{\mu}|\alpha, v, J\rangle|^2$$

where primed and unprimed quantum numbers are final and initial values, respectively. In the above, α_j denotes all other quantum numbers required to specify a given molecular state. The quantity $\langle f|\vec{\mu}|i\rangle$ is the usual notation for the electric dipole matrix element of the transition. As the notation indicates, there is a unique matrix element for each set of quantum numbers,

i. e., for each individual absorption line. Usually the rotational quantum number dependence is not strong, and it is separated as an "F factor," as shown below;

$$|\langle \alpha_j', v', J'|\vec{\mu}|\alpha, v, J\rangle|^2 = |\langle v'|\mu|v\rangle|^2 F(v, v', J, J', \alpha_j, \alpha_j')$$

However, there are also many cases where F may be large and may vary rapidly with quantum number. This is particularly true in some bands of H_2O, N_2O and others for which accidental resonant perturbations occur. It is in the modeling of $\langle f|\vec{\mu}|i\rangle$ from limited data or approximate theory that incorrect values of S are expected to occur.

The Lorentz width depends in a complicated way on the collision processes between the absorbing molecule and its collision partners [8, 9]. It may vary rapidly with rotational state J, and to a lesser extent, with the v state of the colliding molecules. Quantitatively, γ depends on the number of collisions the molecule experiences per unit time. Therefore, γ is the sum of the contributions of the various collision partners. If p_i is the partial pressure of the $i^{\underline{th}}$ molecular constituent [10],

$$\gamma = \gamma_s p_s + \sum_i \gamma_i p_i$$

where s refers to self, and i refers to foreign collision partners. Collectively,

$$\gamma = \gamma_s p_s + \gamma_f p_f$$

where f refers to foreign broadening. In extreme cases, γ_s can be as much as ten times γ_f. Often, it can be only a few times greater. Thus, if mixtures are such that $p_f \sim 10p_s$ or $100p_s$, the effects of self broadening in determining γ are slight. Therefore, enrichments to about one part in 100 can usually be used to determine the desired air broadened γ coefficients, and often even less dilute mixtures may be used with accuracy. For qualitative judgments, the concept of broadening efficiencies or self to foreign broadening

ratio $B = \frac{\gamma_s}{\gamma_f}$ is often used to determine γ for gas mixtures or to predict "safe" gas mixture ratios. However, one should be careful in using B since it is a function of the particular transition involved. Even so, a single value of B is often used as a guide to the ratio of widths found throughout a band. While this practice is relatively crude and inaccurate it is often dictated by a lack of knowledge of both the self and foreign broadened width for all the lines of a band.

3. CONTINUUM ABSORPTION IN THE DF REGION

The H_2O and N_2 continua arise from quite different mechanisms, and consequently they have quite different wavelength and pressure dependencies.

The H_2O continuum is thought to be the accumulation of far wing line absorption originating from lines in the strong vibration-rotation bands of H_2O located on both the long and short wavelength sides of 3.5 μm. Since the distant wings vary slowly with wavelength, the H_2O continuum is not expected to have structure which varies rapidly with wavelength. Also, since individual lines have a self and foreign broadened component, H_2O continuum is expected to have contributions from both, in general. In the distant wings of a Lorentz line, the absorption varies as follows

$$k_{fw} \sim \frac{n_s S_o \gamma}{(\nu - \nu_0)^2}$$

where

$$\gamma = p_s \gamma_s + \sum_i p_i \gamma_i$$

In the above, p_s and p_i are self and foreign gas partial pressures, respectively, γ is the total half width at half height, and n_s is the number density per unit volume of H_2O or other absorber.

The H_2O continuum absorption coefficient is expressed as the sum of contributions from collisions with itself and foreign partners. Following Burch [11, 12],

$$k_c(H_2O) = n_s(C_s^o p_s + C_f^o p_f)$$

where C_s^o and C_f^o are empirical absorption coefficient parameters. In the DF region, Burch has deduced a value of C_s^o for 296°K, based on measurements

of pure H_2O vapor maintained at high temperatures. He also suggested a value of $C_f^o/C_s^o \sim 0.12$, in lieu of measurements of either C_s^o or C_f^o at the lower temperature. It is significant that the H_2O continuum has a mixed dependence on partial pressure of H_2O. Since n_s is proportional to p_s for ideal gases, the self broadening varies quadratically and the foreign broadening varies linearly with p_s.

In his measurements, Burch [12] investigated the H_2O self broadened continuum at several temperatures. He found the data followed the empirical form

$$C_s^o = c \exp (m/T)$$

where our values of m and c are given in Table 1. His data are reproduced for convenience in Figure 1a. It is noteworthy that this data shows an appreciable temperature dependence. Also, for low T, the small number density of H_2O causes difficulty in performing accurate measurements. The curve for 296^o is extrapolated from the higher temperature data. The dashed portion is extrapolated from only one set of data. The self broadened H_2O continuum dependence on T, relative humidity, and wavenumber in the DF region is shown in Figure 1b for a 2 km path. Calculations of H_2O continuum for the midlatitude summer and midlatitude winter models are shown in Figures 1c and 1d.

It is of interest that the dependence of k_c on p_s is quite different near 10.6 μm than it is at ~ 3.8 μm. This is because measured values indicate that a ratio of $C_f^o/C_s^o \simeq 0.005$ occurs for the 10.6 μm region [13]. For the 10.6 μm applications, then, the C_s^o absorption coefficient parameter is much more important than at the shorter wavelength, and for even slightly humid conditions, $k_c(H_2O)$ varies essentially as p_s^2.

The N_2 continuum arises from the electric dipole forbidden fundamental N_2 vibration-rotation band centered at 2400 cm^{-1}. It absorbs via a transition

Table 1.

Evaluated Parameters for C_s^o as a Function of T at 2400 and 2600 cm^{-1} for N_2 and H_2O.

	ν = 2400 cm^{-1}		ν = 2600 cm^{-1}	
	m	c	m	c
	$(^oK^{-1})$	$\frac{cm^2}{molec.\ atm.}$	$(^oK^{-1})$	$\frac{cm^2}{molec.\ atm.}$
N_2	341	1.415×10^{-26}	0	1.55×10^{-27}
H_2O	1305	6.54×10^{-26}	1067	7.1×10^{-26}

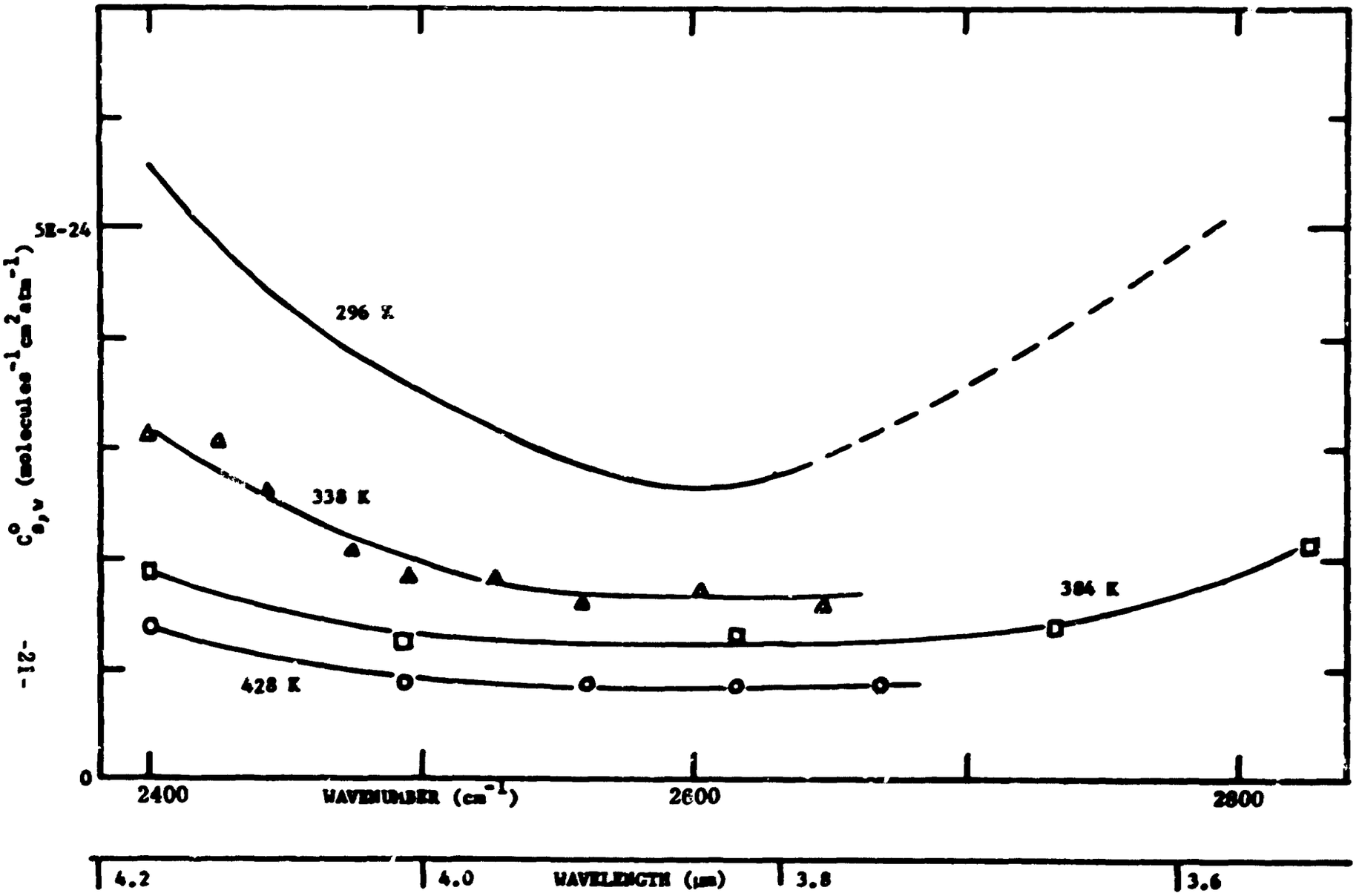

Figure 1a. Spectral Plots of C_s^o Between 2400 and 2820 cm^{-1} for H_2O at Four Temperatures (Reproduced from Ref. 12).

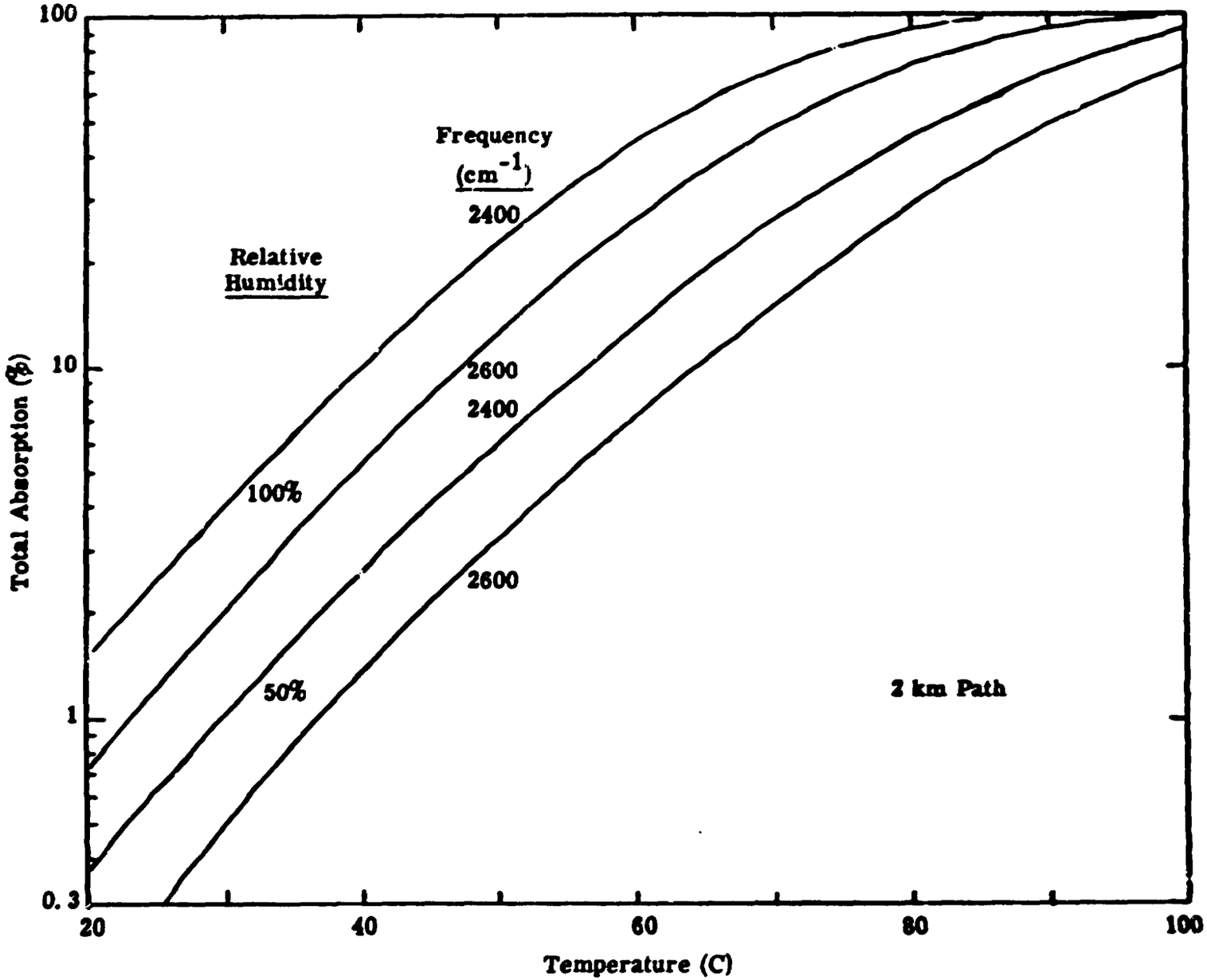

Figure 1b. Total Continuum Absorption Due to Self Broadened H_2O (present calculations based on measurements reported in Ref. 12).

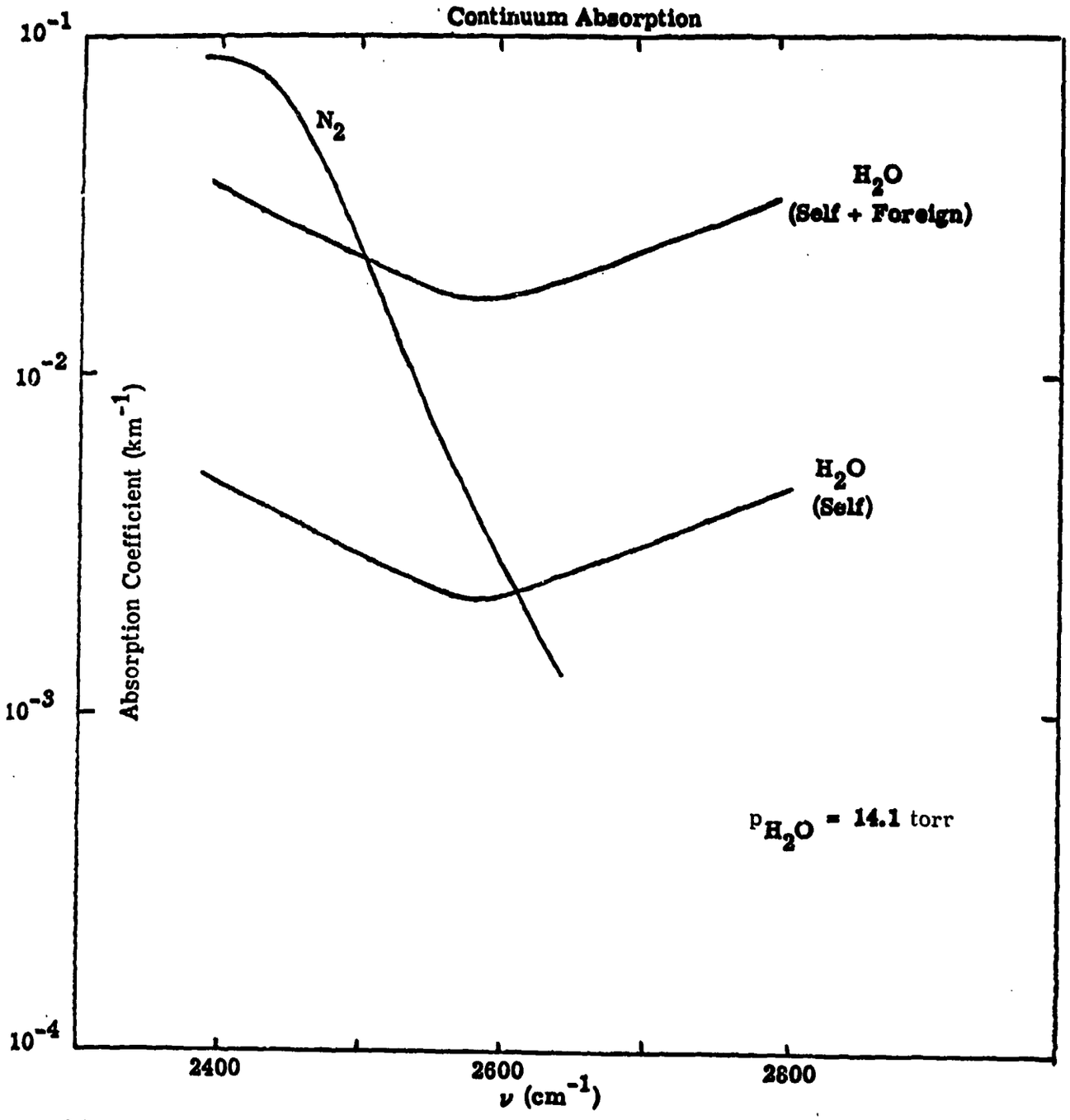

Figure 1c. Calculations of H_2O and N_2 Continuum Absorption Coefficients in the DF Laser Region Based on Data Presented in Ref. 11 and 12.

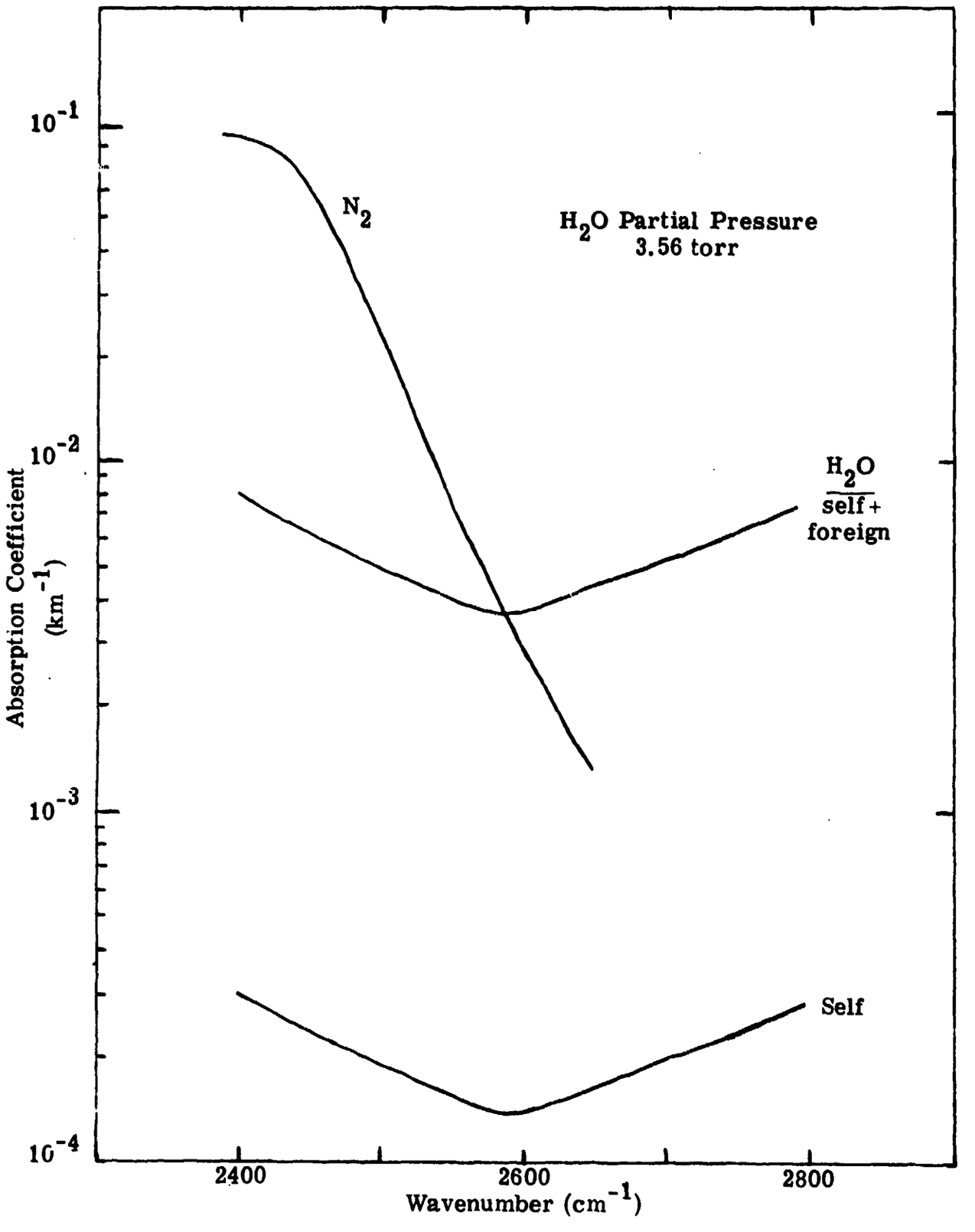

Figure 1d. Calculated H_2O and N_2 Continuum Absorption Coefficients in the DF Laser Region Based on Data Presented in Ref. 11 and 12.

moment induced by collisions with itself or foreign molecules. Since the N_2 absorbs only in the presence of a collision partner, the "rotational line widths" are expected to be very broad -- broader in fact than the approximately 4 cm^{-1} spacings between the transitions. Consequently, the N_2 self broadened continuum, like the H_2O, is expected to show no spectral structure. However, it takes the shape of the R branch envelope of the forbidden vibration-rotation band.

The N_2 continuum absorption coefficient is also written as the sum of contributions from collisions with other N_2 molecules and with foreign species:

$$k_c(N_2) = (C_s^o p_s + C_f^o p_f)n_s$$

where p_s, the partial pressure of N_2, is contained in n_s. Burch's measurements show that N_2-O_2 collisions induce absorption almost as effectively as do N_2 - N_2 collisions. Therefore, if O_2 is taken as the only foreign collision partner, $C_s^o \simeq C_f^o$. To this approximation,

$$k_c(N_2) \simeq C_s^o n_s (p_s + p_f)$$

Therefore, the N_2 continuum varies approximately as the product of the total pressure and the N_2 partial pressure. The N_2 absorption coefficient, to this approximation, is shown in Figures 1c and 1d. It is of interest to compare the pressure dependencies of the H_2O and N_2 continuum absorption coefficients in the DF region. The atmospheric N_2 continuum varies as the square of the partial pressure of N_2, if the mixing ratio of N_2 and O_2 is constant,

$$k_c(N_2) \approx C_s^o n_s p_s \left(1 + \frac{p_f}{p_s}\right)$$

The H_2O continuum, on the other hand, varies more nearly linearly with H_2O partial pressure:

$$k_c(H_2O) \sim C_f^o n_s p_f \left(1 + 8.33 \frac{p_s}{p_f}\right)$$

where C_s^o has been replaced by 8.33 C_f^o, and where $n_s \propto p_s$. We have written $k_c(H_2O)$ in this form to emphasize the importance of C_f^o relative to C_s^o.

The temperature dependence of the N_2 continuum is fairly weak. This has been measured in several laboratories. The results of Burch are shown in Figure 1e.

The discussion in this and in the previous section is intended to place in perspective the several quite different absorption mechanisms. Since the continuum absorption mechanisms are not well understood, we feel that additional clarification of the contributions in the 3.8 μm region is of value. It is important to remember that the H_2O continuum as it occurs in atmospheric absorption is the sum of contributions from H_2O absorbers which collide with both air molecules and other H_2O molecules. Since air is predominantly N_2, the continuum is often considered the sum of H_2O - N_2 (foreign) and H_2O - H_2O (self) absorption coefficients. As pointed out quantitatively above, the self component varies as the square of p_s, and the foreign component varies linearly with the product of $p_s p_f$. Consequently, the (complete) H_2O continuum obeys neither a linear nor square dependence on the pressure p_s. If the self coefficient per molecule (C_s^o) is sufficiently large to surpass or dominate the foreign coefficient, when appropriately weighted by the self and foreign partial pressures, the dependence of the complete H_2O continuum on p_s approaches quadratic. This is the case at 10.6 μm, where the linear contribution is small even for very dry conditions. At 3.8 μm, the magnitude of the continuum caused by H_2O - N_2 collisions is sufficiently large, relative to that caused by H_2O - H_2O collisions, that when weighted properly by p_f, the linear term dominates. The C_s^o contribution is not completely negligible, however, and consequently the dependence on p_s is only approximately linear. Consequently, we prefer to express the absorption coefficient as

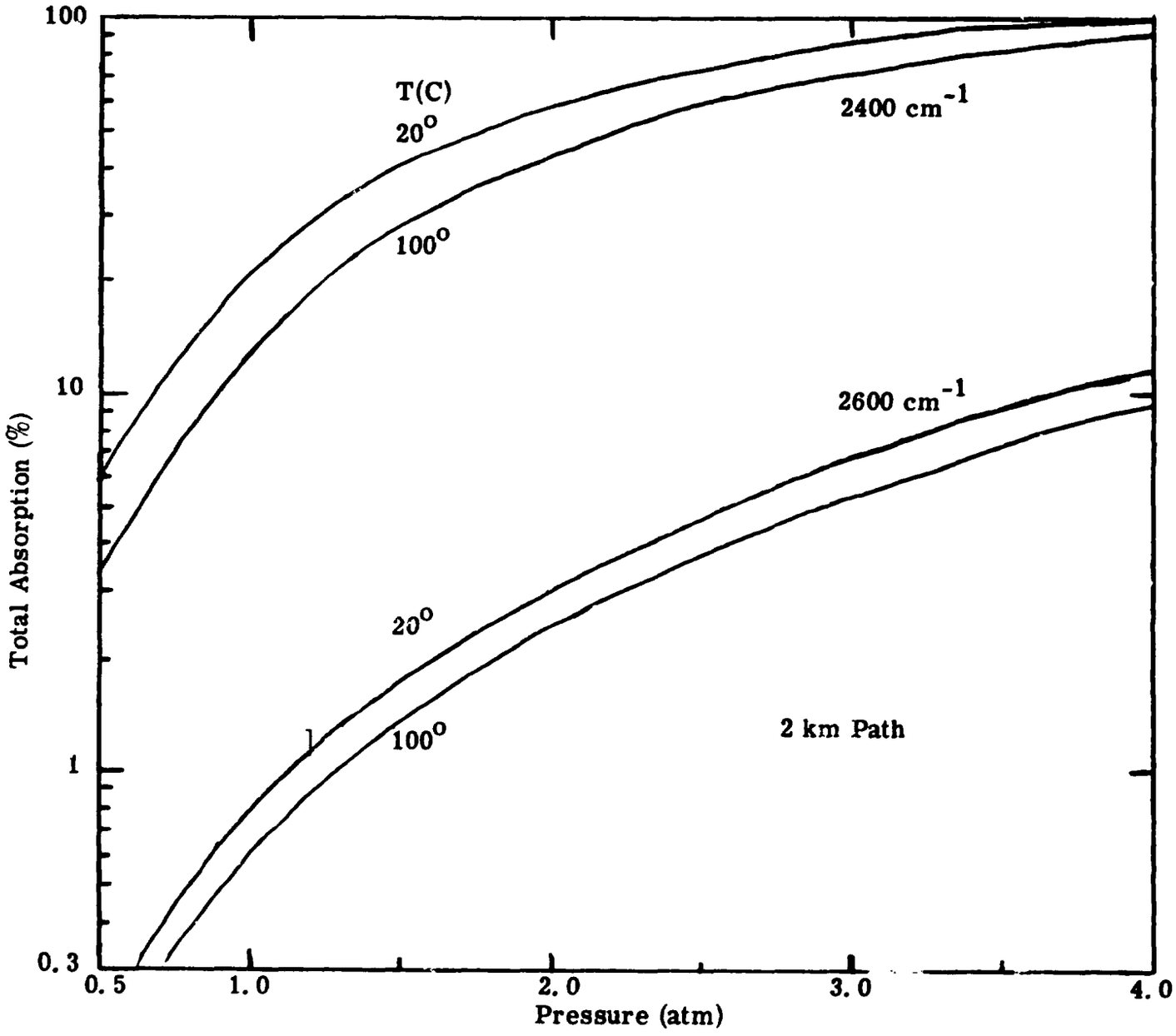

Figure 1e. Calculation of Total Continuum Absorption Due to Self Broadened N_2 Based on Data Presented in Ref. 12.

the sum of linear and square terms. Plots of self broadened and complete H_2O continuum at several partial pressures clearly illustrate this mixed pressure dependence (see Figures 1c and 1d).

In addition to its pressure dependence, the N_2 (induced) continuum is different than the H_2O continuum in a significant way. It necessarily occurs at the wavenumber region where the $v = 0 \rightarrow 1$ vibration-rotation band of N_2 would occur if it were allowed through electric dipole absorption, the mechanism by which molecules normally absorb or emit infrared radiation. The H_2O continuum necessarily occurs far from the center of electric dipole allowed bands, since it is the sum of many distant individual line wing absorptions caused by the normal electric dipole process.

In closing this section dealing with the absorption mechanisms of the continua, we feel it appropriate to comment on the use of the general concept of "broadening efficiencies" or self to foreign absorption coefficients such as C_s^o/C_f^o (for the continua) and B (for the Lorentz line half width).

The ratio $\frac{C_s^o}{C_f^o}$ can be of value in performing specific calculations or estimates of magnitudes, but its use in quantitative discussions or the development of formalisms is not necessary, and it may well lead to confusion. We prefer to use the more general form introduced earlier,

$$k_c = n_s (C_s^o p_s + C_f^o p_f)$$

rather than to express foreign contribution as a function of the self contribution. If the self contribution is factored out to quantify the foreign contribution, their independence may be masked, and one may incorrectly infer a square dependence on pressure (since $n_s \propto p_s$). This view is completely justified since C_s^o and C_f^o are defined as independent empirical coefficients, and they are measured independently of each other, in general.

Another case in point is the parameter B, which is essentially a ratio of self to foreign broadened Lorentz half width γ [14]. The quantity B should not

be confused with the ratio C_s^o/C_f^o which is a modeling parameter which quantifies the magnitude of self and foreign contributions to the continuum absorption coefficient. In the case of H_2O at 3.8 μm, for example, the value $C_f^o/C_s^o \approx 0.12$ is determined empirically from extrapolated data. It is used because far wing calculations obtained by summing specific shapes do not agree with observations, given the measurements accurately quoted by Burch. If the collision mechanisms for $H_2O - H_2O$ and $H_2O - N_2$ collisions both produce a Lorentz line shape, one may expect $B = C_s^o/C_f^o$ if B is constant, line-by-line. This is easily seen as follows by adding the Lorentz line profiles of all contributing lines:

$$k(\nu) = \sum \frac{S^i \gamma^i}{\pi \left| (\nu - \nu_0^i)^2 + (\gamma^i)^2 \right|}$$

Substituting as follows,

$$S^i = S_o^i n_s$$

$$\gamma^i = \gamma_s^i p_s + \gamma_f^i p_f$$

$$k(\nu) = \frac{1}{\pi} \sum_i \left[\frac{S_o^i n_s \gamma_s^i p_s}{(\nu - \nu_0^i)^2 + (\gamma_s^i p_s + \gamma_f^i p_f)^2} + \frac{S_o^i n_s \gamma_f^i p_f}{(\nu - \nu_0^i)^2 + (\gamma_s^i p_s + \gamma_f^i p_f)^2} \right]$$

In the far wings, $|\nu - \nu_0^i| >> \gamma^i$, and $k(\nu) \to k_c(\nu)$:

$$k_c(\nu) = \frac{1}{\pi} \sum_i \left[\frac{S_o^i n_s \gamma_s^i p_s}{(\nu - \nu_0^i)^2} + \frac{S_o^i n_s \gamma_f^i p_f}{(\nu - \nu_0^i)^2} \right]$$

This expression is of the form

$$k_c(\nu) = n_s (C_s^o p_s + C_f^o p_f)$$

where the coefficients C^o have the interpretation:

$$C_s^o = \frac{1}{\pi}\sum_i \frac{S_o^i \gamma_s^i}{(\omega-\nu_0^i)^2}$$

$$C_f^o = \frac{1}{\pi}\sum_i \frac{S_o^i \gamma_f^i}{(\omega-\nu_0^i)^2}$$

The ratio C_s^o/C_f^o then may be written

$$\frac{C_s^o}{C_f^o} = \frac{\sum_i \frac{S_o^i \gamma_s^i}{(\omega-\nu_0^i)^2}}{\sum_i \frac{S_o^i \gamma_f^i}{(\omega-\nu_0^i)^2}}$$

To the extent that, line-by-line, γ_s and γ_f have a constant ratio, the sums above cancel,

$$\frac{\gamma_s^i}{\gamma_f^i} = r$$

and

$$\frac{C_s^o}{C_f^o} = r$$

Analysis of the case where $H_2O - N_2$ and $H_2O - H_2O$ collisions give rise to different shapes is more complicated, but one expects that the ratio $C_s^o/C_f^o \neq r$, in general.

4. MOLECULAR LINE ABSORPTION COEFFICIENTS

In addition to the continuum absorption, atmospheric line absorption caused by N_2O, HDO, H_2O and CH_4 occurs in the DF region. Absorption coefficient calculations have been performed for each individual line of each absorbing molecule which contributes to DF laser absorption. In all, 27 DF laser lines have been investigated. The results are presented in Tables 2 through 28, and in Figures 2 through 28. In addition to displaying the contribution of each line, the total line contribution is given, and the complete absorption coefficient is determined by adding the continua to the total line contribution.

Computations were performed by summing individual Lorentz absorption coefficients, line by line. All contributors whose line centers are within 20 cm^{-1} of the laser frequency under investigation were included in the computation. All line parameter values used in the present calculations were derived from the AFCRL tabulation, using the appropriate temperature corrections. Particular note should be made of the HDO and H_2O line widths. For moderately humid conditions, self broadened half width contributions should be added to the air broadened width values listed in the AFCRL compilation. H_2O - H_2O broadening is about five times as great as H_2O - air broadening, for example [4], and for ~14 torr partial pressure of H_2O, one would expect ~10% contribution from the H_2O - H_2O collisions. Accordingly, this contribution has been included in the parameters used in the present calculations, for the few H_2O lines that occur. The γ_s values were adapted from the calculations of Benedict and Kaplan [15]. The HDO contributors will not encounter significant HDO collision partners. They will encounter a significant number of collisions with the "foreign" H_2O molecules. The air broadened widths of HDO used in the compilation are not based on measurement, and the HDO - H_2O widths have never been investigated to our knowledge. The lack of information on the HDO width precludes inclusion of the HDO - H_2O correction, and accordingly all HDO widths were taken from the AFCRL compilation.

TABLE 2. CONTRIBUTORS TO ATMOSPHERIC MOLECULAR ABSORPTION OF THE P3(12) DF LINE (MIDLATITUDE SUMMER, SEA LEVEL)

LINE NO.	FREQ	SPECTROSCOPIC IDENTIFICATION		STRENGTH	HALF WIDTH	ABSORPT COEF	% LINES	% TOTAL
		ROTATIONAL	VIBRATIONAL					
M1	2444.723	P15D	V1+3V2-V2	4.34E-22	.084	2.444E-05	0.60	0.02
M2	2444.906	P20	3V1-V1	4.75E-21	.081	5.595E-04	13.73	0.57
M3	2445.452	P14C	V1+3V2-V2	4.31E-22	.085	2.408E-04	5.91	0.24
M4	2445.580	P14D	V1+3V2-V2	4.30E-22	.085	8.814E-05	2.16	0.09
M5	2445.778	P19	3V1-V1	4.90E-21	.081	3.635E-04	8.92	0.37
C1	2445.444	R22	V1+V3 /1	3.57E-24	.071	2.225E-03	54.59	2.25

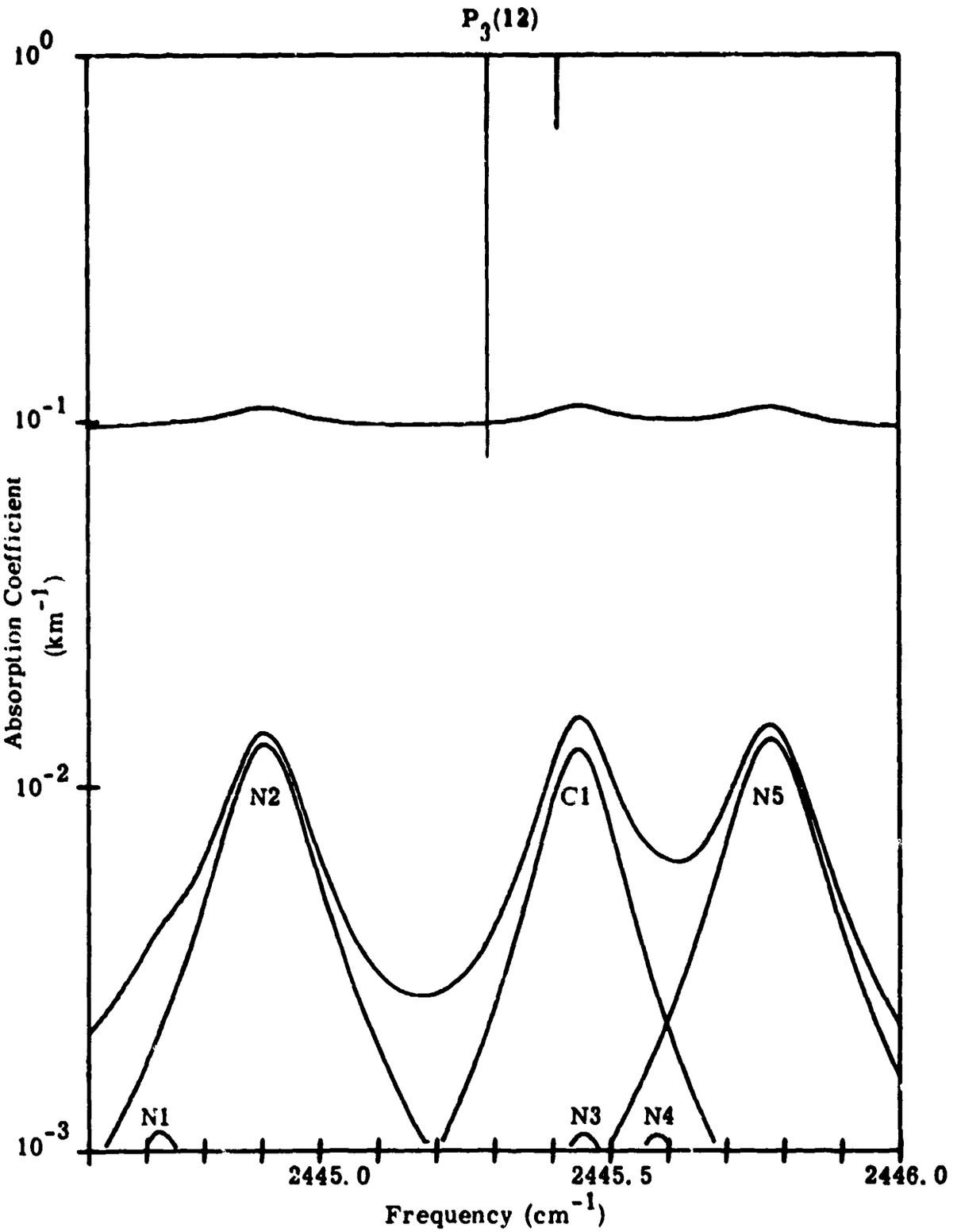

Figure 2. Contributors to the Molecular Absorption of the $P_3(12)$ DF Line (Midlatitude Summer, Sea Level).

TABLE 3. CONTRIBUTORS TO ATMOSPHERIC MOLECULAR ABSORPTION OF THE P3(11) DF LINE (MIDLATITUDE SUMMER, SEA LEVEL)

LINE NO.	FREQ	SPECTROSCOPIC IDENTIFICATION						STRENGTH	HALF WIDTH	ABSORPT COEF	% LINES	% TOTAL
			ROTATIONAL				VIBRATIONAL					
H1	2471.150	8	6	1	7	5	2	V2	5.30E-26	.046	1.001E-03	10.33	1.27
H2	2471.350	8	8	0	7	5	3	V2	1.66E-26	.045	4.707E-03	48.57	5.97
D1	2471.295	15	1	14	16	1	15	V1	2.75E-27	.031	4.128E-04	4.26	0.52
D2	2471.379	15	2	14	16	2	15	V1	2.75E-27	.031	4.907E-04	5.06	0.62
N1	2470.665			R21				V1+4V2-2V2	4.20E-23	.080	0.0	0.0	0.0
N2	2470.718			R15D				V1+3V2-V2	4.68E-22	.084	2.198E-05	0.23	0.03
N3	2471.100			R10				3V1-V1	4.96E-21	.088	1.502E-03	15.49	1.90
N4	2471.258			R16C				V1+3V2-V2	4.67E-22	.083	6.247E-04	6.45	0.79
N5	2471.537			R16D				V1+3V2-V2	4.66E-22	.083	1.861E-04	1.92	0.24
N6	2471.917			R11				3V1-V1	5.18E-21	.087	2.976E-04	3.07	0.38
C1	2471.060			R17				V1+V2+V3-V1-V2	7.70E-26	.073	1.664E-05	0.17	0.02
C2	2471.732			R18				V1+V2+V3-V1-V2	7.59E-26	.072	0.0	0.0	0.0

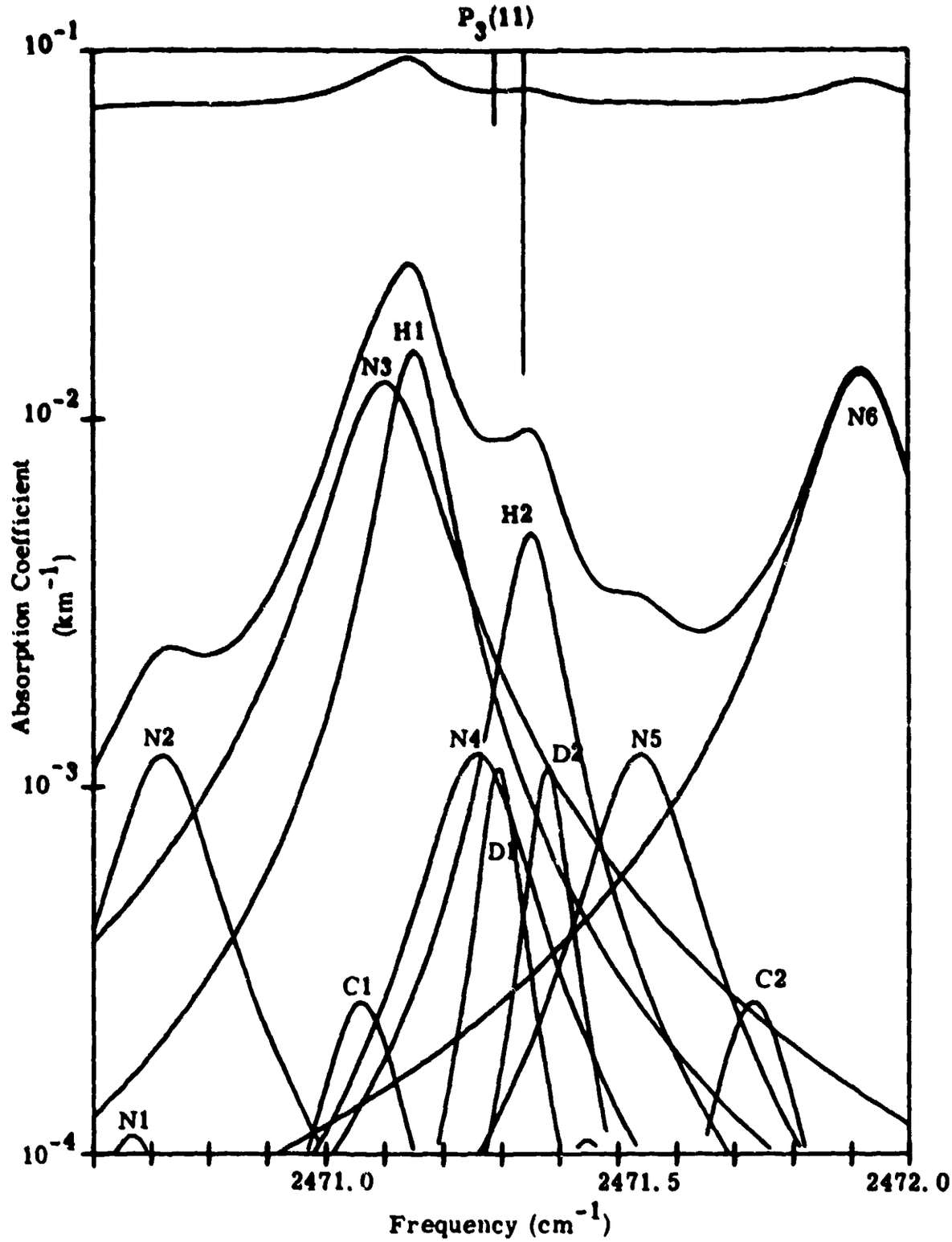

Figure 3. Contributors to the Molecular Absorption of the $P_3(11)$ DF Line (Midlatitude Summer, Sea Level).

TABLE 4. CONTRIBUTORS TO ATMOSPHERIC MOLECULAR ABSORPTION OF THE P3(10) DF LINE (MIDLATITUDE SUMMER, SEA LEVEL)

LINE NO.	FREQ	SPECTROSCOPIC IDENTIFICATION		STRENGTH	HALF WIDTH	ABSORPT COEF	% LINES	% TOTAL
		ROTATIONAL	VIBRATIONAL					
H1	2496.570	9 8 2 3 5 3	V2	2.38E-26	.048	4.133E-03	90.09	7.78
H2	2497.330	9 8 1 8 5 4	V2	7.15E-26	.047	1.022E-04	2.23	0.19
M1	2496.122	R42	3V1-V1	6.21E-22	.073	4.091E-05	0.89	0.08
M2	2496.391	P64	2V1	3.24E-23	.059	7.902E-06	0.17	0.01
M3	2496.860	R43	3V1-V1	5.34E-22	.073	1.261E-04	2.75	0.24

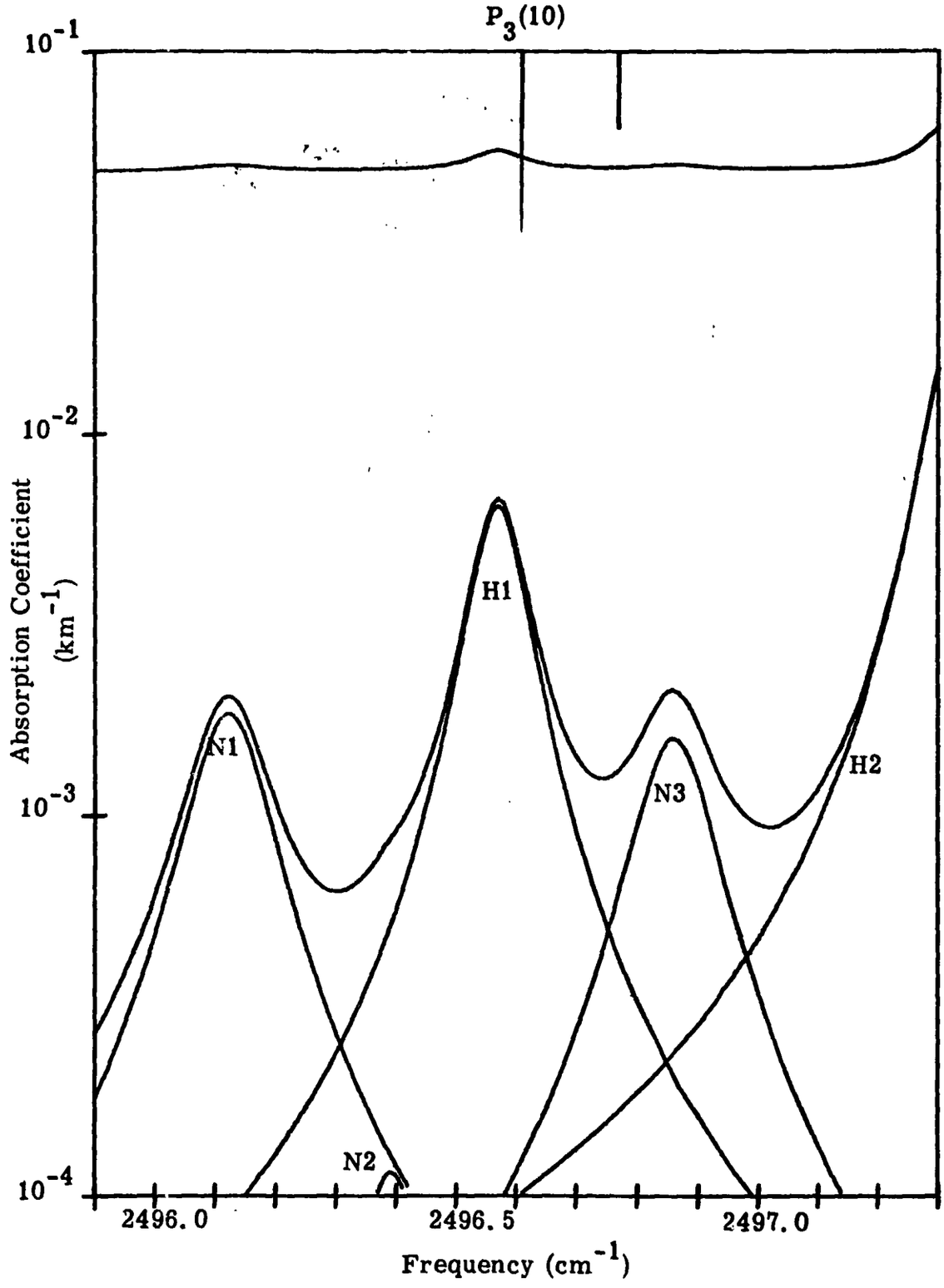

Figure 4. Contributors to the Molecular Absorption of the $P_3(10)$ DF Line (Midlatitude Summer, Sea Level).

TABLE 5. CONTRIBUTORS TO ATMOSPHERIC MOLECULAR ABSORPTION OF THE P2(13) DF LINE (MIDLATITUDE SUMMER, SEA LEVEL)

LINE NO.	FREQ	SPECTROSCOPIC IDENTIFICATION		STRENGTH	HALF WIDTH	ABSORPT COEF	% LINES	% TOTAL
		ROTATIONAL	VIBRATIONAL					
H1	2500.000 9	2 7 8 1 8	V1-V2	1.05E-26	.069	1.017E-04	20.61	0.22
D1	2499.768 12	2 10 13 2 11	V1	2.57E-26	.040	5.226E-05	10.59	0.11
N1	2499.779	R47	3V1-V1	2.78E-22	.071	1.448E-05	2.93	0.03
N2	2500.106	P61	2V1	6.66E-23	.060	1.729E-05	3.50	0.04
N3	2500.500	R48	3V1-V1	2.34E-22	.070	9.570E-05	19.39	0.21

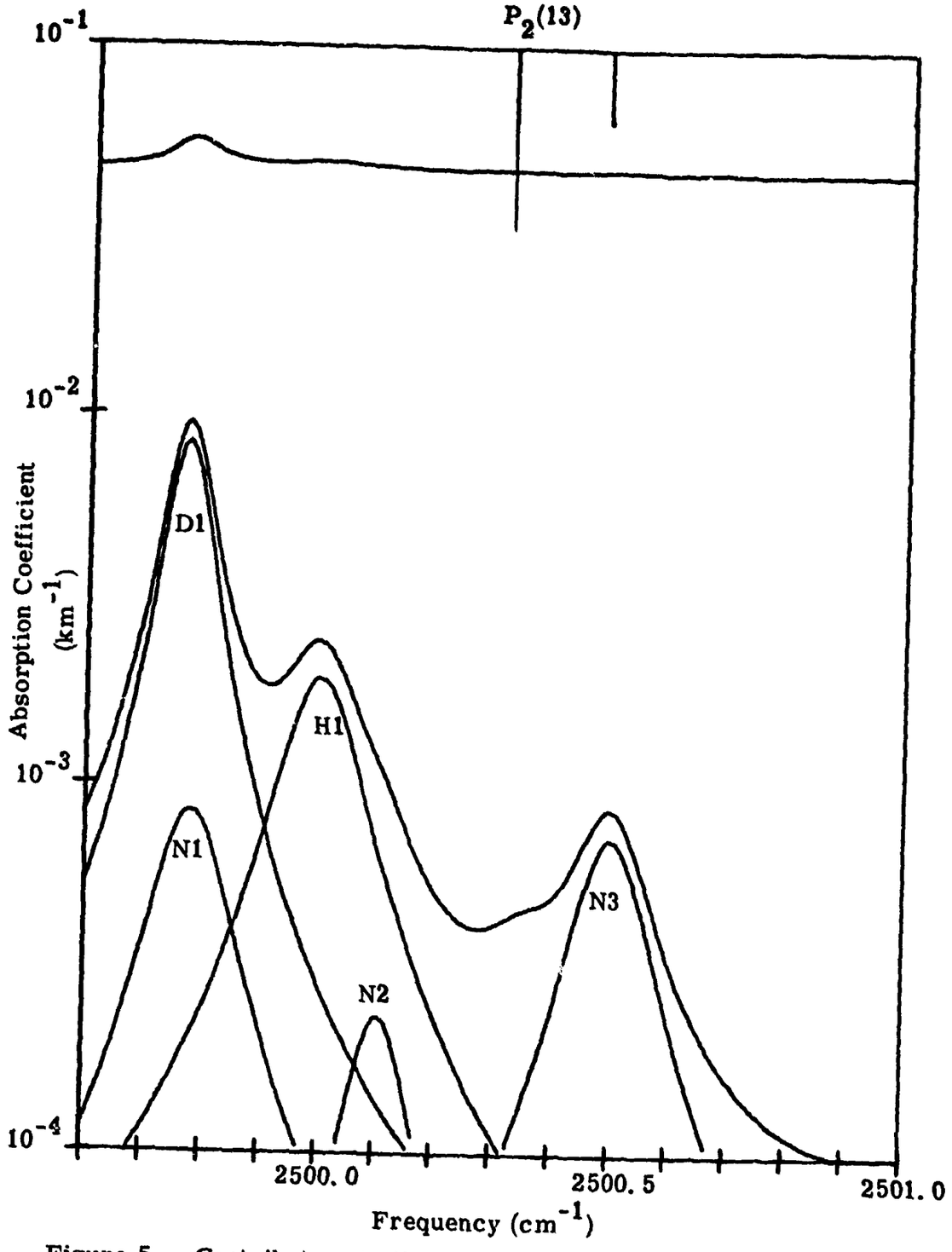

Figure 5. Contributors to the Molecular Absorption of the $P_2(13)$ DF Line (Midlatitude Summer, Sea Level).

TABLE 6. CONTRIBUTORS TO ATMOSPHERIC MOLECULAR ABSORPTION OF THE P3(9) DF LINE (MIDLATITUDE SUMMER, SEA LEVEL)

LINE NO.	FREQ	SPECTROSCOPIC IDENTIFICATION		STRENGTH	HALF WIDTH	ABSORPT COEF	% LINES	% TOTAL
		ROTATIONAL	VIBRATIONAL					
H1	2522.570 10 8 2 9 5 5	V2		1.76E-26	.048	2.093E-05	3.13	0.06
D1	2521.006 6 2 5 7 3 4	V1		1.30E-26	.083	2.444E-05	3.66	0.07
D2	2522.407 11 3 9 12 3 10	V1		5.78E-26	.044	1.024E-04	15.32	0.29
N1	2521.256 P43	2V1		2.20E-21	.073	1.129E-04	16.89	0.32
N2*	2521.440 P15	2V1		8.32E-23	.084	1.090E-05	1.63	0.03
N3	2521.739 P32	3V-V1		5.27E-23	.076	7.852E-05	11.75	0.22
N4*	2522.333 P14	2V1		8.24E-23	.085	5.605E-06	0.84	0.02
N5	2522.372 P42	2V1		2.56E-21	.074	1.296E-04	19.38	0.37

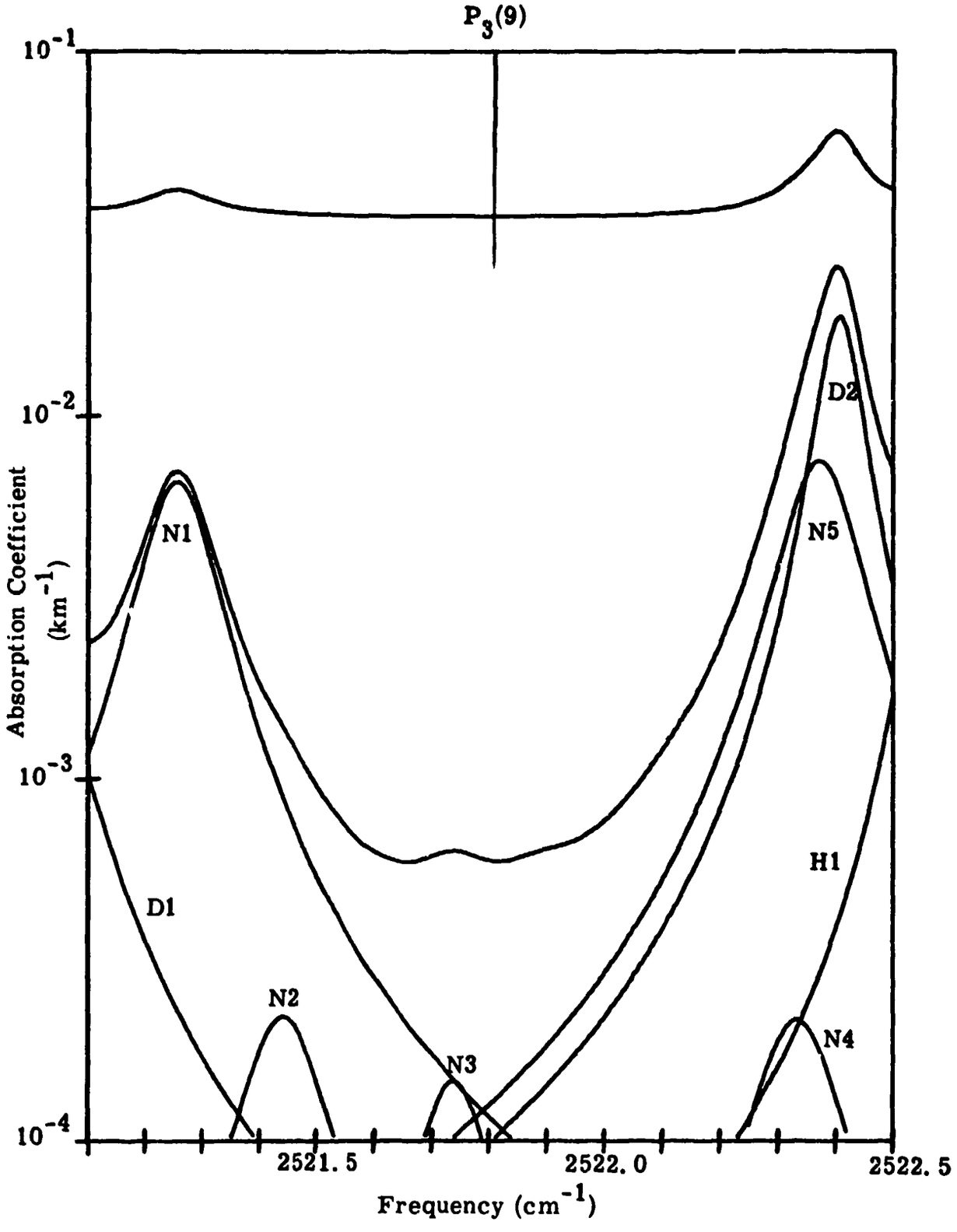

Figure 6. Contributors to the Molecular Absorption of the $P_3(9)$ DF Line (Midlatitude Summer, Sea Level).

TABLE 7. CONTRIBUTORS TO ATMOSPHERIC MOLECULAR ABSORPTION OF THE P2(12) DF LINE (MIDLATITUDE SUMMER, SEA LEVEL)

LINE NO.	FREQ	SPECTROSCOPIC IDENTIFICATION		STRENGTH	HALF WIDTH	ABSORPT COEF	% LINES	% TOTAL
		ROTATIONAL	VIBRATIONAL					
D1	2527.189	3 1 3 4 3 2	V1	7.83E-27	.087	1.176E-04	10.07	0.35
D2	2527.952	14 0 14 14 2 13	V1	5.33E-28	.031	0.0	0.0	0.0
N1	2526.773	P38	2V1	4.49E-21	.075	1.513E-04	12.96	0.45
N2	2526.785	P27	3V-V1	8.19E-23	.077	2.836E-06	0.24	0.01
N3*	2527.156	P29	2V1	3.82E-23	.077	6.263E-06	0.54	0.02
N4	2527.180	P50C	2V1+V2-V2	3.39E-23	.069	5.613E-06	0.48	0.02
N5*	2527.565	P8	2V1	6.19E-23	.091	7.303E-05	6.26	0.22
N6	2527.777	P26	3V-V1	8.80E-23	.078	1.463E-05	1.25	0.04
N7	2527.857	P37	2V1	5.10E-21	.075	5.438E-04	46.61	1.61
N8	2528.935	P36	2V1	5.77E-21	.075	4.449E-05	3.81	0.13

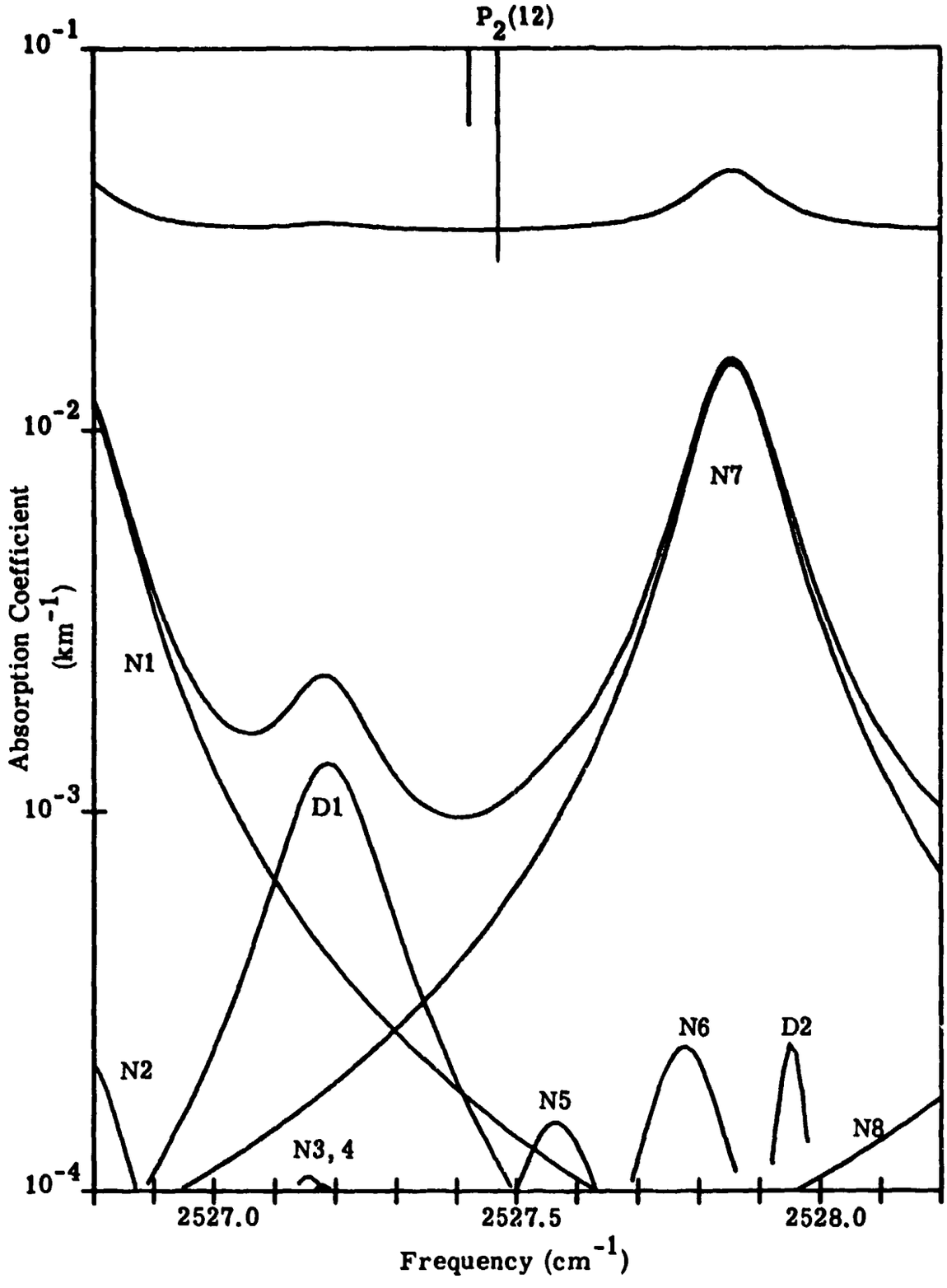

Figure 7. Contributors to the Molecular Absorption of the $P_2(12)$ DF Line (Midlatitude Summer, Sea Level).

TABLE 8. CONTRIBUTORS TO ATMOSPHERIC MOLECULAR ABSORPTION OF THE P3(8) OF LINE (MIDLATITUDE SUMMER, SEA LEVEL)

LINE NO.	FREQ	SPECTROSCOPIC IDENTIFICATION ROTATIONAL	VIBRATIONAL	STRENGTH	HALF WIDTH	ABSORPT COEF	% LINES	% TOTAL
J1	2546.993	9 2 7 10 2 8	V1	3.20E-25	.066	7.863E-04	3.16	1.53
N1	2545.293	P20	2V1	2.06E-20	.081	3.204E-04	1.29	0.62
N2	2545.939	P33C	2V1+V2-V2	4.11E-22	.076	3.548E-05	0.14	0.07
N3	2546.194	P33D	2V1+V2-V2	4.10E-22	.076	1.843E-04	0.74	0.36
N4	2546.260	P19	2V1	2.13E-20	.081	2.067E-02	83.03	40.24
N5*	2546.352	R15	2V1	8.96E-23	.084	2.276E-04	0.91	0.44
N6	[illegible]366	P6	3V-V1	7.79E-23	.093	1.792E-04	0.72	0.35
N7*	2[illegible].505	P9	2V1	5.84E-23	.090	4.484E-05	0.18	0.09
N8	2546.987	P32C	2V1+V2-V2	4.50E-22	.076	0.0	0.0	0.0
N9*	2547.060	R16	2V1	8.94E-23	.083	0.0	0.0	0.0
N10	2547.219	P18	2V1	2.18E-20	.082	5.510E-04	2.21	1.07
M1	2545.680	P6	2V4	7.43E-23	.055	0.0	0.0	0.0
M2	2546.420	P6	2V4	7.81E-23	.055	9.914E-04	3.98	1.93

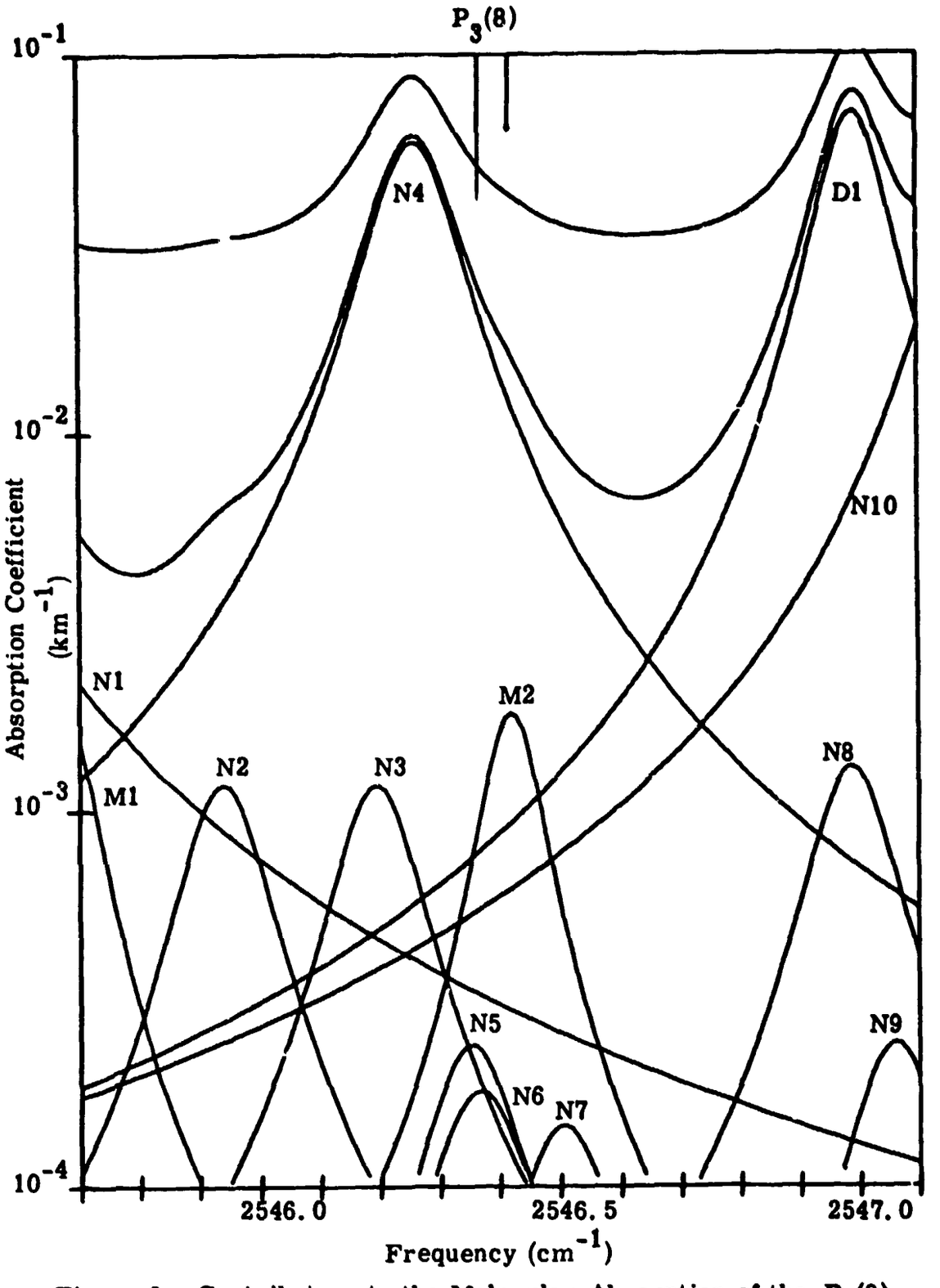

Figure 8. Contributors to the Molecular Absorption of the $P_3(8)$ DF Line (Midlatitude Summer, Sea Level).

TABLE 9. CONTRIBUTORS TO ATMOSPHERIC MOLECULAR ABSORPTION OF THE P2(11) DF LINE (MIDLATITUDE SUMMER, SEA LEVEL)

LINE NO.	FREQ	SPECTROSCOPIC IDENTIFICATION		STRENGTH	HALF WIDTH	ABSORPT COEF	% LINES	% TOTAL
		ROTATIONAL	VIBRATIONAL					
D1	2553.110	9 4 6 10 4 7	V1	1.42E-25	.064	1.777E-04	1.74	0.51
D2	2553.630	8 2 7 9 3 6	2V2	1.15E-27	.071	0.0	0.0	0.0
N1	2552.836	P12	2V1	2.13E-20	.087	3.221E-04	3.15	0.92
N2	2553.287	P26D	2V1+V2-V2	7.62E-22	.078	2.752E-05	0.27	0.08
N3	2553.749	P11	2V1	2.05E-20	.088	7.164E-03	70.14	20.43
N4*	2553.813	R26	2V1	6.11E-23	.077	3.430E-05	0.34	0.10
N5	2554.142	P25C	2V1+V2-V2	8.17E-22	.078	3.908E-04	3.83	1.11
N6	2554.278	P25D	2V1+V2-V2	8.15E-22	.078	1.379E-04	1.35	0.39
N7*	2554.456	R27	2V1	5.70E-23	.077	0.0	0.0	0.0
N8	2554.655	P10	2V1	1.95E-20	.089	8.182E-04	8.01	2.33
N9	2555.554	P9	2V1	1.83E-20	.090	1.472E-04	1.44	0.42
M1	2553.380	P5	2V4	3.35E-23	.055	0.0	0.0	0.0
M2	2553.500	P5	2V4	2.97E-23	.055	0.0	0.0	0.0
M3	2553.580	P5	2V4	4.46E-23	.055	2.028E-05	0.20	0.06
M4	2554.280	P5	2V4	5.20E-23	.055	3.700E-05	0.36	0.11

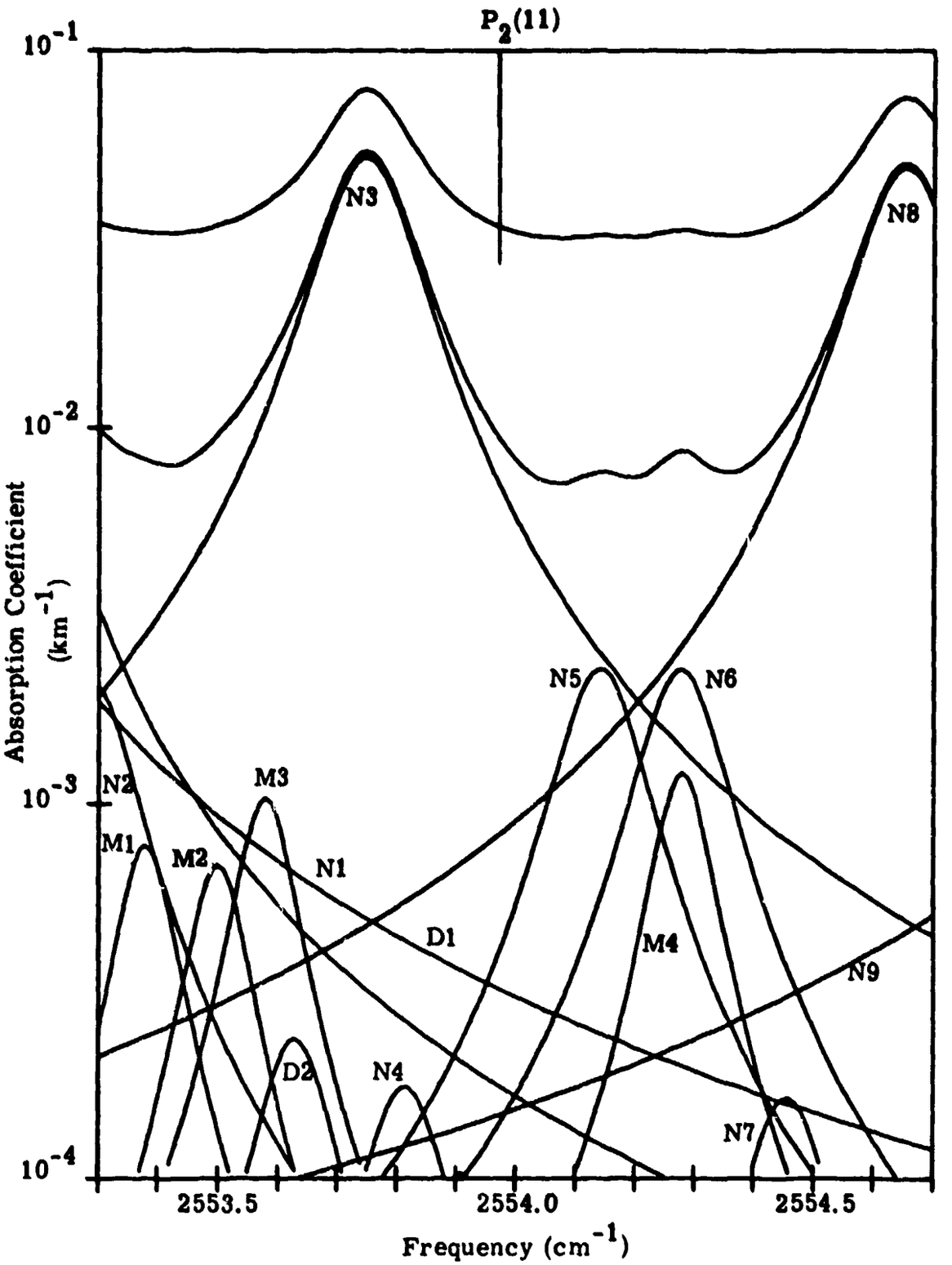

Figure 9. Contributors to the Molecular Absorption of the $P_2(11)$ DF Line (Midlatitude Summer, Sea Level).

TABLE 10. CONTRIBUTORS TO ATMOSPHERIC MOLECULAR ABSORPTION OF THE P3(7) DF LINE (MIDLATITUDE SUMMER, SEA LEVEL)

LINE NO.	FREQ	SPECTROSCOPIC IDENTIFICATION							STRENGTH	HALF WIDTH	ABSORPT COEF	% LINES	% TOTAL
		ROTATIONAL						VIBRATIONAL					
H1	2571.190	13	8	6	12	5	7	V2	3.94E-27	.055	0.0	0.0	0.0
D1	2569.890	8	8	1	9	8	2	V1	2.31E-27	.035	0.0	0.0	0.0
D2	2569.890	8	8	0	9	8	1	V1	2.31E-27	.035	0.0	0.0	0.0
D3	2569.961	9	2	8	10	1	9	V1	2.00E-26	.052	5.011E-05	0.13	0.08
D4	2570.140	8	4	4	9	4	5	V1	2.62E-25	.081	2.162E-03	5.66	3.58
D5	2570.381	8	7	2	9	7	3	V1	1.24E-26	.040	3.910E-04	1.02	0.65
D6	2570.381	8	7	1	9	7	2	V1	1.24E-26	.040	3.910E-04	1.02	0.65
D7	2570.902	8	6	2	9	6	3	V1	4.37E-26	.049	1.986E-04	0.52	0.33
D8	2570.905	8	6	3	9	6	4	V1	4.37E-26	.049	1.957E-04	0.51	0.32
D9	2571.162	8	5	3	9	5	4	V1	1.19E-25	.063	2.543E-04	0.67	0.42
M1	2569.800			R7				2V1	1.75E-20	.091	6.997E-04	1.83	1.16
M2	2570.196			P8C				2V1+V2-V2	8.41E-22	.091	1.580E-04	0.41	0.26
M3	2570.200			P8D				2V1+V2-V2	8.41E-22	.091	1.618E-04	0.42	0.27
M4*	2570.262			R20				2V1	7.03E-23	.080	0.0	0.0	0.0
M5	2570.313			R24				3V-V1	1.06E-22	.078	3.941E-05	0.10	0.07
M6	2570.397			P20C				2V1+2V2-2V2	5.50E-23	.081	4.954E-05	0.13	0.08
M7	2570.403			P20D				2V1+2V2-2V2	5.50E-23	.081	5.317E-05	0.14	0.09
M8	2570.486			P11				2V1+2V2-2V2	5.93E-23	.088	1.349E-04	0.35	0.22
M9	2570.576			R8				2V1	1.91E-20	.090	3.093E-02	80.95	51.20
M10*	2570.944			R21				2V1	6.76E-23	.080	0.0	0.0	0.0
M11	2570.988			R25				3V-V1	9.94E-23	.078	0.0	0.0	0.0
M12	2571.081			P7C				2V1+V2-V2	7.57E-22	.092	4.597E-05	0.12	0.08
M13	2571.082			P7D				2V1+V2-V2	7.57E-22	.092	4.581E-05	0.12	0.08
M14	2571.346			R9				2V1	2.04E-20	.089	5.780E-04	1.51	0.96
N1	2570.100			P3				2V4	3.35E-23	.055	0.0	0.0	0.0
N2	2570.830			P3				2V4	2.23E-23	.055	0.0	0.0	0.0

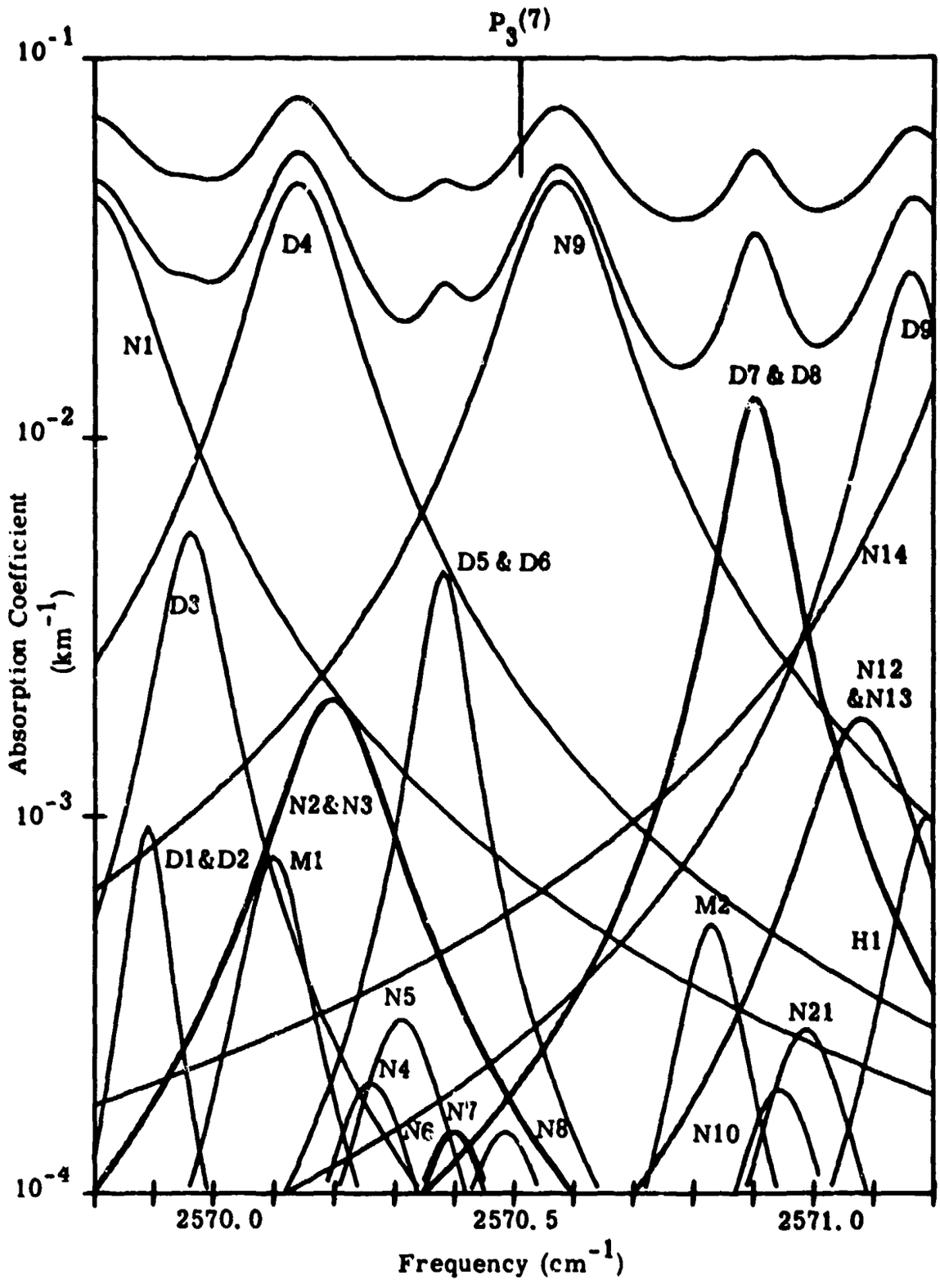

Figure 10. Contributors to the Molecular Absorption of the $P_3(7)$ DF Line (Midlatitude Summer, Sea Level).

TABLE 11. CONTRIBUTORS TO ATMOSPHERIC MOLECULAR ABSORPTION OF THE P2(10) DF LINE (MIDLATITUDE SUMMER, SEA LEVEL)

LINE NO.	FREQ	SPECTROSCOPIC IDENTIFICATION							STRENGTH	HALF WIDTH	ABSORPT COEF	% LINES	% TOTAL
		ROTATIONAL						VIBRATIONAL					
D1	2578.807	9	1	9	10	1	10	V1	8.65E-25	.038	2.639E-04	1.03	0.56
D2	2579.747	8	4	4	9	5	5	2V2	1.28E-27	.070	0.0	0.0	0.0
D3	2579.837	7	3	6	8	2	7	V1	3.08E-26	.064	2.688E-04	1.04	0.57
D4	2580.138	7	4	4	7	5	3	V1	1.89E-27	.073	3.464E-04	1.35	0.74
D5	2580.386	7	4	3	7	5	2	V1	1.89E-27	.067	3.345E-05	0.13	0.07
D6	2581.046	8	2	7	9	2	8	V1	8.46E-25	.052	8.222E-04	3.19	1.76
D7	2582.303	7	2	5	8	2	6	V1	1.17E-24	.083	3.118E-04	1.21	0.67
M1	2579.362			R20				2V1	2.20E-20	.080	6.130E-04	2.38	1.31
M2	2579.565			R2C				2V1+V2-V2	3.27E-22	.094	0.0	0.0	0.0
M3	2579.573			R2D				2V1+V2-V2	3.27E-22	.094	0.0	0.0	0.0
M4	2579.645			P10D				2V1+2V2-2V2	5.04E-23	.089	0.0	0.0	0.0
M5	2579.645			P10C				2V1+2V2-2V2	5.04E-23	.089	0.0	0.0	0.0
M6	2580.049			R21				2V1	2.11E-20	.080	2.014E-02	78.27	43.04
M7	2580.376			R3C				2V1+V2-V2	4.54E-22	.094	1.697E-04	0.66	0.36
M8	2580.389			R3D				2V1+V2-V2	4.54E-22	.094	1.537E-04	0.60	0.33
M9	2580.538			P9C				2V1+2V2-2V2	4.68E-23	.090	0.0	0.0	0.0
M10	2580.730			R22				2V1	2.02E-20	.079	1.078E-03	4.19	2.30

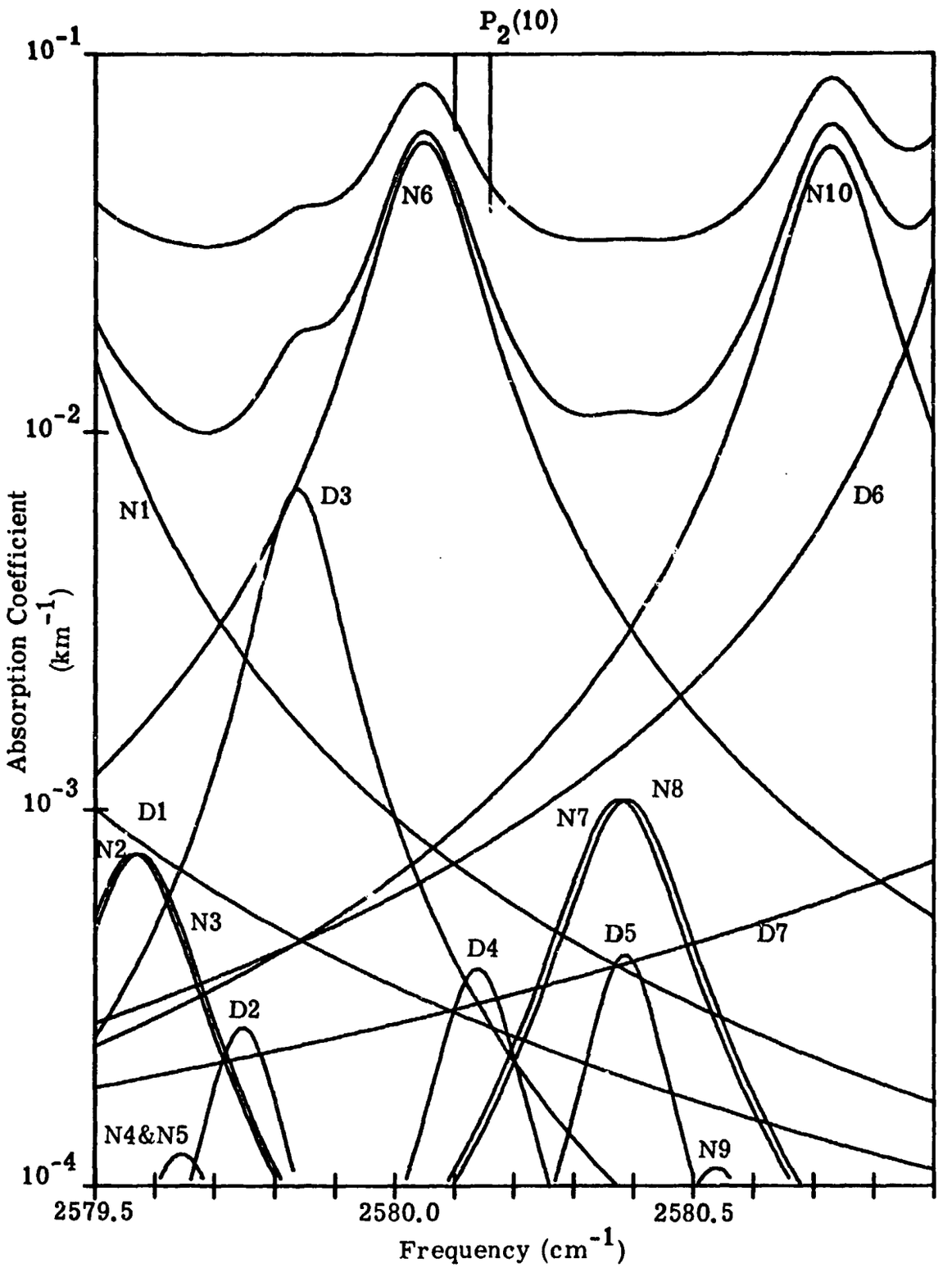

Figure 11. Contributors to the Molecular Absorption of the $P_2(10)$ DF Line (Midlatitude Summer, Sea Level).

TABLE 12. CONTRIBUTORS TO ATMOSPHERIC MOLECULAR ABSORPTION OF THE P3(6) DF LINE (MIDLATITUDE SUMMER, SEA LEVEL)

LINE NO.	FREQ	SPECTROSCOPIC IDENTIFICATION						STRENGTH	HALF WIDTH	ABSORPT COEF	% LINES	% TOTAL
		ROTATIONAL					VIBRATIONAL					
H1	2594.423	8	2	7	9	5	4	2V2	1.74E-26	.061	3.720E-04	4.16	1.29
H2	2594.620	14	5	9	13	2	12	V2	1.14E-26	.051	5.299E-05	0.59	0.18
D1	2591.220	7	1	6	8	1	7	V1	1.55E-24	.066	1.669E-04	1.87	0.58
D2	2593.244	8	0	8	9	0	9	V1	1.50E-24	.044	1.001E-03	11.20	3.47
D3	2593.618	8	1	8	9	1	9	V1	1.50E-24	.044	2.590E-03	28.99	8.98
D4	2593.980	8	1	8	9	0	9	V1	7.80E-26	.043	7.699E-04	8.62	2.67
D5	2594.223	12	2	11	12	2	10	V1	3.47E-27	.038	1.267E-03	14.18	4.39
D6	2594.707	10	0	10	10	1	9	V1	6.27E-27	.039	1.564E-05	0.18	0.05
D7	2594.905	10	1	10	10	1	9	V1	1.72E-26	.039	2.150E-05	0.24	0.07
D8	2596.738	7	2	6	8	2	7	V1	1.43E-24	.062	2.083E-04	2.33	0.72
N1	2593.839			R21C				2V1+V2-V2	1.07E-21	.080	1.180E-04	1.32	0.41
N2	2593.998			R44				2V1	1.98E-21	.073	5.354E-04	5.99	1.86
N3	2594.002			R17				2V1+2V2-2V2	6.87E-23	.082	2.070E-05	0.23	0.07
N4	2594.021			R21D				2V1+V2-V2	1.07E-21	.080	3.750E-04	4.20	1.30
N5	2594.523			R22C				2V1+V2-V2	1.02E-21	.079	1.919E-04	2.15	0.67
N6	2594.524			R45				2V1	1.69E-21	.072	2.907E-04	3.25	1.01
N7	2594.704			R18				2V1+2V2-2V2	6.74E-23	.081	0.0	0.0	0.0
N8	2594.720			R22D				2V1+V2-V2	1.02E-21	.079	7.177E-05	0.80	0.25
M1	2593.910			P1				2V4	2.23E-23	.055	1.499E-05	0.17	0.05

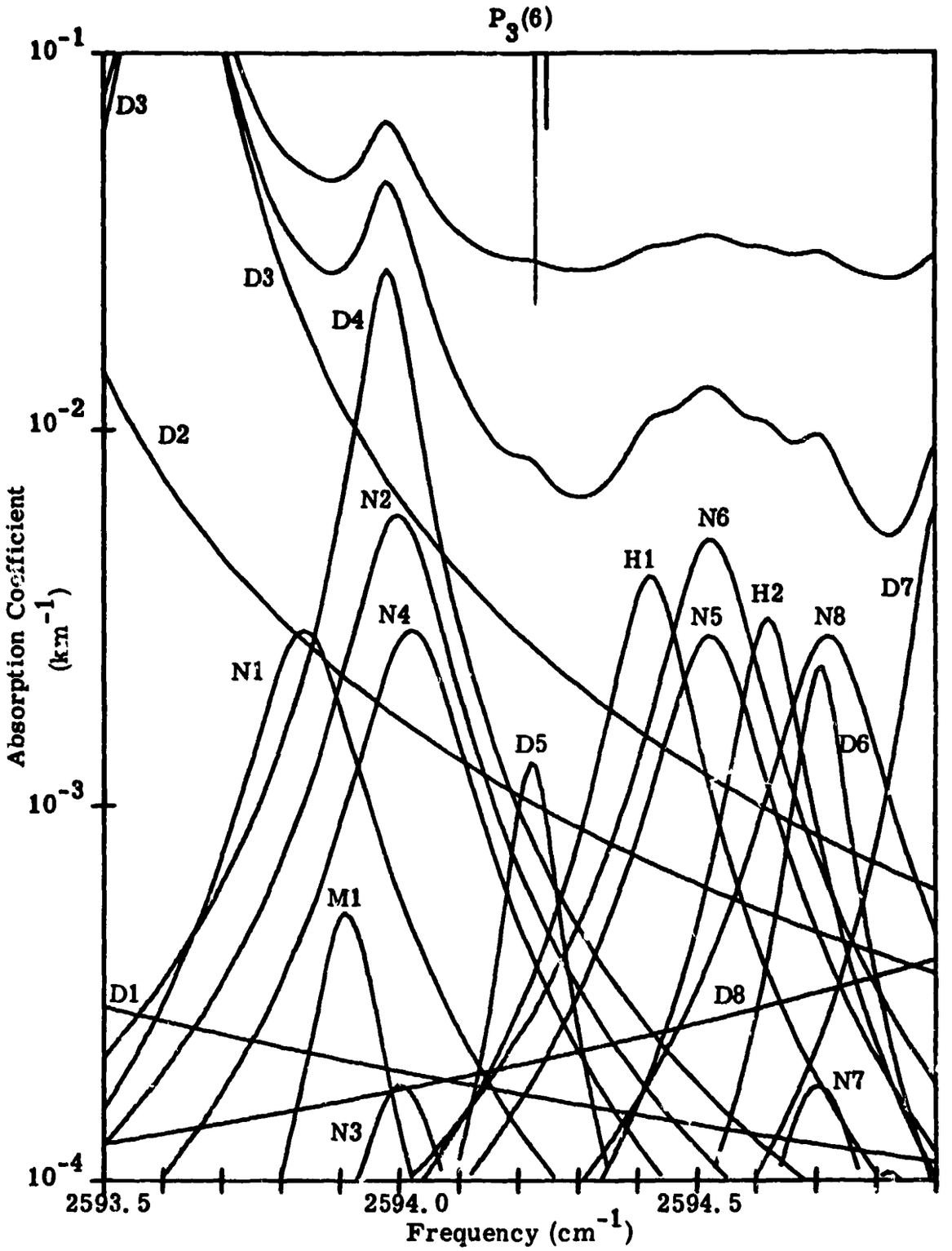

Figure 12. Contributors to the Molecular Absorption of the $P_3(6)$ DF Line (Midlatitude Summer, Sea Level).

TABLE 13. CONTRIBUTORS TO ATMOSPHERIC MOLECULAR ABSORPTION OF THE P2(9) DF LINE (MIDLATITUDE SUMMER, SEA LEVEL)

LINE NO.	FREQ	SPECTROSCOPIC IDENTIFICATION							STRENGTH	HALF WIDTH	ABSORPT COEF	% LINES	% TOTAL
		ROTATIONAL						VIBRATIONAL					
D1	2605.183	6	3	3	7	3	4	V1	1.27E-24	.087	3.410E-03	15.52	8.21
D2	2605.419	3	1	2	3	3	1	V1	6.04E-27	.085	3.649E-05	0.17	0.09
D3	2605.999	9	1	8	9	3	7	V1	2.24E-26	.057	9.409E-04	4.28	2.27
D4	2606.311	6	[illegible]	5	7	1	6	V1	2.51E-24	.077	1.432E-02	65.17	34.50
D5	2606.326	8	3	6	8	4	5	V1	6.06E-27	.082	3.400E-05	0.15	0.08
D6	2606.517	6	6	1	7	6	2	V1	5.91E-26	.042	8.624E-05	0.39	0.21
D7	2606.517	6	6	0	7	6	1	V1	5.91E-26	.042	8.624E-05	0.39	0.21
D8	2607.194	6	4	2	7	4	3	V1	6.37E-25	.074	3.954E-04	1.80	0.95
D9	2607.626	7	0	7	8	0	8	V1	2.43E-24	.052	6.074E-04	2.76	1.46

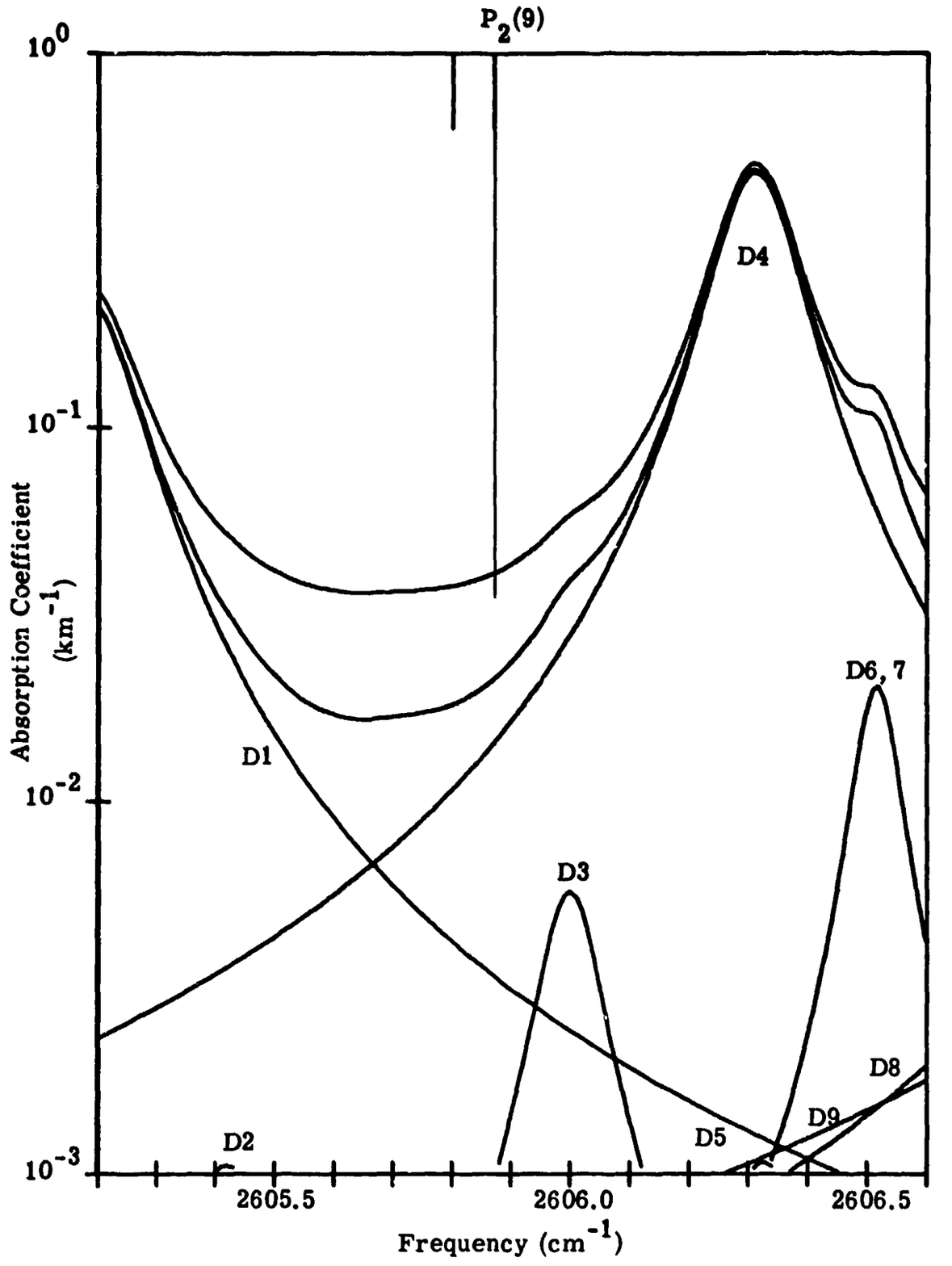

Figure 13. Contributors to the Molecular Absorption of the $P_2(9)$ DF Line (Midlatitude Summer, Sea Level).

TABLE 14. CONTRIBUTORS TO ATMOSPHERIC MOLECULAR ABSORPTION OF THE P3(5) DF LINE (MIDLATITUDE SUMMER, SEA LEVEL)

LINE NO.	FREQ	SPECTROSCOPIC IDENTIFICATION						STRENGTH	HALF WIDTH	ABSORPT COEF	% LINES	% TOTAL
		ROTATIONAL					VIBRATIONAL					
M1	2616.290	13	4	9	12	1	12	V2	5.69E-26	.050	3.244E-05	1.25	0.15
D1	2612.541	6	2	5	7	2	6	V1	2.21E-24	.072	9.962E-05	3.82	0.45
D2	2617.489	12	1	11	13	2	12	2V2	5.61E-28	.033	3.634E-05	1.39	0.16
D3	2617.604	9	3	6	9	4	5	V1	3.90E-27	.082	1.053E-04	4.04	0.47
D4	2617.726	8	0	8	8	2	7	V1	5.97E-26	.052	4.475E-04	17.18	2.02
D5	2617.799	11	0	11	12	1	12	2V2	3.38E-27	.032	1.034E-05	0.40	0.05
D6	2617.847	11	0	11	12	0	12	2V2	3.50E-26	.032	8.494E-05	3.26	0.38
D7	2617.854	12	3	9	13	3	10	2V2	2.60E-27	.056	1.040E-05	0.40	0.05
D8	2618.012	11	1	11	12	1	12	2V2	3.50E-26	.032	4.487E-05	1.72	0.20
D9	2618.060	11	1	11	12	0	12	2V2	3.38E-27	.032	3.718E-06	0.14	0.02
D10	2619.762	5	2	3	6	2	4	V1	2.84E-24	.091	6.945E-04	26.66	3.13
D11	2621.733	6	0	6	7	0	7	V1	3.62E-24	.064	1.845E-04	7.08	0.83
D12	2622.108	5	1	4	6	1	5	V1	3.71E-24	.087	2.179E-04	8.37	0.98
D13	2622.860	6	1	6	7	1	7	V1	3.59E-24	.063	1.133E-04	4.35	0.51
M1	2617.290	R3						2V4	2.23E-23	.055	9.045E-05	3.47	0.41

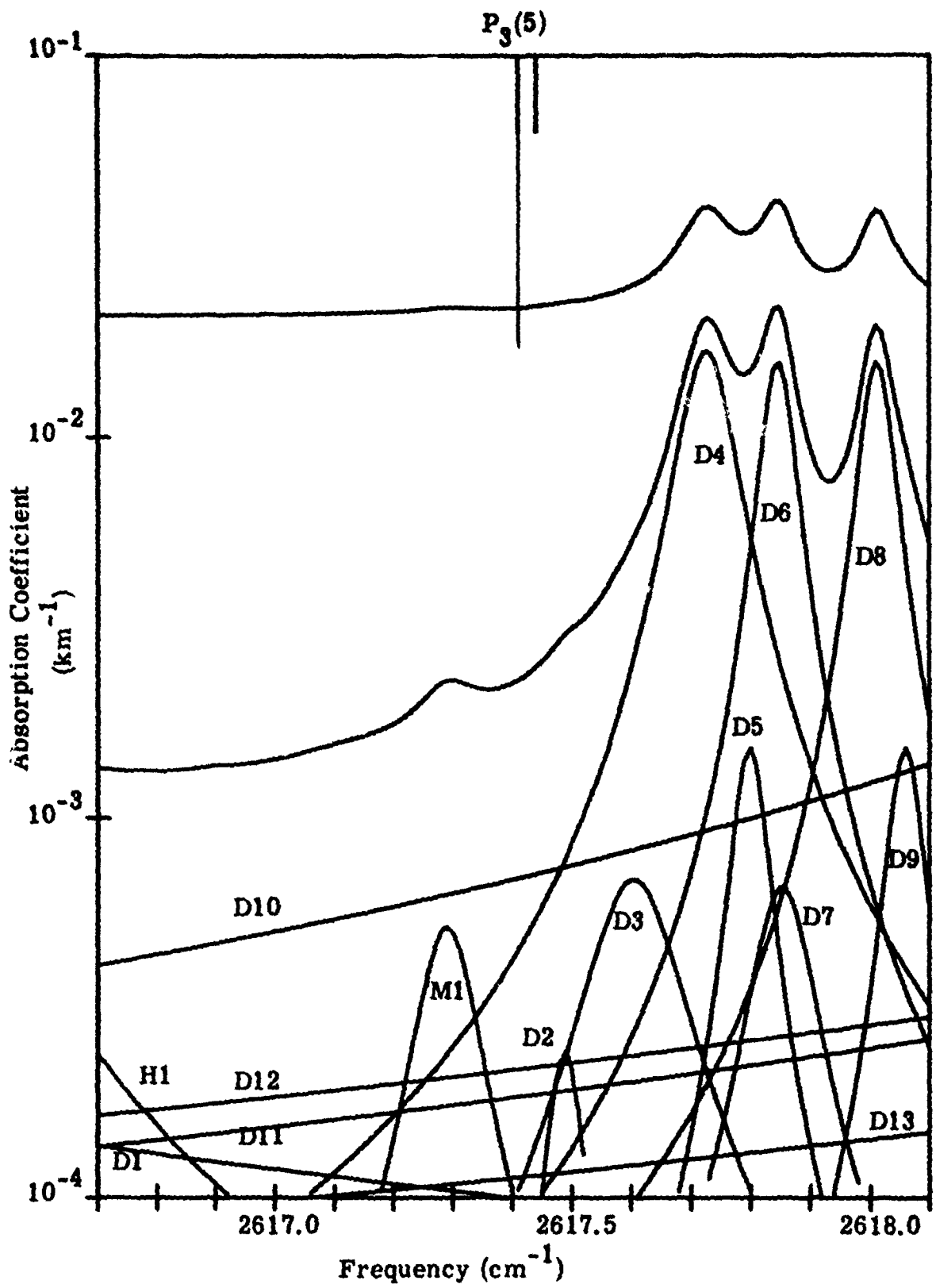

Figure 14. Contributors to the Molecular Absorption of the $P_3(5)$ DF Line (Midlatitude Summer, Sea Level).

TABLE 15. CONTRIBUTORS TO ATMOSPHERIC MOLECULAR ABSORPTION OF THE P2(8) DF LINE (MIDLATITUDE SUMMER, SEA LEVEL)

LINE NO.	FREQ	SPECTROSCOPIC IDENTIFICATION						STRENGTH	HALF WIDTH	ABSORPT COEF	% LINES	% TOTAL
		ROTATIONAL					VIBRATIONAL					
M1	2631.008	9	1	9	10	2	8	2V2	3.95E-26	.050	3.209E-03	24.97	9.80
D1	2628.459	5	2	4	6	2	5	V1	3.09E-24	.081	5.965E-04	4.64	1.82
D2	2630.411	11	3	8	12	3	9	2V2	6.78E-27	.065	1.509E-05	0.12	0.05
D3	2631.071	7	1	7	7	2	6	V1	3.25E-26	.061	6.571E-03	51.13	20.08
D4	2631.259	12	0	12	12	1	11	2V2	3.95E-28	.033	0.0	0.0	0.0
D5	2631.361	12	1	12	12	1	11	2V2	5.17E-28	.033	0.0	0.0	0.0
D6	2635.600	5	0	5	6	0	6	V1	4.99E-24	.077	3.127E-04	2.43	0.96
D7	2637.359	5	1	5	6	1	6	V1	4.90E-24	.076	1.569E-04	1.22	0.48
D8	2638.557	4	1	3	5	1	4	V1	4.96E-24	.082	1.357E-04	1.06	0.41
M1	2630.480		R4					2V4	5.58E-23	.055	0.0	0.0	0.0
M2	2631.080		R4					2V4	3.35E-23	.055	7.526E-04	5.86	2.30
M3	2631.340		R4					2V4	5.20E-23	.055	5.606E-05	0.44	0.17
M4	2631.470		R4					2V4	7.06E-23	.055	3.384E-05	0.26	0.10

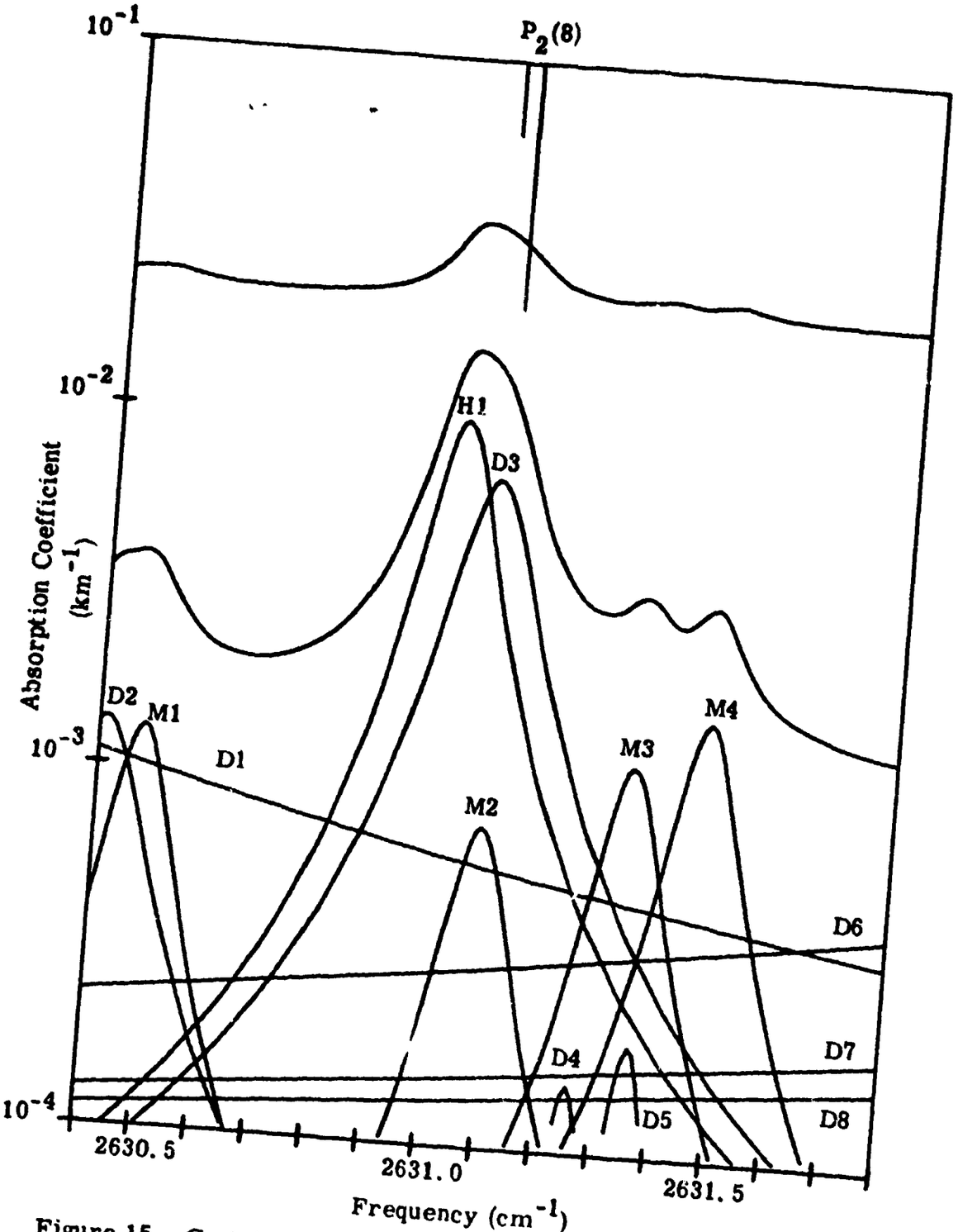

Figure 15. Contributors to the Molecular Absorption of the $P_2(8)$ DF Line (Midlatitude Summer, Sea Level).

TABLE 18. CONTRIBUTORS TO ATMOSPHERIC MOLECULAR ABSORPTION OF THE P2(7) DF LINE (MIDLATITUDE SUMMER, SEA LEVEL)

LINE NO.	FREQ	SPECTROSCOPIC IDENTIFICATION							STRENGTH	HALF WIDTH	ABSORPT COEF	% LINES	% TOTAL
		ROTATIONAL						VIBRATIONAL					
D1	2655.459	3	1	2	4	1	3	V1	5.85E-24	.095	3.084E-02	68.96	47.85
D2	2655.746	4	1	4	5	0	5	V1	2.65E-25	.091	6.173E-03	13.80	9.58
D3	2657.330	3	2	1	4	2	2	V1	3.90E-24	.091	2.861E-03	6.40	4.44
M1	2655.960	P12						V2+V4	1.08E-22	.055	2.371E-03	5.30	3.68
M2	2656.210	P12						V2+V4	1.15E-22	.055	1.309E-04	0.29	0.20
M3	2656.360	P12						V2+V4	8.92E-23	.055	0.0	0.0	0.0
M4	2656.440	P12						V2+V4	8.92E-23	.055	0.0	0.0	0.0

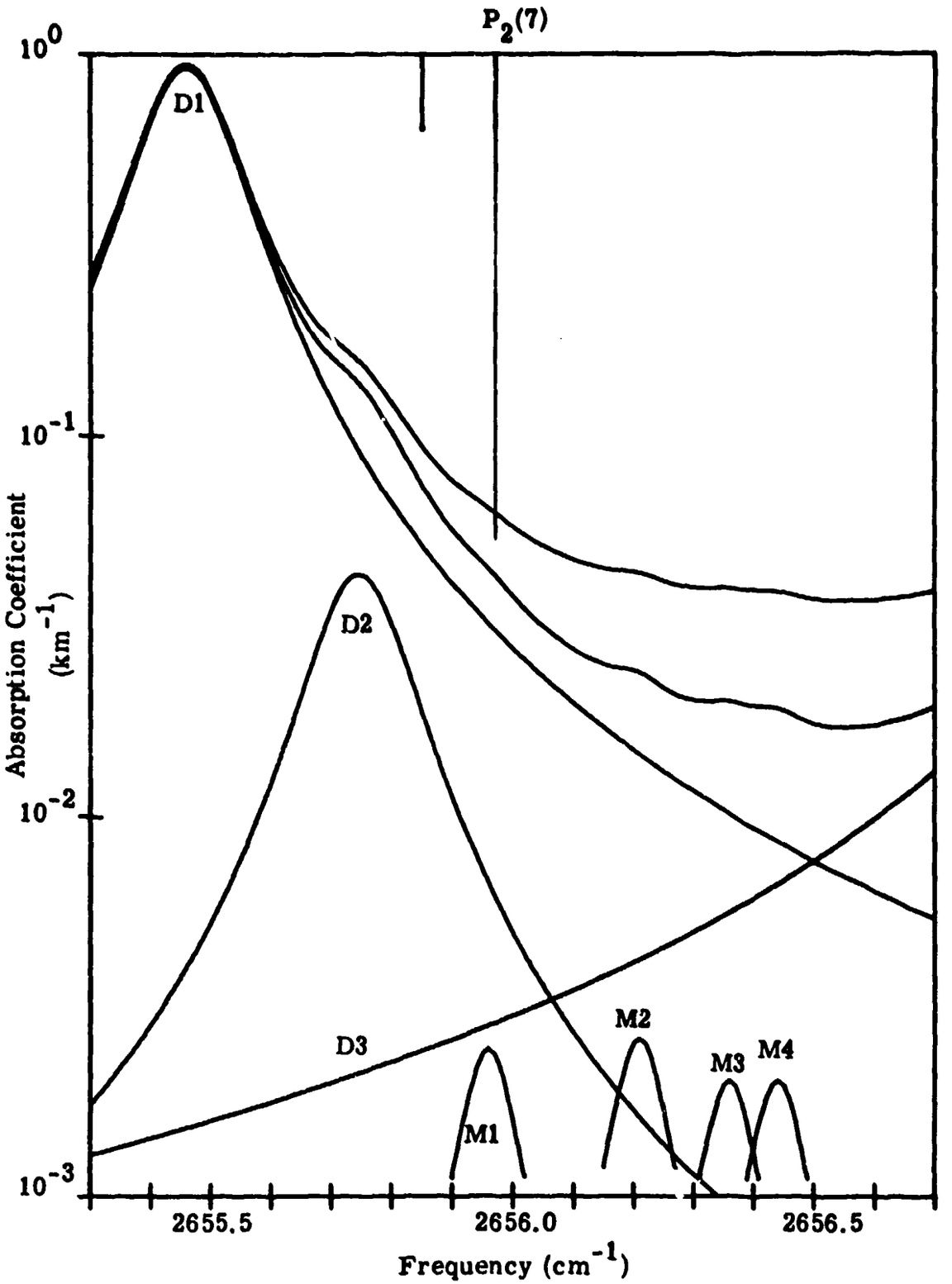

Figure 16. Contributors to the Molecular Absorption of the $P_2(7)$ DF Line (Midlatitude Summer, Sea Level).

TABLE 17. CONTRIBUTORS TO ATMOSPHERIC MOLECULAR ABSORPTION OF THE P1(10) DF LINE (MIDLATITUDE SUMMER, SEA LEVEL)

LINE NO.	FREQ	SPECTROSCOPIC IDENTIFICATION							STRENGTH	HALF WIDTH	ABSORPT COEF	% LINES	% TOTAL
		ROTATIONAL						VIBRATIONAL					
D1	2660.518	3	2	2	4	2	3	V1	3.99E-24	.089	2.426E-04	1.50	0.66
D2	2663.293	3	0	3	4	0	4	V1	7.22E-24	.095	2.825E-03	17.45	7.73
D3	2664.542	6	1	5	7	2	6	2V2	1.85E-26	.076	4.757E-05	0.29	0.13
D4	2664.799	6	1	6	6	1	5	V1	2.34E-25	.077	1.611E-03	9.95	4.41
D5	2664.947	6	3	4	7	2	5	V1	2.22E-26	.092	4.176E-04	2.58	1.14
D6	2665.471	9	4	5	10	3	8	V1	2.48E-27	.068	3.152E-05	0.19	0.09
D7	2666.295	3	1	3	4	1	4	V1	6.70E-24	.094	7.826E-03	48.35	21.41
M1	2664.770	R8						2V4	7.81E-23	.055	2.910E-05	0.18	0.08
M2	2665.070	R8						2V4	7.43E-23	.055	2.609E-04	1.61	0.71
M3	2665.160	R8						2V4	8.92E-23	.055	1.345E-03	8.31	3.68
M4	2665.270	P11						V2+V4	6.32E-23	.055	5.513E-04	3.41	1.51

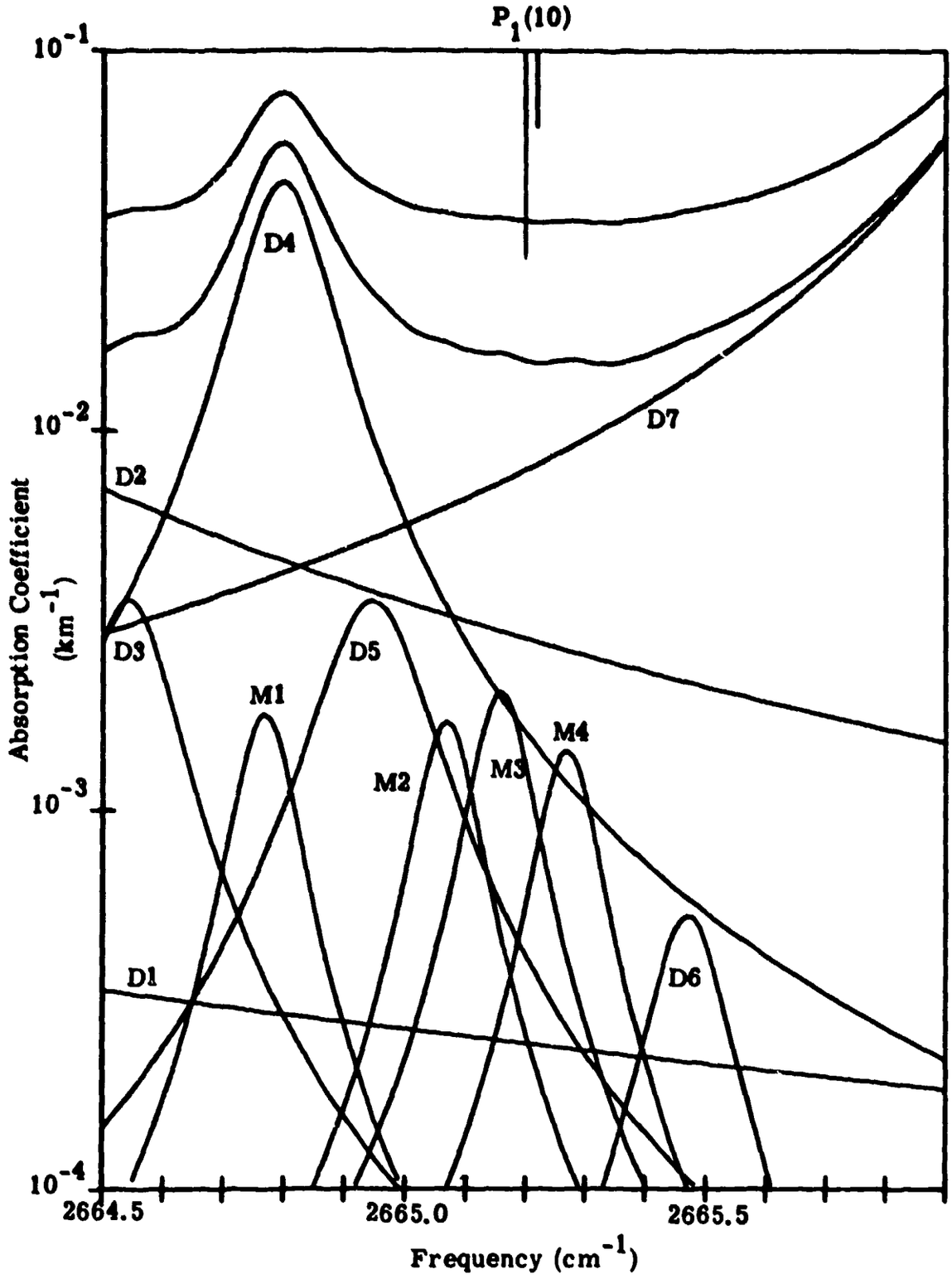

Figure 17. Contributors to the Molecular Absorption of the $P_1(10)$ DF Line (Midlatitude Summer, Sea Level).

TABLE 18. CONTRIBUTORS TO ATMOSPHERIC MOLECULAR ABSORPTION OF THE P2(6) DF LINE (MIDLATITUDE SUMMER, SEA LEVEL)

LINE NO.	FREQ	SPECTROSCOPIC IDENTIFICATION							STRENGTH	HALF WIDTH	ABSORPT COEF	% LINES	% TOTAL
		ROTATIONAL						VIBRATIONAL					
M1	2680.875	9	2	7	10	5	6	2V2	6.32E-26	.065	1.634E-04	0.33	0.23
D1	2677.722	2	0	2	3	0	3	V1	7.31E-24	.100	1.678E-03	3.41	2.37
D2	2679.785	2	1	1	2	2	0	V1	9.53E-26	.095	5.356E-04	1.09	0.76
D3	2680.006	9	1	9	9	1	8	2V2	5.33E-27	.045	0.0	0.0	0.0
D4	2680.620	5	1	4	5	2	3	V1	1.54E-25	.091	1.689E-03	3.43	2.39
D5	2680.738	5	1	5	5	1	4	V1	4.18E-25	.086	2.475E-03	5.03	3.50
D6	2680.759	2	1	2	3	1	3	V1	6.30E-24	.097	3.846E-02	78.14	54.42
D7	2680.796	1	0	1	2	1	2	V1	2.18E-25	.103	1.221E-03	2.48	1.73
D8	2681.052	6	1	5	7	1	6	2V2	3.78E-25	.077	7.182E-04	1.46	1.02
M1	2680.000	P10						V2+V4	7.06E-23	.055	6.031E-05	0.12	0.09

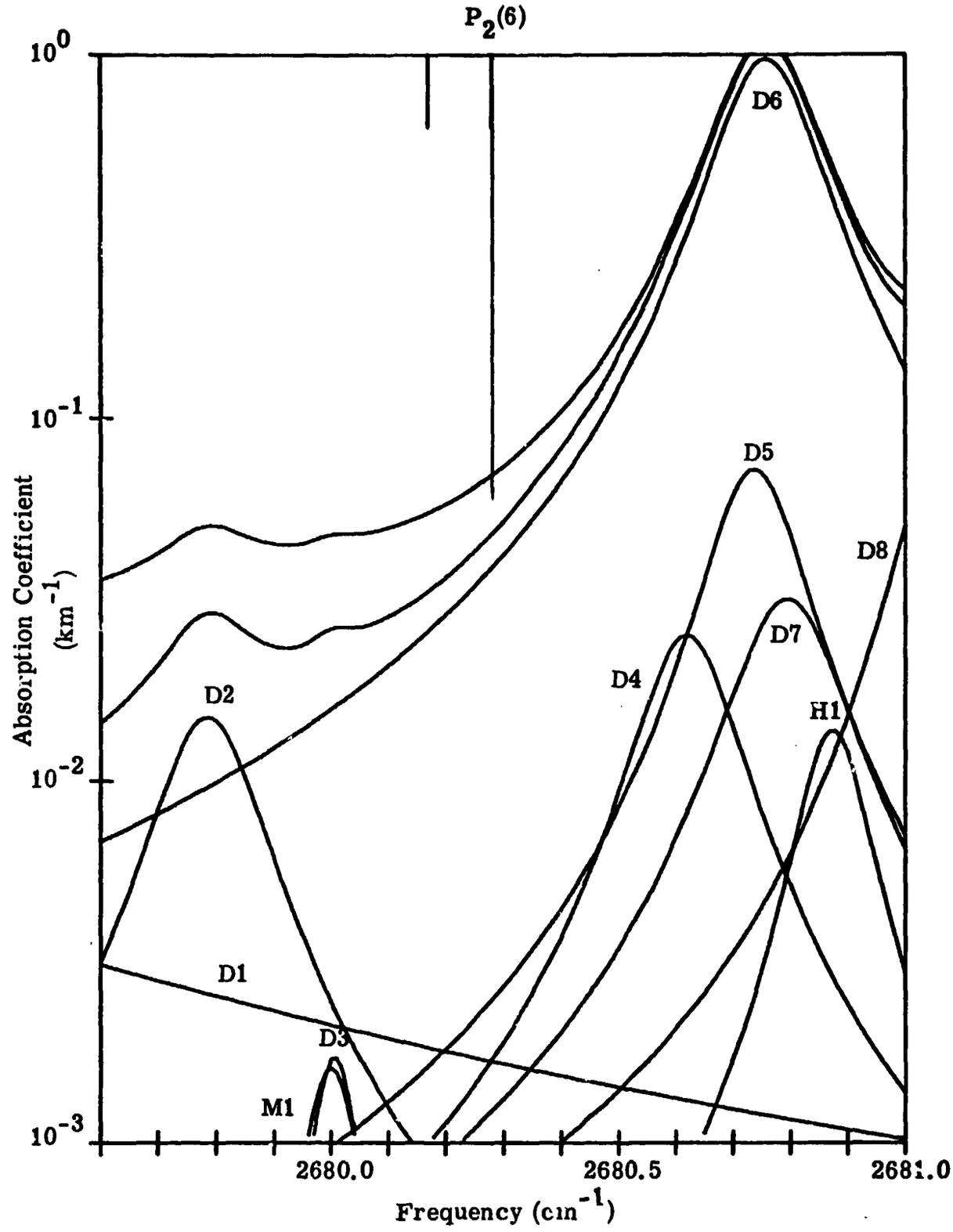

Figure 18. Contributors to the Molecular Absorption of the $P_2(6)$ DF Line (Midlatitude Summer, Sea Level).

TABLE 19. CONTRIBUTORS TO ATMOSPHERIC MOLECULAR ABSORPTION OF THE P1(9) DF LINE (MIDLATITUDE SUMMER, SEA LEVEL)

LINE NO.	FREQ	SPECTROSCOPIC IDENTIFICATION							STRENGTH	HALF WIDTH	ABSORPT COEF	% LINES	% TOTAL
		ROTATIONAL						VIBRATIONAL					
H1	2691.154	3	1	3	4	4	0	3V2-V2	9.00E-27	.078	1.492E-04	0.83	0.37
H2	2691.649	5	1	4	6	4	3	3V2-V2	3.17E-25	.079	5.861E-03	32.64	14.55
D1	2689.785	1	1	0	2	1	1	V1	4.20E-24	.103	2.687E-03	14.96	6.67
D2	2691.319	5	3	2	4	4	1	V1	1.19E-27	.075	9.770E-05	0.54	0.24
D3	2691.435	13	5	9	13	5	8	V1	1.97E-27	.061	3.623E-04	2.02	0.90
D4	2691.449	7	1	6	7	3	5	2V2	5.78E-27	.073	8.522E-04	4.75	2.12
D5	2692.750	1	0	1	2	0	2	V1	6.15E-24	.105	5.871E-03	32.70	14.58
D6	2693.495	5	1	4	6	1	5	2V2	5.60E-25	.087	1.821E-04	1.01	0.45
D7	2695.208	1	1	1	2	1	2	V1	4.38E-24	.098	4.892E-04	2.72	1.21
M1	2691.590			P9				V2+V4	1.08E-22	.055	2.106E-04	1.17	0.52
M2	2691.660			P9				V2+V4	8.18E-23	.055	8.647E-05	0.48	0.21

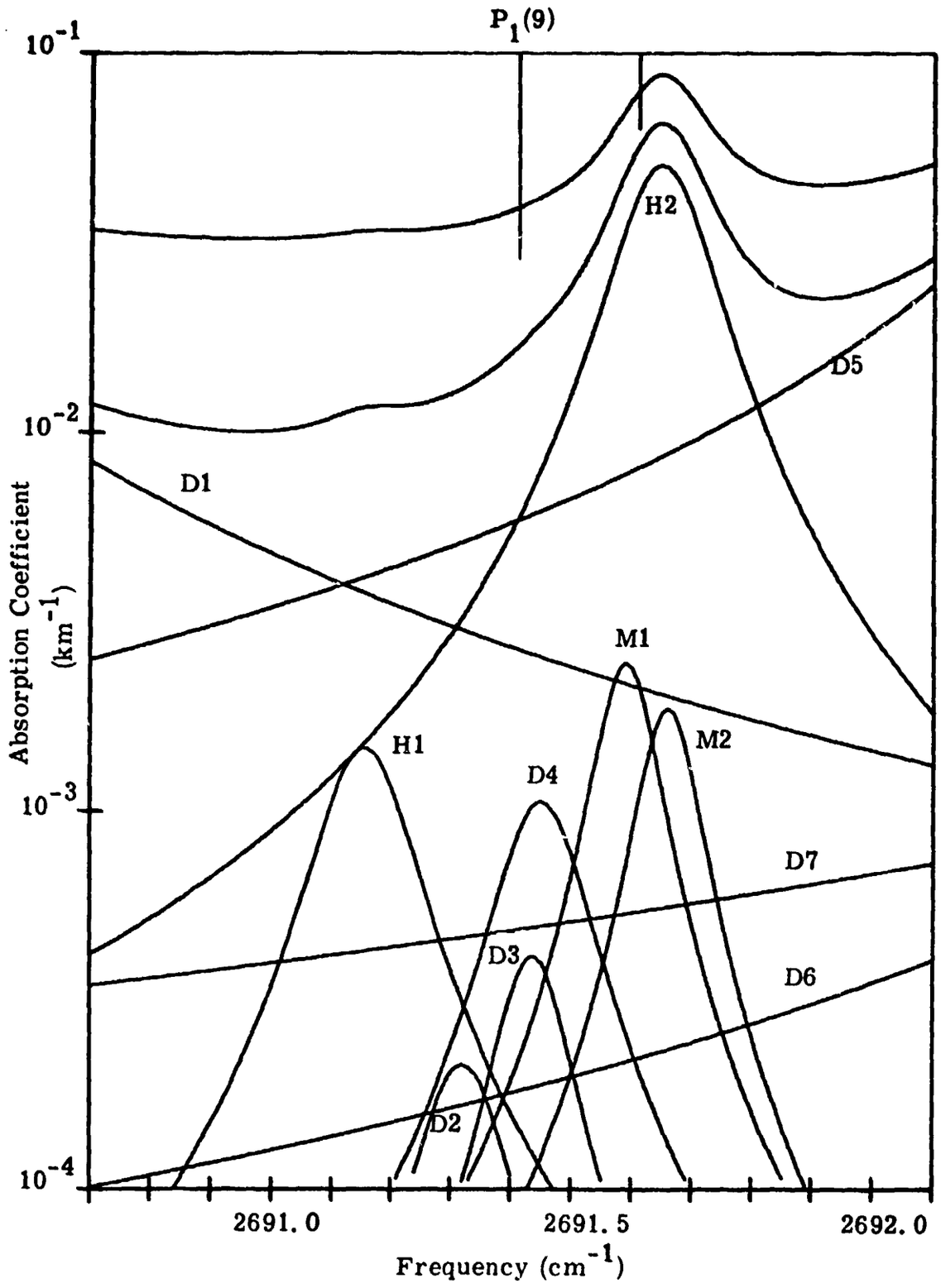

Figure 19. Contributors to the Molecular Absorption of the $P_1(9)$ DF Line (Midlatitude Summer, Sea Level).

TABLE 20. CONTRIBUTORS TO ATMOSPHERIC MOLECULAR ABSORPTION OF THE P2(5) DF LINE (MIDLATITUDE SUMMER, SEA LEVEL)

LINE NO.	FREQ	SPECTROSCOPIC IDENTIFICATION							STRENGTH	HALF WIDTH	ABSORPT COEF	% LINES	% TOTAL
		ROTATIONAL						VIBRATIONAL					
D1	2702.119	5	2	3	6	2	4	2V2	4.30E-25	.091	1.678E-04	3.44	0.59
D2	2702.157	5	1	5	6	1	6	2V2	7.37E-25	.076	2.513E-04	5.16	0.89
D3	2702.868	2	0	2	2	1	1	V1	3.21E-25	.102	3.953E-04	8.11	1.40
D4	2703.093	8	3	6	8	3	5	V1	2.22E-25	.079	3.259E-04	6.69	1.15
D5	2703.329	10	7	3	10	7	4	V1	1.60E-26	.043	2.314E-05	0.47	0.08
D6	2703.329	10	7	4	10	7	3	V1	1.60E-26	.043	2.314E-05	0.47	0.08
D7	2704.080	9	9	0	9	9	1	V1	6.81E-27	.032	2.800E-04	5.75	0.99
D8	2704.080	9	9	1	9	9	0	V1	6.81E-27	.032	2.800E-04	5.75	0.99
D9	2704.180	3	0	3	2	2	0	V1	1.42E-26	.094	4.104E-04	8.42	1.45
D10	2704.256	6	0	6	6	2	5	2V2	2.11E-26	.074	2.847E-04	5.84	1.01
D11	2704.458	5	1	5	6	0	6	2V2	6.39E-26	.080	3.250E-04	6.67	1.15
D12	2704.470	8	5	3	9	4	6	V1	2.28E-27	.064	8.736E-06	0.18	0.03
D13	2704.599	10	6	5	10	6	4	V1	2.92E-26	.051	5.561E-05	1.14	0.20
D14	2704.622	10	6	4	10	6	5	V1	2.92E-26	.051	5.172E-05	1.06	0.18
D15	2706.216	3	1	3	3	1	2	V1	1.30E-24	.097	3.784E-04	7.76	1.34
D16	2706.426	1	0	1	1	1	0	V1	2.49E-25	.107	6.699E-05	1.37	0.24
D17	2707.102	4	1	3	5	1	4	2V2	7.48E-25	.092	1.055E-04	2.16	0.37
D18	2708.179	0	0	0	1	0	1	V1	3.61E-24	.103	3.178E-04	6.52	1.13

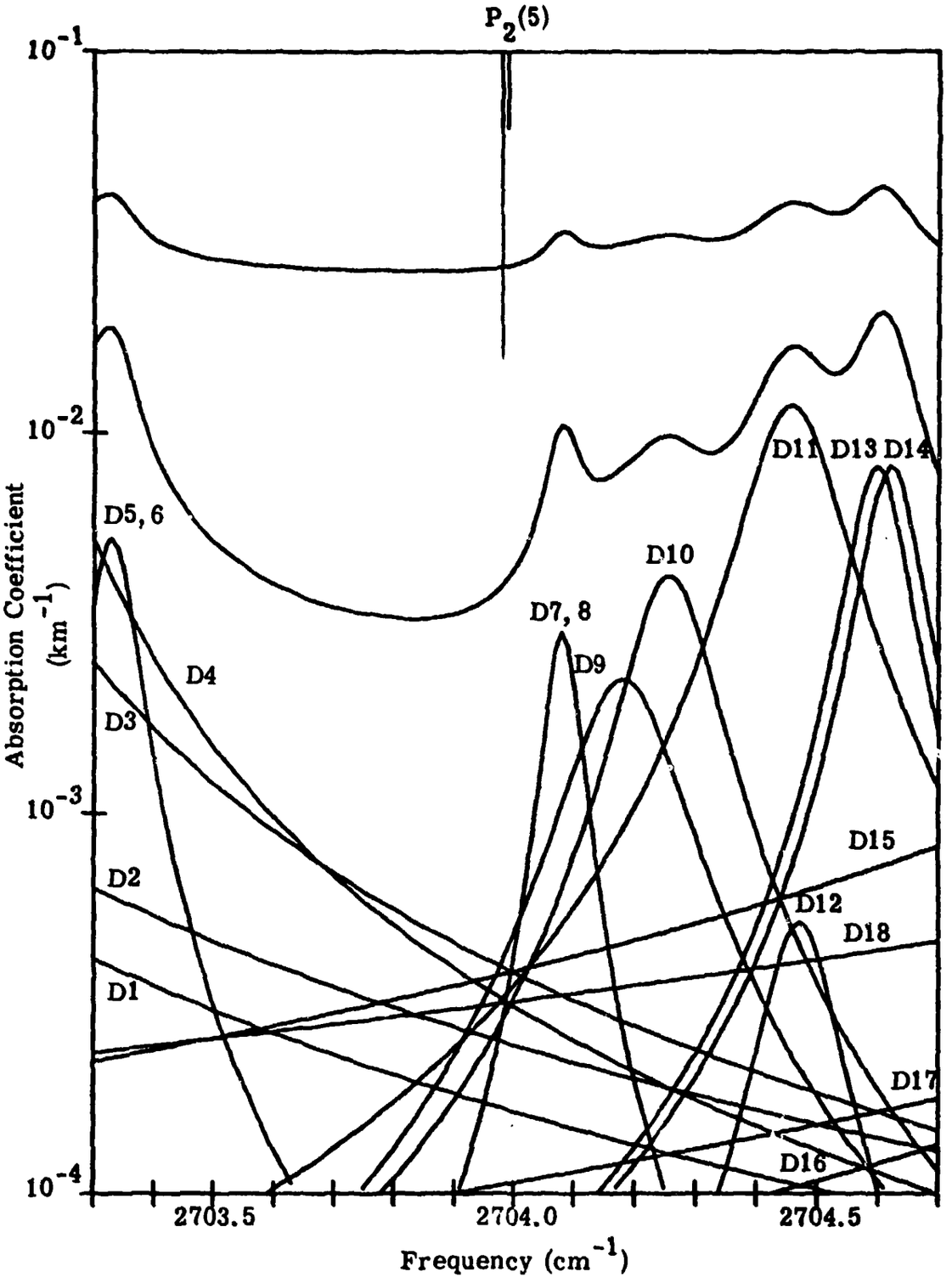

Figure 20. Contributors to the Molecular Absorption of the $P_2(5)$ DF Line (Midlatitude Summer, Sea Level).

TABLE 21. CONTRIBUTORS TO ATMOSPHERIC MOLECULAR ABSORPTION OF THE P1(8) DF LINE (MIDLATITUDE SUMMER, SEA LEVEL)

LINE NO.	FREQ	SPECTROSCOPIC IDENTIFICATION							STRENGTH	HALF WIDTH	ABSORPT COEF	% LINES	% TOTAL
		ROTATIONAL						VIBRATIONAL					
H1	2717.920	14	4	10	13	1	13	V2	7.36E-27	.047	0.0	0.0	0.0
D1	2716.271	4	2	3	4	2	2	V1	2.24E-24	.090	1.877E-03	2.27	1.75
D2	2716.810	6	4	3	6	4	2	V1	1.17E-24	.070	2.279E-03	2.75	2.12
D3	2716.859	4	2	2	5	1	5	V1	2.20E-26	.087	0.0	0.0	0.0
D4	2716.910	10	5	6	11	5	7	2V2	5.27E-27	.058	0.0	0.0	0.0
D5	2716.913	6	4	2	6	4	3	V1	1.17E-24	.070	3.085E-03	3.72	2.87
D6	2716.933	5	3	2	5	4	1	2V2	1.12E-26	.075	0.0	0.0	0.0
D7	2716.997	5	2	3	6	0	6	V1	2.38E-26	.081	9.690E-05	0.12	0.09
D8	2717.136	5	1	5	5	2	4	2V2	3.10E-26	.083	2.303E-04	0.28	0.21
D9	2717.189	6	3	4	6	4	3	2V2	1.01E-26	.084	9.850E-05	0.12	0.09
D10	2717.456	3	0	3	4	1	4	2V2	8.34E-26	.094	7.693E-03	9.29	7.17
D11	2717.658	5	2	4	4	3	1	V1	8.34E-27	.082	4.719E-04	0.57	0.44
D12	2717.751	5	5	0	5	5	1	V1	1.79E-24	.047	2.567E-02	31.00	23.91
D13	2717.751	5	5	1	5	5	0	V1	1.79E-24	.047	2.567E-02	31.00	23.91
D14	2717.822	6	2	4	7	0	7	V1	1.22E-26	.074	1.539E-04	0.19	0.14
D15	2717.898	7	3	5	7	4	4	2V2	7.66E-27	.084	0.0	0.0	0.0
D16	2718.549	5	3	3	5	3	2	V1	2.04E-24	.082	2.413E-03	2.91	2.25
D17	2718.647	5	4	2	5	4	1	V1	2.21E-24	.066	1.749E-03	2.11	1.63
D18	2718.682	5	4	1	5	4	2	V1	2.21E-24	.066	1.644E-03	1.99	1.53
D19	2720.838	1	1	1	1	1	0	V1	5.01E-24	.102	7.057E-04	0.85	0.66

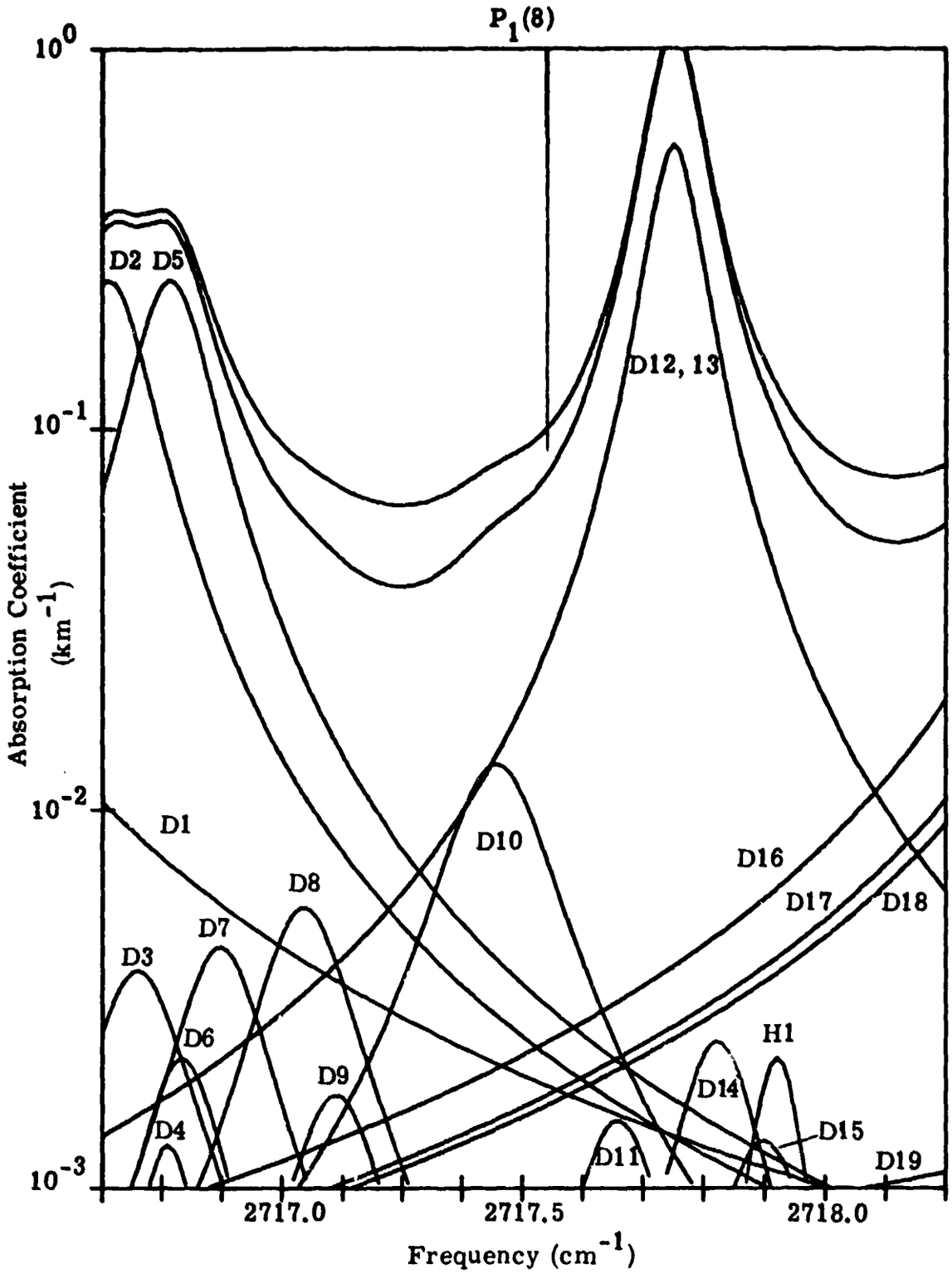

Figure 21. Contributors to the Molecular Absorption of the $P_1(8)$ DF Line (Midlatitude Summer, Sea Level).

TABLE 22. CONTRIBUTORS TO ATMOSPHERIC MOLECULAR ABSORPTION OF THE P2(4) DF LINE (MIDLATITUDE SUMMER, SEA LEVEL)

LINE NO.	FREQ	SPECTROSCOPIC IDENTIFICATION							STRENGTH	HALF WIDTH	ABSORPT COEF	% LINES	% TOTAL
		ROTATIONAL						VIBRATIONAL					
M1	2727.322	3	1	2	4	4	1	3V2-V2	7.08E-26	.077	7.980E-03	21.12	12.62
M2	2727.730	11	8	4	10	3	7	V2	7.09E-27	.058	5.099E-05	0.13	0.06
M3	2729.017	6	1	6	7	2	5	3V2-V2	1.03E-24	.078	4.561E-04	1.21	1.21
D1	2722.664	2	2	1	2	2	0	V1	7.63E-24	.091	5.134E-04	1.36	0.81
D2	2723.338	2	2	0	2	2	1	V1	7.64E-24	.091	6.997E-04	1.85	1.11
D3	2723.777	3	2	1	3	2	2	V1	4.18E-24	.090	4.757E-04	1.26	0.75
D4	2725.682	4	2	2	4	2	3	V1	2.30E-24	.090	1.173E-03	3.11	1.86
D5	2726.161	1	1	0	1	1	1	V1	5.08E-24	.102	5.704E-03	15.10	9.02
D6	2726.956	8	3	5	8	4	4	2V2	5.32E-27	.083	3.950E-05	0.10	0.06
D7	2727.092	4	2	2	4	3	1	2V2	2.76E-26	.086	4.225E-04	1.12	0.67
D8	2727.260	7	4	4	8	4	5	2V2	6.79E-26	.069	3.740E-03	9.90	5.92
D9	2727.528	5	3	2	6	3	3	2V2	2.64E-25	.085	1.192E-02	31.54	18.85
D10	2727.824	5	2	3	4	3	2	V1	9.46E-27	.087	6.524E-05	0.17	0.10
D11	2727.870	9	3	6	9	3	7	V1	9.87E-26	.073	4.693E-04	1.24	0.74
D12	2728.060	2	0	2	3	1	3	2V2	8.24E-26	.100	2.858E-04	0.76	0.45
M1	2726.790	PT						V2+V4	1.08E-22	.055	0.0	0.0	0.0
M2	2726.910	PT						V2+V4	1.19E-22	.055	0.0	0.0	0.0

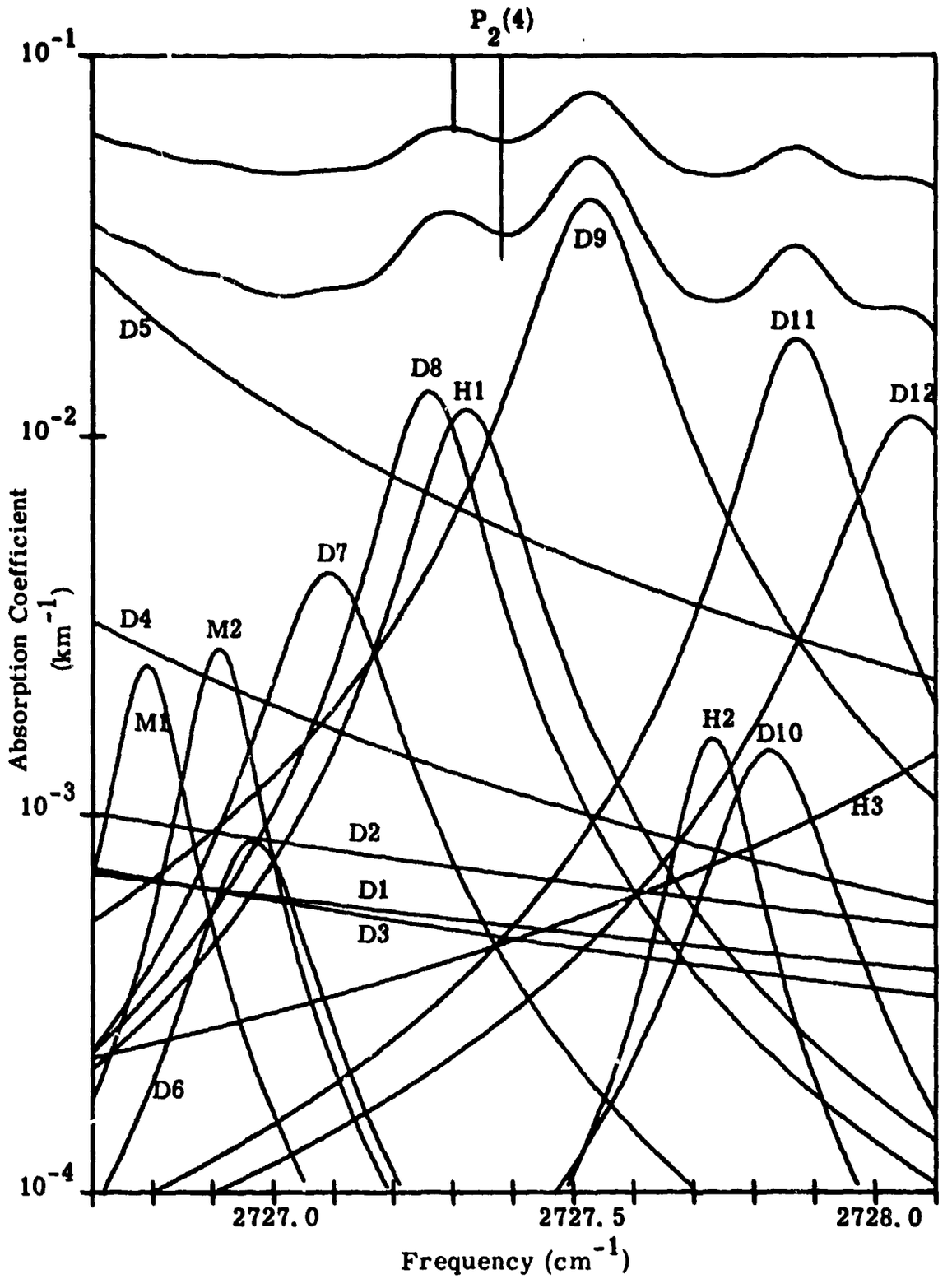

Figure 22. Contributors to the Molecular Absorption of the $P_2(4)$ DF Line (Midlatitude Summer, Sea Level).

TABLE 23. CONTRIBUTORS TO ATMOSPHERIC MOLECULAR ABSORPTION OF THE P1(7) DF LINE (MIDLATITUDE SUMMER, SEA LEVEL)

LINE NO.	FREQ	SPECTROSCOPIC IDENTIFICATION							STRENGTH	HALF WIDTH	ABSORPT COEF	% LINES	% TOTAL
		ROTATIONAL						VIBRATIONAL					
D1	2738.923	1	0	1	0	0	0	V1	3.94E-24	.103	3.631E-04	1.38	0.68
D2	2742.366	6	4	3	7	4	4	2V2	9.86E-26	.069	2.265E-04	0.86	0.42
D3	2742.530	7	2	5	7	3	4	2V2	1.86E-26	.087	9.369E-05	0.35	0.18
D4	2742.722	9	3	7	8	4	4	V1	1.23E-27	.075	0.0	0.0	0.0
D5	2742.882	2	1	1	2	0	2	V1	4.31E-25	.103	2.090E-02	79.19	39.18
D6	2742.914	9	2	7	10	0	10	V1	8.38E-28	.053	4.128E-05	0.16	0.08
D7	2743.234	9	2	8	8	3	5	V1	1.93E-27	.079	4.612E-05	0.17	0.09
D8	2743.576	4	3	1	5	3	2	2V2	3.00E-25	.082	1.194E-03	4.52	2.24
D9	2743.941	2	1	2	3	1	3	2V2	9.46E-25	.097	1.637E-03	6.20	3.07
D10	2744.147	4	3	2	5	3	3	2V2	3.02E-25	.079	2.825E-04	1.07	0.53
M1	2742.550	P6						V2+V4	1.71E-22	.055	5.199E-05	0.20	0.10
M2	2742.730	P6						V2+V4	1.78E-22	.055	1.364E-04	0.52	0.26

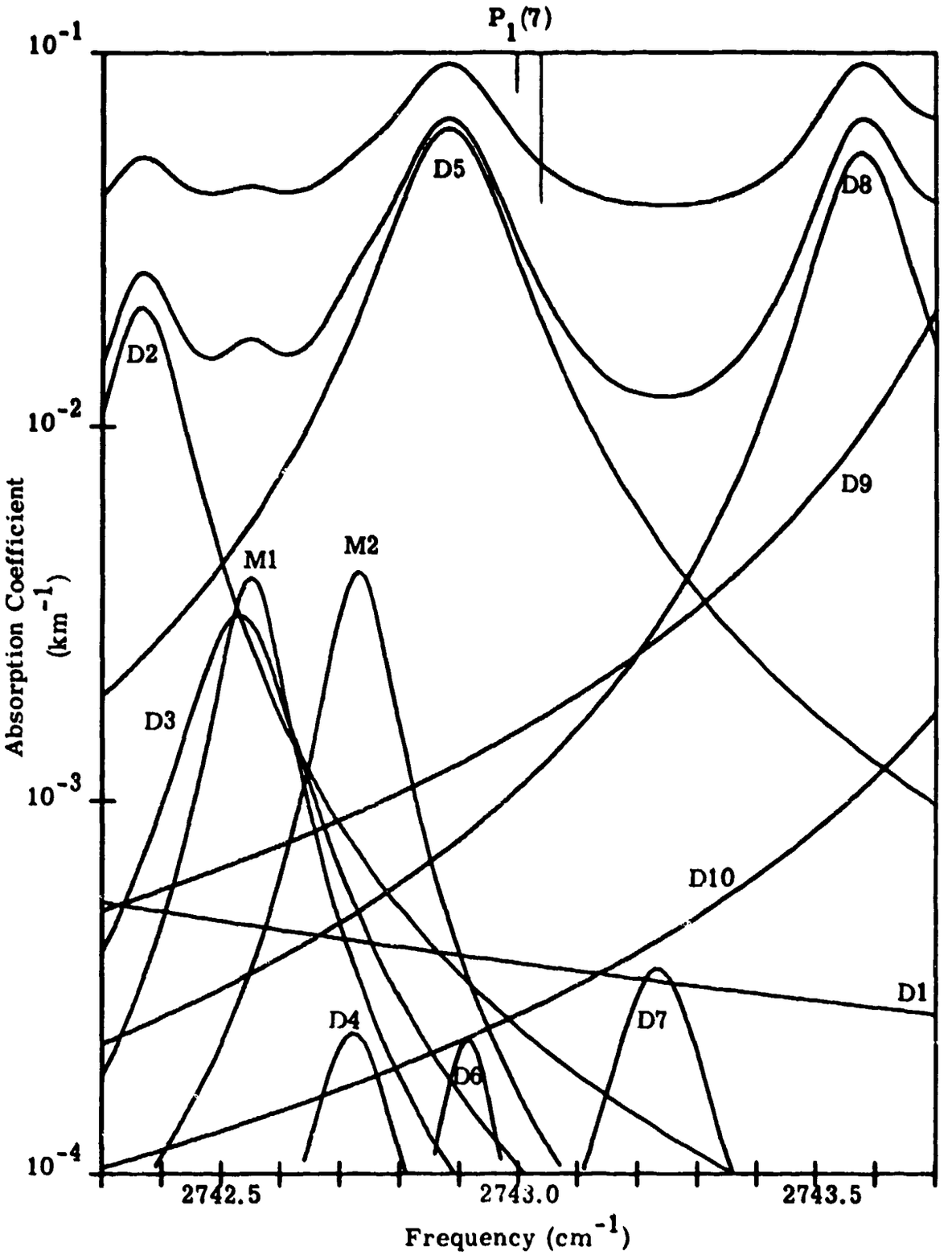

Figure 23. Contributors to the Molecular Absorption of the $P_1(7)$ DF Line (Midlatitude Summer, Sea Level).

TABLE 24. CONTRIBUTORS TO ATMOSPHERIC MOLECULAR ABSORPTION OF THE P2(3) DF LINE (MIDLATITUDE SUMMER, SEA LEVEL)

LINE NO.	FREQ	SPECTROSCOPIC IDENTIFICATION							STRENGTH	HALF WIDTH	ABSORPT COEF	% LINES	% TOTAL
		ROTATIONAL						VIBRATIONAL					
M1	2749.730	9	3	7	10	4	6	3V2-V2	4.00E-26	.072	3.626E-04	2.74	0.89
D1	2747.412	4	1	3	4	1	4	V1	8.54E-25	.092	1.693E-04	1.28	0.41
D2	2749.920	4	0	4	4	1	3	2V2	7.80E-26	.093	4.248E-03	32.09	10.39
D3	2750.503	4	1	3	4	2	2	2V2	7.17E-26	.092	4.623E-04	3.49	1.13
D4	2751.342	2	1	2	1	1	1	V1	5.13E-24	.098	4.513E-03	34.10	11.04
D5	2751.443	1	0	1	2	0	2	2V2	9.23E-25	.105	7.481E-04	5.65	1.83
D6	2753.545	2	0	2	1	0	1	V1	7.30E-24	.105	9.454E-04	7.14	2.31
D7	2756.558	2	1	1	1	1	0	V1	5.07E-24	.103	1.858E-04	1.40	0.45
M1	2749.490			P6				V2+V4	1.82E-22	.055	4.046E-05	0.31	0.10
M2	2750.160			P5				V2+V4	8.92E-23	.055	4.155E-04	3.14	1.02
M3	2750.430			P5				V2+V4	6.32E-23	.055	3.024E-05	0.23	0.07
M4	2750.620			P5				V2+V4	7.06E-23	.055	1.519E-05	0.11	0.04

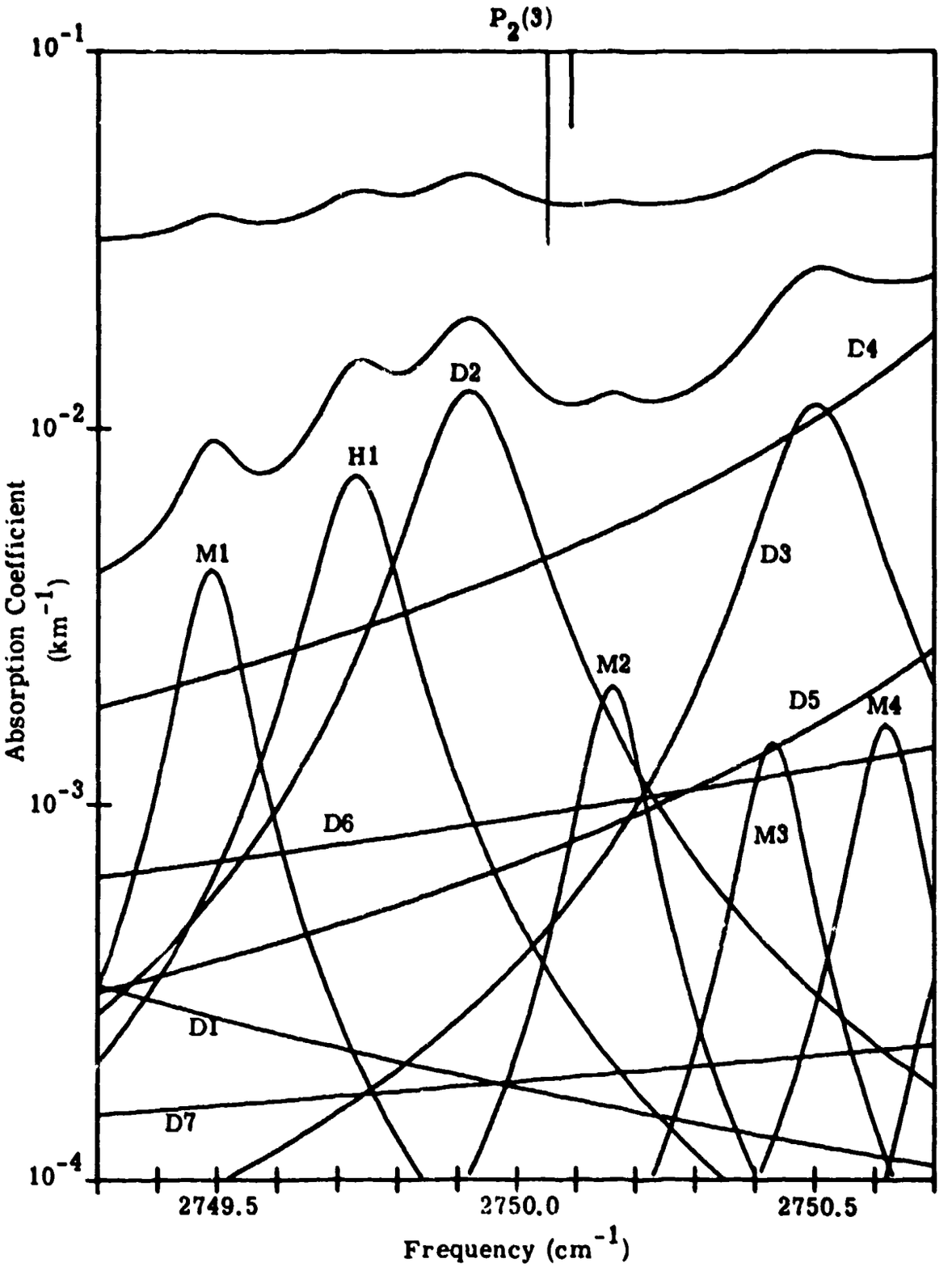

Figure 24. Contributors to the Molecular Absorption of the $P_2(3)$ DF Line (Midlatitude Summer, Sea Level).

TABLE 25. CONTRIBUTORS TO ATMOSPHERIC MOLECULAR ABSORPTION OF THE P1(6) DF LINE (MIDLATITUDE SUMMER, SEA LEVEL)

LINE NO.	FREQ	SPECTROSCOPIC IDENTIFICATION							STRENGTH	HALF WIDTH	ABSORPT COEF	% LINES	% TOTAL
		ROTATIONAL						VIBRATIONAL					
D1	2764.551	3	1	3	2	1	2	V1	7.97E-24	.097	1.028E-03	1.86	1.21
D2	2767.277	3	0	3	2	0	2	V1	9.41E-24	.100	3.409E-02	61.59	40.15
D3	2767.371	8	2	6	8	1	7	V1	8.80E-26	.075	3.249E-04	0.59	0.38
D4	2767.574	5	1	4	4	2	3	V1	5.88E-26	.091	6.467E-04	1.17	0.75
D5	2767.593	9	3	6	9	2	7	V1	4.80E-26	.082	5.266E-04	0.95	0.62
D6	2767.878	7	2	5	6	3	4	V1	1.12E-26	.085	1.650E-03	2.98	1.94
D7	2768.260	11	3	8	11	2	9	V1	1.08E-26	.065	8.227E-05	0.15	0.10
D8	2768.634	3	2	2	2	2	1	V1	3.90E-24	.091	1.013E-02	18.30	11.93
D9	2769.897	3	2	1	2	2	0	V1	3.90E-24	.090	1.339E-03	2.42	1.58
M1	2767.960	P4						V2+V4	2.12E-22	.055	2.902E-03	5.24	3.42
M2	2768.270	P4						V2+V4	2.16E-22	.055	1.176E-04	0.21	0.14
M3	2768.590	P4						V2+V4	6.69E-23	.055	0.0	0.0	0.0

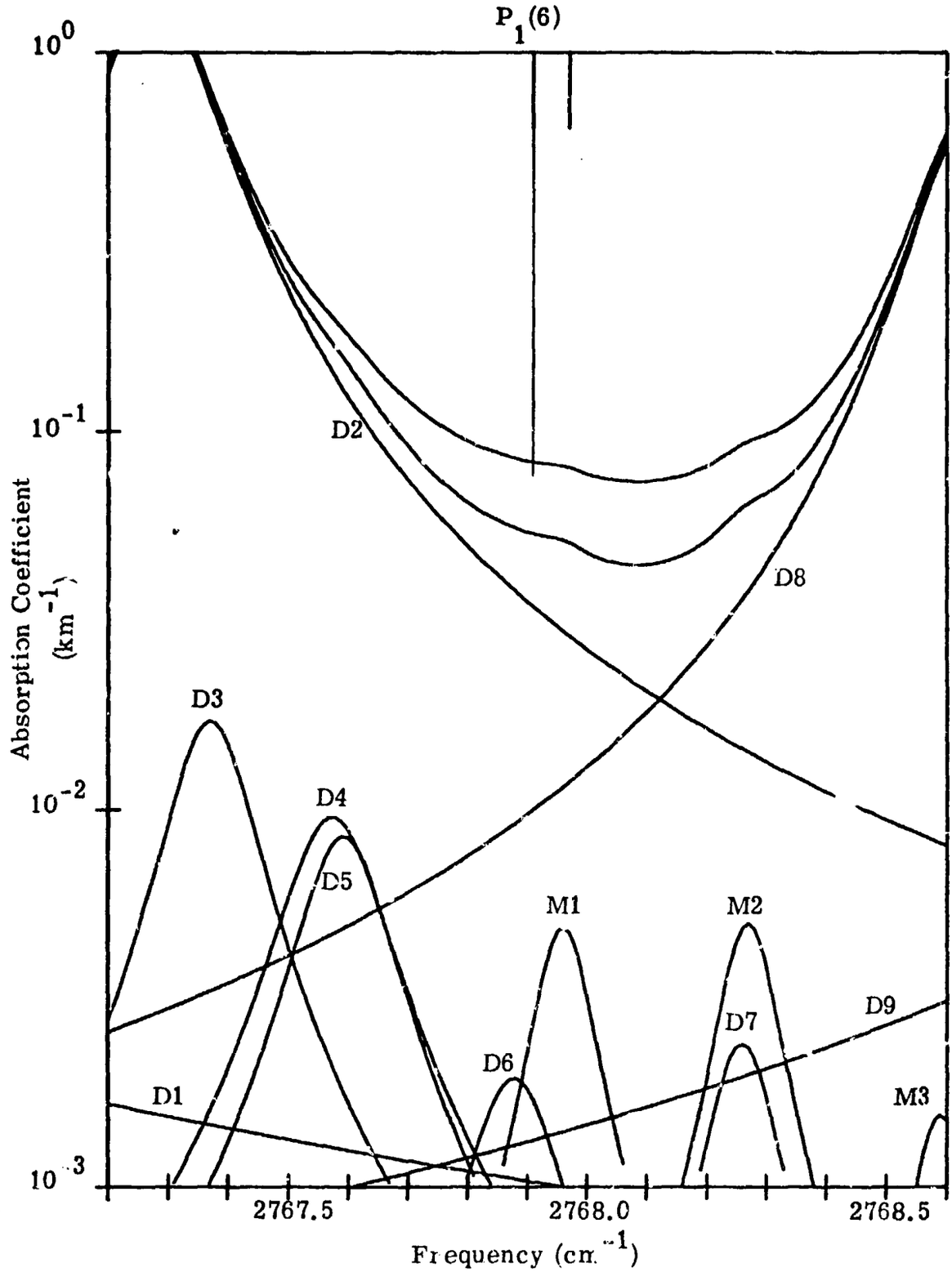

Figure 25. Contributors to the Molecular Absorption of the $P_1(6)$ DF Line (Midlatitude Summer, Sea Level).

TABLE 26. CONTRIBUTORS TO ATMOSPHERIC MOLECULAR ABSORPTION OF THE P1(5) DF LINE (MIDLATITUDE SUMMER, SEA LEVEL)

LINE NO.	FREQ	SPECTROSCOPIC IDENTIFICATION							STRENGTH	HALF WIDTH	ABSORPT COEF	% LINES	% TOTAL
		ROTATIONAL						VIBRATIONAL					
H1	2791.340	8	3	6	9	4	5	3V2-V2	5.47E-25	.076	4.697E-04	1.32	0.69
H2	2791.366	5	1	5	6	2	4	3V2-V2	1.14E-24	.086	1.191E-03	3.35	1.76
D1	2789.593	5	1	5	4	1	4	V1	8.95E-24	.087	1.444E-03	4.07	2.13
D2	2791.390	5	2	4	5	0	5	V1	2.52E-25	.084	2.874E-04	0.81	0.42
D3	2791.759	5	0	5	4	0	4	V1	9.42E-24	.088	2.662E-02	74.99	39.24
D4	2792.595	2	2	1	3	1	2	2V2	8.63E-27	.094	3.601E-04	1.01	0.53
D5	2792.708	10	4	6	10	3	7	V1	1.60E-26	.086	2.481E-04	0.70	0.37
M1	2791.750	P3						V2+V4	1.45E-22	.055	0.0	0.0	0.0
M2	2792.140	P3						V2+V4	2.60E-22	.055	2.016E-04	0.57	0.30
M3	2792.580	P3						V2+V4	1.12E-22	.055	3.373E-04	0.95	0.50

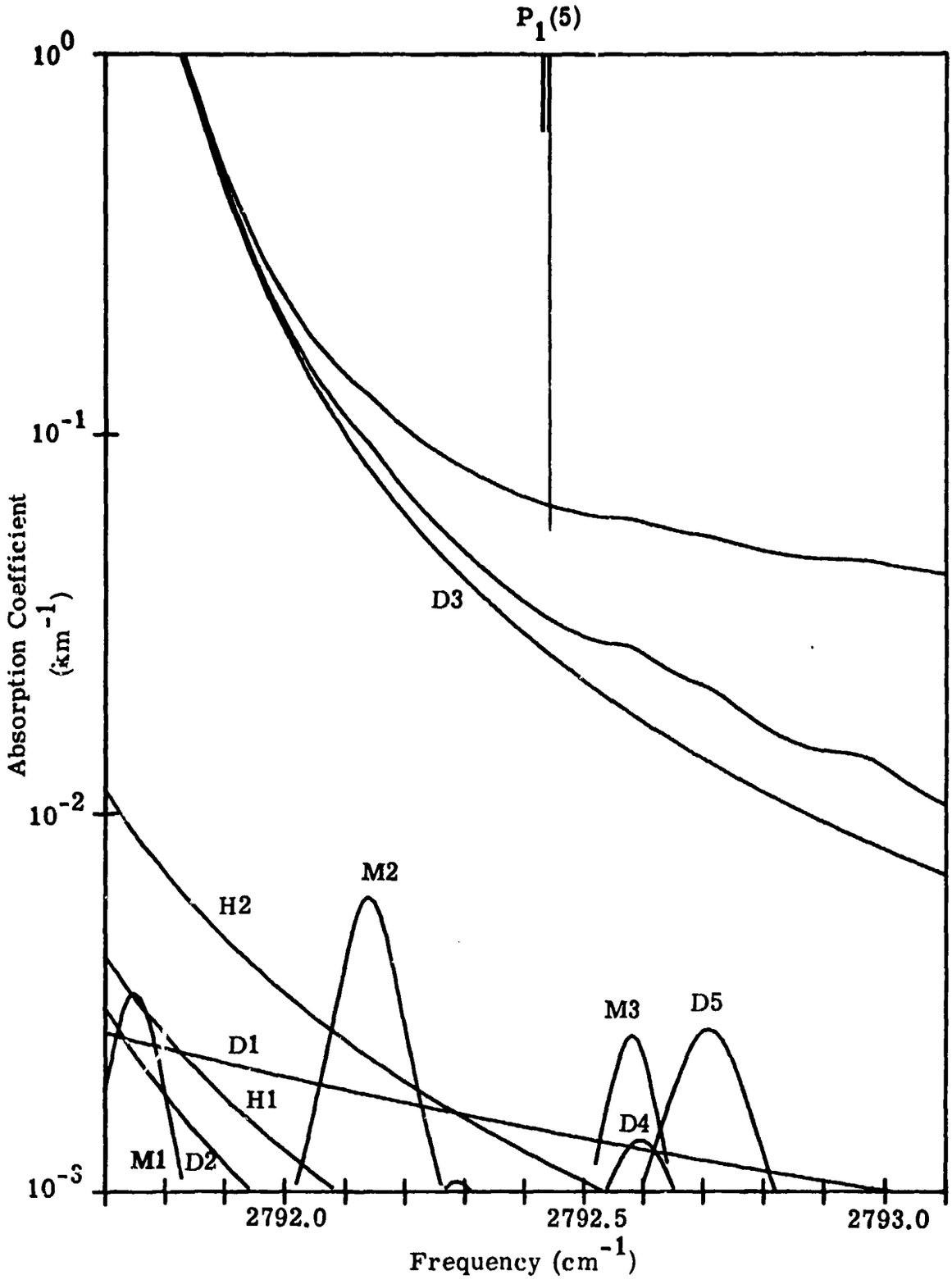

Figure 26. Contributors to the Molecular Absorption of the $P_1(5)$ DF Line (Midlatitude Summer, Sea Level).

TABLE 27. CONTRIBUTORS TO ATMOSPHERIC MOLECULAR ABSORPTION OF THE P1(4) DF LINE (MIDLATITUDE SUMMER, SEA LEVEL)

LINE NO.	FREQ	SPECTROSCOPIC IDENTIFICATION							STRENGTH	HALF WIDTH	ABSORPT COEF	% LINES	% TOTAL
		ROTATIONAL						VIBRATIONAL					
H1	2815.801	11	1	10	11	4	7	2V2	5.55E-27	.057	0.0	0.0	0.0
H2	2816.559	8	2	7	8	5	4	2V2	3.25E-26	.058	6.466E-04	1.02	0.65
D1	2813.829	7	0	7	6	0	6	V1	6.23E-24	.064	9.276E-04	1.46	0.94
D2	2814.993	6	1	5	5	1	4	V1	6.40E-24	.087	4.425E-03	6.99	4.50
D3	2815.712	3	0	3	2	1	2	2V2	7.32E-26	.098	2.500E-04	0.39	0.25
D4	2815.957	4	1	3	4	1	4	2V2	1.28E-25	.092	1.024E-03	1.62	1.04
D5	2816.219	1	1	1	0	0	0	2V2	6.60E-26	.100	3.263E-03	5.15	3.32
D6	2816.324	8	3	6	8	1	7	V1	5.74E-26	.066	9.613E-03	15.18	9.78
D7	2816.378	9	3	7	9	1	8	V1	4.04E-26	.057	9.614E-03	15.18	9.78
D8	2816.437	7	4	3	7	3	4	V1	7.45E-26	.087	7.242E-03	11.43	7.37
D9	2816.757	2	2	0	1	0	1	V1	3.99E-26	.098	3.559E-04	0.56	0.36
D10	2816.950	4	1	3	3	2	2	2V2	1.85E-26	.094	7.360E-05	0.12	0.07
D11	2816.989	6	2	4	5	2	3	V1	4.95E-24	.091	1.676E-02	26.46	17.05
N1	2815.768	R22						V2+V3	7.08E-22	.079	0.0	0.0	0.0
N2	2816.449	R23						V2+V3	6.71E-22	.079	8.557E-04	1.35	0.87
M1	2815.740	P1						V2+V4	1.78E-22	.055	0.0	0.0	0.0
M2	2816.320	P1						V2+V4	2.45E-22	.055	3.611E-03	5.70	3.67
M3	2816.700	P1						V2+V4	2.53E-22	.055	1.529E-04	0.24	0.15

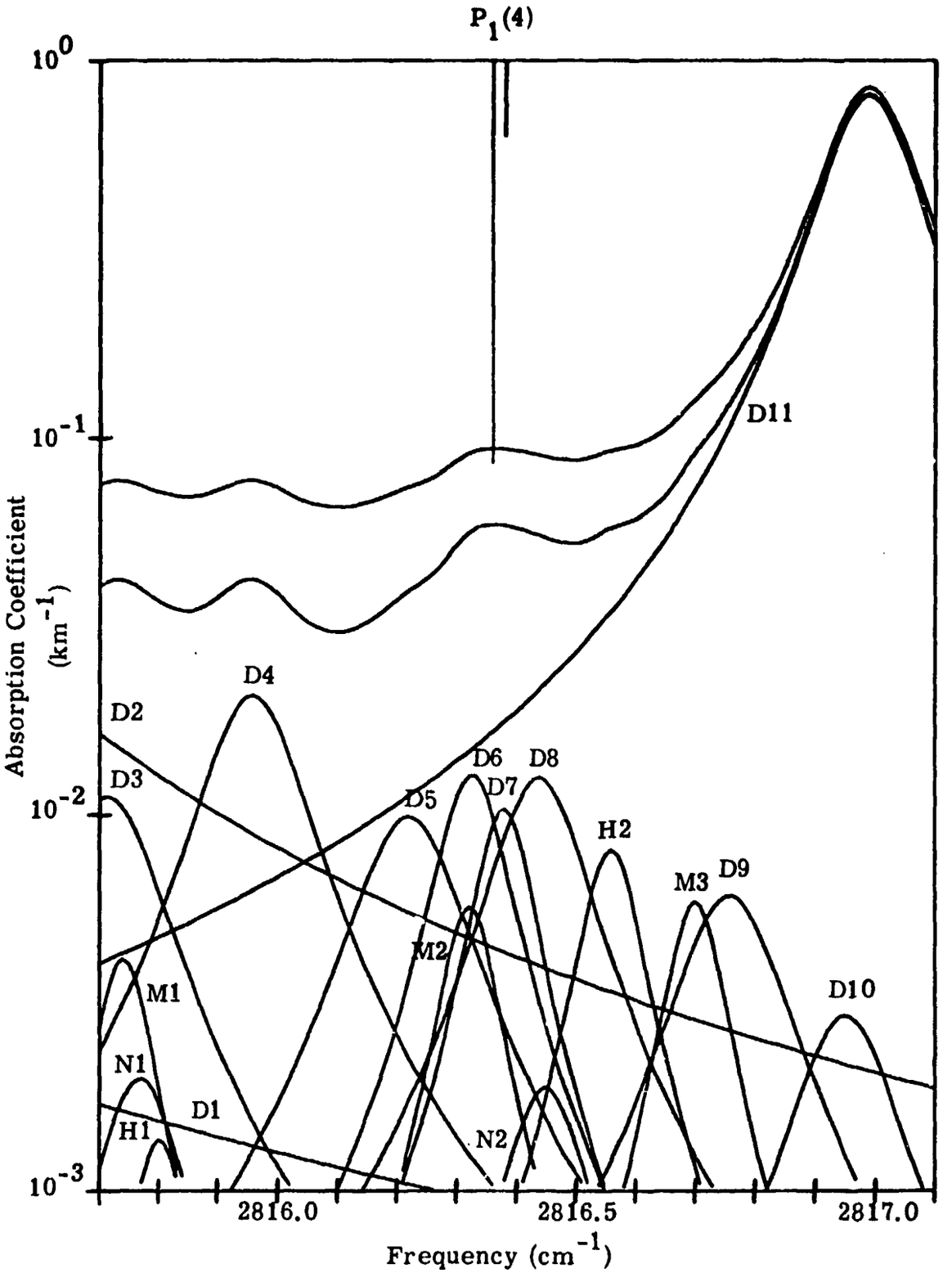

Figure 27. Contributors to the Molecular Absorption of the $P_1(4)$ DF Line (Midlatitude Summer, Sea Level).

TABLE 28. CONTRIBUTORS TO ATMOSPHERIC MOLECULAR ABSORPTION OF THE P1(3) DF LINE (MIDLATITUDE SUMMER, SEA LEVEL)

LINE NO.	FREQ	SPECTROSCOPIC IDENTIFICATION							STRENGTH	HALF WIDTH	ABSORPT COEF	% LINES	% TOTAL
		ROTATIONAL						VIBRATIONAL					
H1	2839.800	8	4	4	9	5	5	3V2-V2	1.76E-25	.070	2.895E-02	50.29	30.51
D1	2837.984	8	3	6	7	3	5	V1	1.70E-24	.072	6.124E-04	1.06	0.65
D2	2838.483	8	1	7	7	1	6	V1	3.11E-24	.066	1.975E-03	3.43	2.08
D3	2838.504	3	1	2	2	1	1	2V2	1.16E-24	.097	1.129E-03	1.96	1.19
D4	2839.772	11	2	10	11	1	11	V1	8.24E-27	.057	2.881E-03	5.00	3.04
D5	2839.786	4	2	2	4	1	3	2V2	9.22E-26	.094	1.333E-02	23.15	14.04
D6	2839.867	11	2	10	11	0	11	V1	1.63E-26	.035	9.891E-04	1.72	1.04
D7	2840.038	9	5	4	9	4	5	V1	1.72E-26	.078	2.878E-04	0.50	0.30
D8	2840.110	3	1	3	2	0	2	2V2	1.16E-25	.102	1.594E-03	2.77	1.68
D9	2840.407	11	4	8	11	2	9	V1	4.56E-27	.054	0.0	0.0	0.0
D10	2840.432	5	2	3	5	1	4	2V2	8.34E-26	.094	2.928E-04	0.51	0.31
D11	2841.449	4	1	4	3	1	3	2V2	1.38E-24	.094	7.603E-04	1.32	0.80
D12	2841.574	4	0	4	3	0	3	2V2	1.51E-24	.095	7.283E-04	1.27	0.77
M1	2839.910	P17						V3	1.12E-22	.055	3.729E-04	0.65	0.39
M2	2840.000	P17						V3	1.12E-22	.055	1.452E-04	0.25	0.15
M3	2840.330	P17						V3	1.12E-22	.055	0.0	0.0	0.0
M4	2840.360	P17						V3	1.12E-22	.055	0.0	0.0	0.0

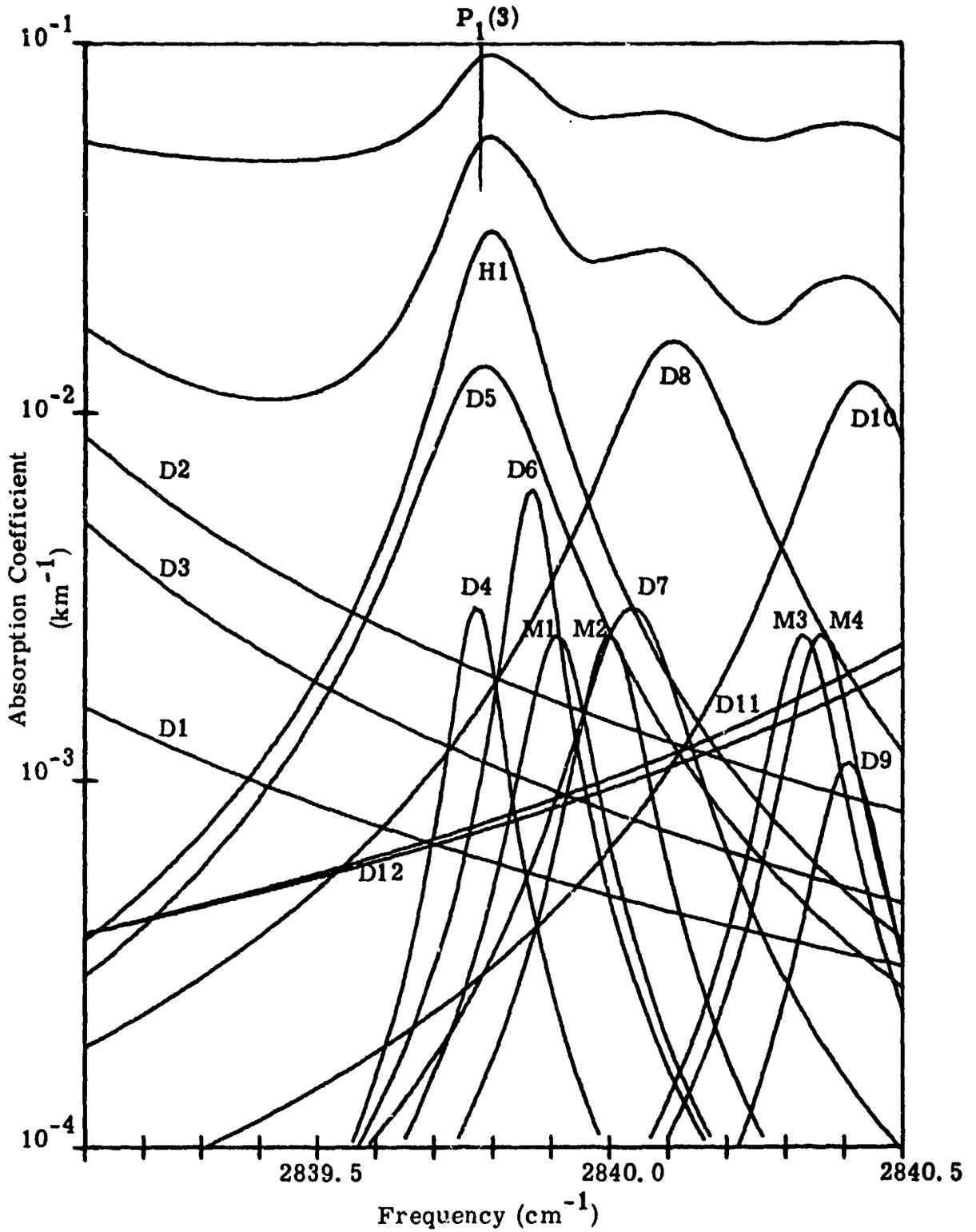

Figure 28. Contributors to the Molecular Absorption of the $P_1(3)$ DF Line (Midlatitude Summer, Sea Level).

The input parameters and line computation procedures were purposely chosen for direct comparison with calculations performed at other laboratories. The most significant difference between the curves presented here and the calculations of McClatchey, et. al. [6, 7], is in the H_2O continuum. Long first pointed out that the original AFCRL calculations should be corrected for the continuum, and he included the contribution in his tables [16]. We include it in our curves since it is important at the temperature and humidity chosen for our calculations. The good agreement between our calculations and Long's can best be seen by comparing the total of the line and continuum contributions in our curves with Tables III and VI of Long. In an erratum to Reference 7, the authors point out that extinction caused by scattering is competitive with or even greater than molecular absorption except for very humid conditions. We have purposely restricted the present investigation to molecular absorption. This is a natural division since molecular extinction and energy transfer mechanisms differ in principle from those of aerosols. Very importantly for the high energy laser (HEL) application considered here, molecular absorption is the starting point for thermal blooming, a phenomenon which contributes non-linearly to beam degradation. The absorption portion of the extinction caused by aserosols can be expected to contribute to the blooming by a somewhat different mechanism and thus should be treated independent of either molecular absorption or scattering. Scattering contributes to energy loss linearly; consequently, it cannot be treated equivalent to absorption, for HEL applications. We also include the continuum absorption along with the line absorption to maintain internal consistency. Our curves show that at the given conditions, for eighteen out of twenty-seven DF lines, the H_2O continuum contributes more than any single line contributor, and it is the second most important contributor for all other lines. In most cases, no contributor is dominant, but in all cases, the H_2O continuum is significant. (At higher altitudes or dryer conditions, of course, the uniformly mixed gases become much more important.)

Presentation of the Results

All calculations are presented on logarithmic plots of $k(\nu)$ versus wavenumber at each of 27 DF laser wavelengths. Each line is identified by a letter and a numeral. The code is as follows:

Letter	Specie
H	H_2O
D	HDO
M	CH_4
N	N_2O
C	CO_2

In addition, an asterisk next to an N indicates an isotope of N_2O. Individual specie lines are identified in order of increasing value of line center position, by numerals 1, 2, 3, ..., etc. For example, M3 identifies the methane contributor which has the third lowest wavenumber location. The numeral designations begin from 1 for each DF laser line. The laser line location used by McClatchey is designated by a vertical line near the center of the figure. Recent calculations by Yin [16] indicate some significant discrepancies with the values used by McClatchey. For completeness, both laser positions are indicated, with the values due to Yin designated by the shorter line.

Considerable information is contained in the descriptive table which accompanies each plot of $k(\nu)$. Each column of the tables will now be described in turn.

Column 1, Line No. Line identity as described above.

Column 2, FREQ. Wavenumber position of the absorbing line, as taken from the AFCRL compilation.

Column 3, SPECTROSCOPIC IDENTIFICATION. Rotation and vibration transition identification of the absorbing line. For each molecule, the description is as follows:

HDO, H_2O	ROTATIONAL	VIBRATIONAL
	$J^u\ K_a^u\ K_c^u\ \ J^l\ K_a^l\ K_c^l$	V mode designation

J and K are the usual water vapor rotational quantum numbers. u and ℓ refer to upper and lower levels involved in the transition. The vibrational mode designations refer to the fundamental, overtone, combination or "hot" band responsible for the vibrational mode change. Since there are three fundamental vibrations, ν_1, ν_2, ν_3, typical designations are:

V Mode Designation	$(V_1^u$	V_2^u	$V_3^u \leftarrow V_1^\ell$	V_2^ℓ	$V_3^\ell)$	
V1	1	0	0 ← 0	0	0	
2V2	0	2	0 ← 0	0	0	
V2	0	1	0 ← 0	0	0	
3V2-V2	0	3	0 ← 0	1	0	(hot)

N_2O ROTATIONAL VIBRATIONAL

P, Q, or R V mode designation

The standard notation P, Q, R is used for rotational transitions $\Delta J = -1, 0, 1$, respectively. As is the case for HDO and H_2O, three vibrational frequencies exist for N_2O. The contributing modes for N_2O are as follows:

V Mode Designation	V_1^u	V_2^u	$V_3^u \leftarrow V_1^\ell$	V_2^ℓ	V_3^ℓ
V1+2V2	1	2	0 ← 0	0	0
V1+3V2-V2	1	3	0 ← 0	1	0
V1+4V2-2V2	1	4	0 ← 0	2	0
2V1	2	0	0 ← 0	0	0
2V1+2V2-2V2	2	2	0 ← 0	2	0
3V1-V1	3	0	0 ← 1	0	0
V2+V3	0	1	1 ← 0	0	0
2V1+V2-V2	2	1	0 ← 0	1	0

CH_4 ROTATIONAL VIBRATIONAL

P, Q, or R V Mode Designation

Because of methane's spherical symmetry, higher order splitting may occur for each P, Q, or R line. Values listed in the AFCRL compilation are included here, but the precise identification of each component within a ΔJ transition is not included. Splittings and other parameters listed in the compliation were derived from older work, and are highly suspect since the theory is complicated and the data base is inadequate. It is felt that a precise distinction between the lines for a given ΔJ should be made when more reliable parameters become available.

Vibrational mode designations are also presented in the simplified form, for the reasons mentioned above, and because the present application does not require use of the ℓ quantum numbers. The relationship of the present mode description to that of the AFCRL tabulation is as follows,

V Mode Designation	V_1^u	V_2^u	V_3^u	$V_4^u \leftarrow V_1^l$	V_2^l	V_3^l	V_4^l
2V4	0	0	0	2 ← 0	0	0	0
V2+V4	0	1	0	1 ← 0	0	0	0
V3	0	0	1	0 ← 0	0	0	0

Column 4, STRENGTH. Strength values are presented in the basic unit cm/molecule. All tabulated values are for the conditions of the midlatitude summer model, which is defined as follows

$P = 1$ atm

$T = 294^{\circ}K$

Water vapor pressure = 14.26 torr (Humidity = 77%)

Strength values of each molecule are weighted by natural isotopic abundances, but not by mixing ratios. A HDO line strength, for example, is diminished by the accepted atmospheric abundance factor of 0.0003. An estimate of laboratory absorption would require an adjustment of the listed S value to account for the amount of enhancement over natural abundance. The natural mixing ratios used here are listed as follows [5]:

Constituent	ppm by volume
CO_2	330
N_2O	0.28
CH_4	1.6

Column 6, ABSORPT COEF. Calculated absorption coefficient at the DF wavelength are tabulated in units km^{-1}.

Column 7, % LINES. Percent contribution of each line to the total line absorption coefficient.

Column 8, % TOTAL. Percent contribution of each line to the total (line + continuum) absorption coefficient.

A summary of the absorption coefficients is presented in Table 28a. Only the N_2 continuum contribution is not listed explicitly. This value can be obtained by subtracting line total and H_2O continuum from the total given in the last column.

In concluding the discussion of the present calculations, attention is drawn to the fact that the absorption coefficient profile of each line contributor has been displayed, rather than just the total absorptance or absorption coefficient. The additional effort required for this was deemed necessary to designate the precise contributor and absorption phenomena which dominate the absorption. With this display also, the overall impact of errors in assumed S, γ, $\delta\nu$, wing or continuum can be more readily assessed. For example, certain DF lines can easily be seen to be insensitive to possible errors in S, γ, or $\delta\nu$, whereas others are very sensitive to these parameters.

Table 28a. Atmospheric Molecular Absorption of DF Laser Lines Due to Various Species (Midlatitude Summer, Sea Level)

DF Line	Freq.	Absorption Coefficient x 10^3 (km^{-1}) H_2O	HDO	N_2O	CH_4	Line Total	H_2O Cont.	Total[1]
$P_3(12)$	2445.29	.0221	.0042	1.668	--	4.076[2]	28.78	98.72
$P_3(11)$	2471.34	5.719	.9183	3.025	--	9.692[3]	25.45	78.83
$P_3(10)$	2498.61	4.258	.0443	.2727	.0133	4.588	22.71	53.15
$P_2(13)$	2500.32	.1142	.0898	.2869	.0028	.4936	22.34	46.60
$P_3(9)$	2521.81	.0436	.1740	.4480	.0027	.6684	20.09	35.42
$P_2(12)$	2527.47	.0066	.1841	.9574	.0187	1.167	19.59	33.70
$P_3(8)$	2546.37	.0425	1.061	22.78	1.021	24.90	18.20	51.38
$P_2(11)$	2553.97	.0089	.4645	9.663	.0776	10.21	17.77	35.06
$P_3(7)$	2570.51	.0656	4.391	33.72	.0317	38.21	17.06	60.42
$P_2(10)$	2580.16	.0085	2.523	23.20	.0025	25.73	16.80	46.79
$P_3(6)$	2594.23	.4684	6.420	2.029	.0177	8.935	16.63	28.83
$P_2(9)$	2605.87	.0105	21.53	.3572	.0726	21.97	16.90	41.52
$P_3(5)$	2617.41	.0481	2.443	.0108	.1030	2.605	17.46	22.20
$P_2(8)$	2631.09	3.233	8.749	--	.8683	12.85	18.20	32.72
$P_2(7)$	2655.97	.0100	42.14	--	2.577	44.73	19.73	64.46
$P_1(10)$	2665.20	.0348	13.95	--	2.201	16.19	20.36	36.55
$P_2(6)$	2680.28	.2990	48.44	--	.4865	49.23	21.46	70.69
$P_1(9)$	2691.409	6.131	11.52	--	.3021	17.96	22.32	40.28
$P_2(5)$	2703.98	.0285	4.843	--	.0018	4.874	23.36	28.23
$P_1(8)$	2717.536	.1175	82.69	--	.0021	82.81	24.54	107.35
$P_2(4)$	2727.38	8.754	28.91	--	.1117	37.78	25.44	63.22
$P_1(7)$	2743.028	.0539	26.08	.0039	.2489	26.39	26.95	53.34
$P_2(3)$	2750.05	.4094	12.28	.0310	.5156	13.24	27.66	40.90
$P_1(6)$	2767.914	.0205	51.99	.0932	3.042	55.35	29.55	84.90
$P_1(5)$	2792.437	1.855	32.19	.7993	.6274	35.50	32.35	67.85
$P_1(4)$	2816.362	1.992	56.57	.9431	3.842	63.34	34.93	98.27
$P_1(3)$	2839.779	29.97	26.89	--	.7161	57.57	37.32	94.89

1. Includes N_2 continuum.
2. Includes CO_2 absorption coefficient of 2.382×10^{-3} km^{-1}.
3. Includes CO_2 absorption coefficient of 3.109×10^{-5} km^{-1}.

Attention is also called to the fact that the entries in the "% lines" column does not add up to 100%. The difference between 100% and the total in this column is the percent contribution of lines within the twenty cm^{-1} cutoff distance that contribute, but which individually are too weak to be included in the curves. The larger this number, and the more it arises from absorption lines centered near the 20 cm^{-1} limit, the greater is the chance that near wing non-Lorentz shape effects may occur. We have not investigated the extent to which this may be the case.

5. CH_4 ABSORPTION COEFFICIENTS FOR LABORATORY CONDITIONS

For very dry conditions, and for applications at high altitudes greater than 5 km, CH_4 is expected to be a major contributor to molecular absorption of DF laser radiation. For relatively humid sea level applications, current AFCRL line parameter values indicate that CH_4 should contribute very little to the line absorption at DF frequencies. However, current methane line parameters (splittings, strengths and widths) are suspect since the data on which they are based is old, and because low order approximations to the strength and splitting theory were used. The dominant CH_4 band in the more transparent DF region is the $\nu_2 + \nu_4$ combination. The strengths of the $2\nu_4$ band which contributes in the low frequency region has recently been updated by Fox [17]. The new values have not been used in the present calculations since the $2\nu_4$ contribution is very small. Also, an average value of 0.055 cm^{-1} was used for the Lorentz half width in this region. Therefore, it is not unreasonable to expect that CH_4 absorption coefficients may well be factors of 2-10 in error. Recent airborne measurements of stratospheric CH_4 indicate that the strengths of these lines may be greatly underestimated [18]. Consequently, current predicted values of only several percent contribution of methane may in reality be considerably larger.

To assist laboratory measurements of DF laser absorption by CH_4, calculation of methane absorption coefficients for optimum laboratory conditions have been performed. For optimum measurements, CH_4-air mixtures must be enriched with CH_4 well above the levels which occur naturally. This can be done with confidence since, as discussed in Section 2, the self broadening enters the line absorption linearly through the Lorentz half width. Thus, for a 1.6 ppm naturally occurring CH_4 abundance, N_2 or O_2 broadening is orders of magnitude more dominant than CH_4 self broadening. Recent CH_4 self broadening investigations indicate that self and air broadening of CH_4 are comparable. Consequently, even an enrichment to 10 parts air to 1 part CH_4 will only result in an expected contribution to $k(\nu)$ of order 10%.

Twenty-one DF lines have been selected for investigation. The selection is based on importance of the DF line, and the significant occurrence of CH_4 absorption for each. A path of 1 km is assumed, and air/CH_4 ratios have been chosen arbitrarily to predict absorption in the range 10% to 50%. Laboratory temperature was assumed to be heated to 303°K, since a slightly elevated temperature may be maintained accurately. Four sets of mixtures were chosen for absorption predictions in the desired range. The volume mixing ratios for the four sets of conditions are given in Table 29. The results are shown in Figures 29 through 49. Lines are identified as in the previous section. Because of the large enrichment of CH_4, a number of lines occur which did not contribute earlier.

Table 29. Values Used in Methane Calculations

$P = 1$ atm (only N_2 and CH_4)

$T = 303^{o}K$

N_2 to CH_4 Ratio (Volume Basis)	Figures
5000	29-32
860	33-40
95	41-44
25	45-49

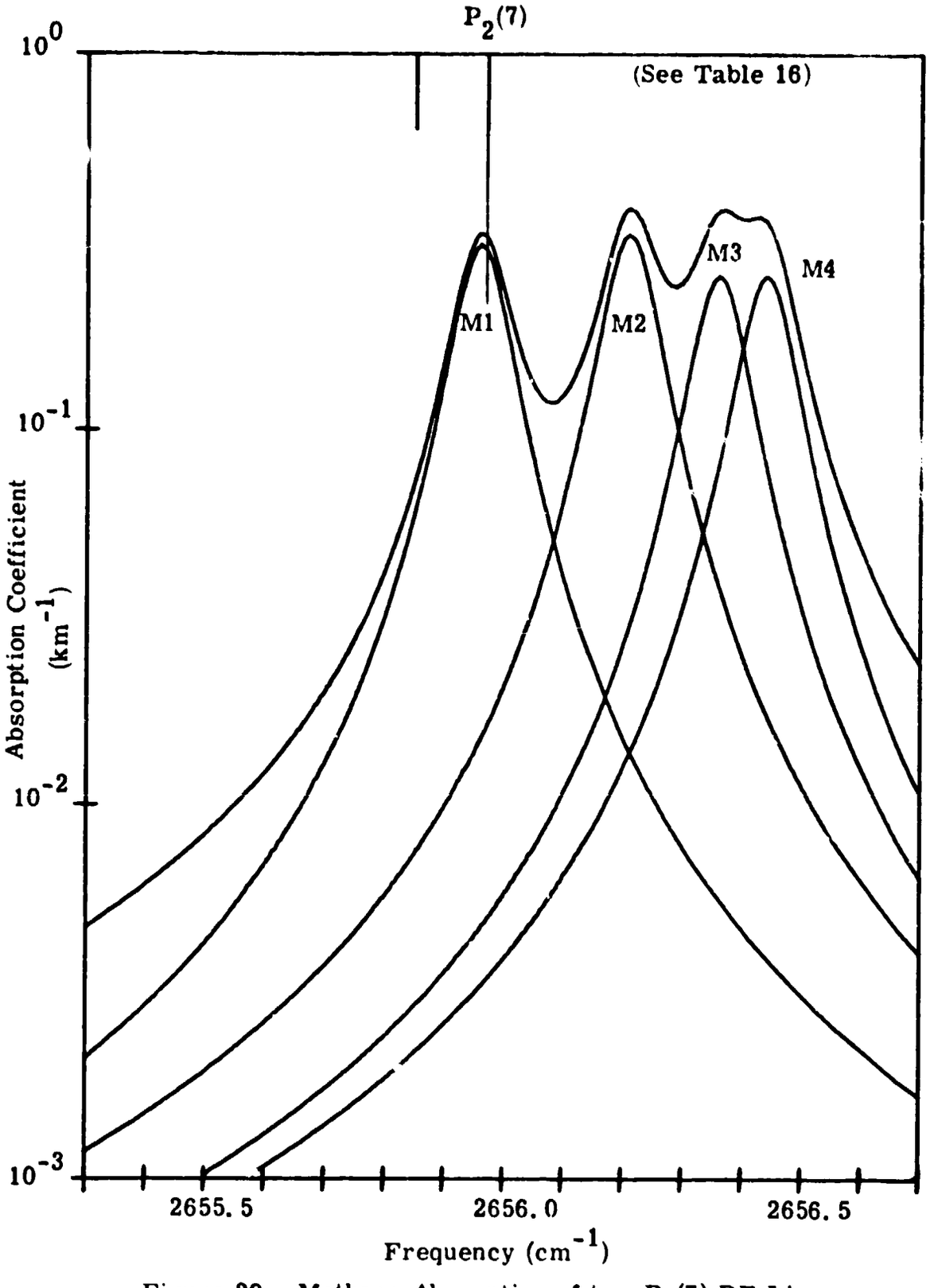

Figure 29. Methane Absorption of the $P_2(7)$ DF Line.

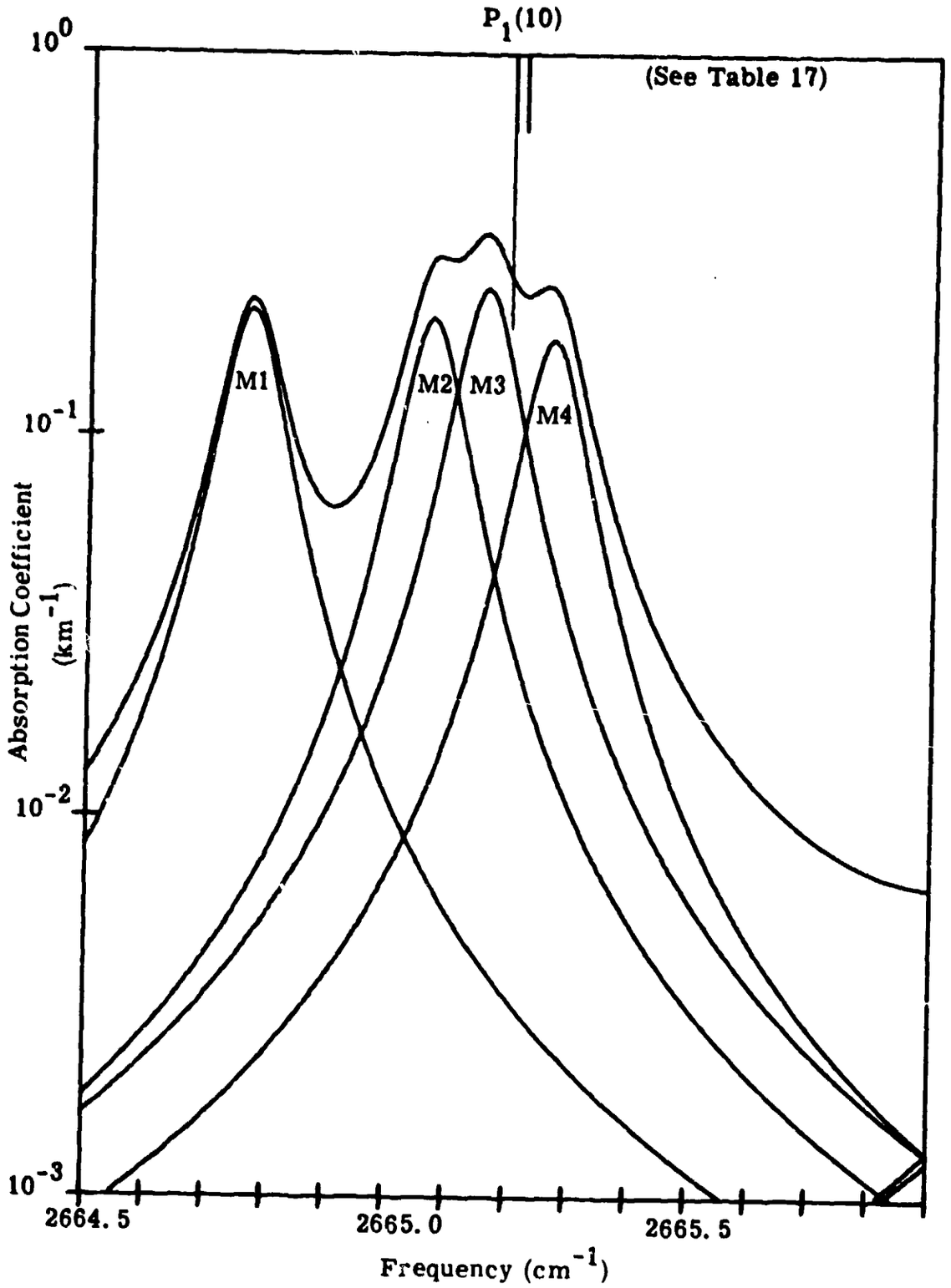

Figure 30. Methane Absorption of the $P_1(10)$ DF Line.

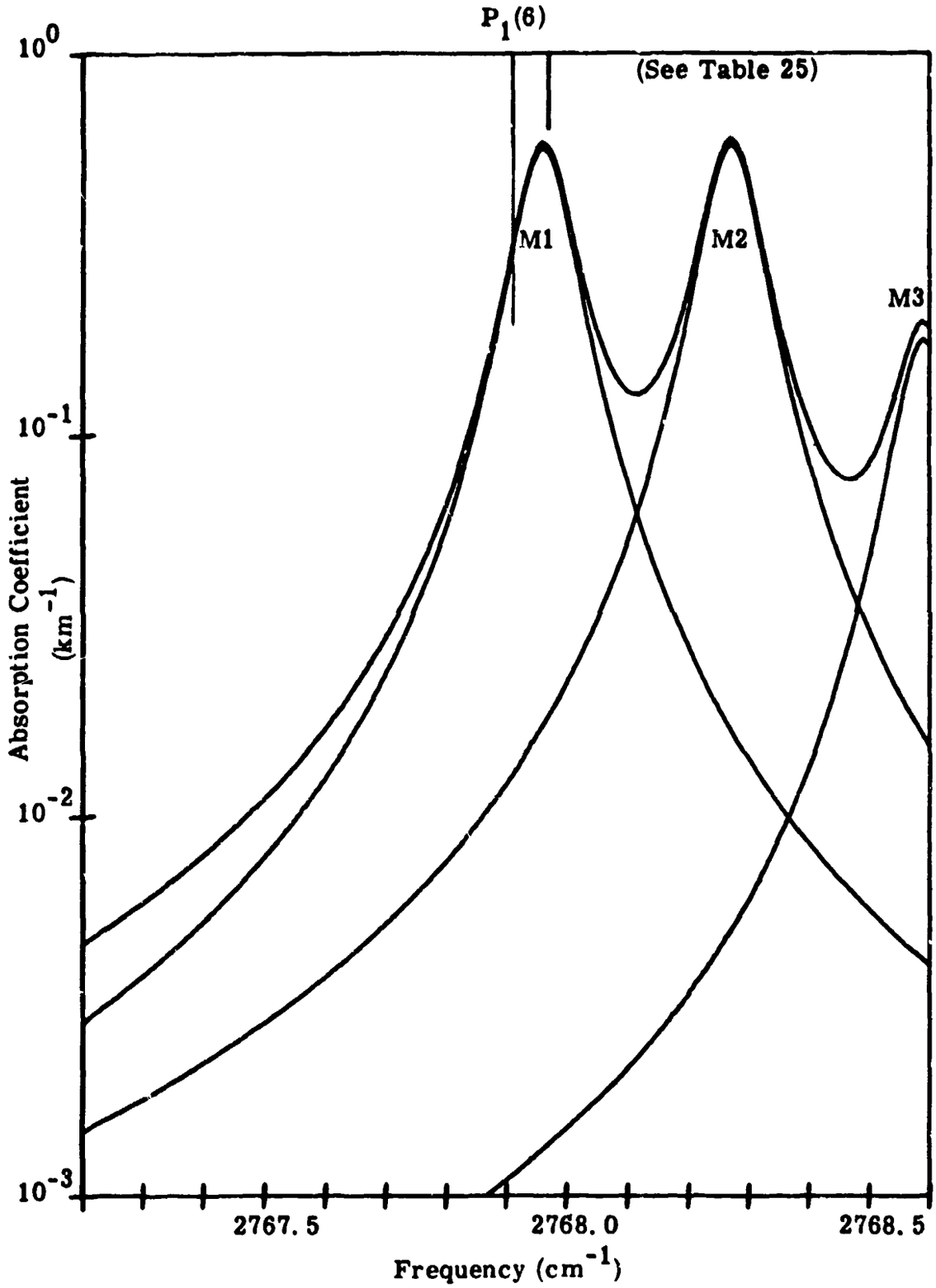

Figure 31. Methane Absorption of the $P_1(6)$ DF Line.

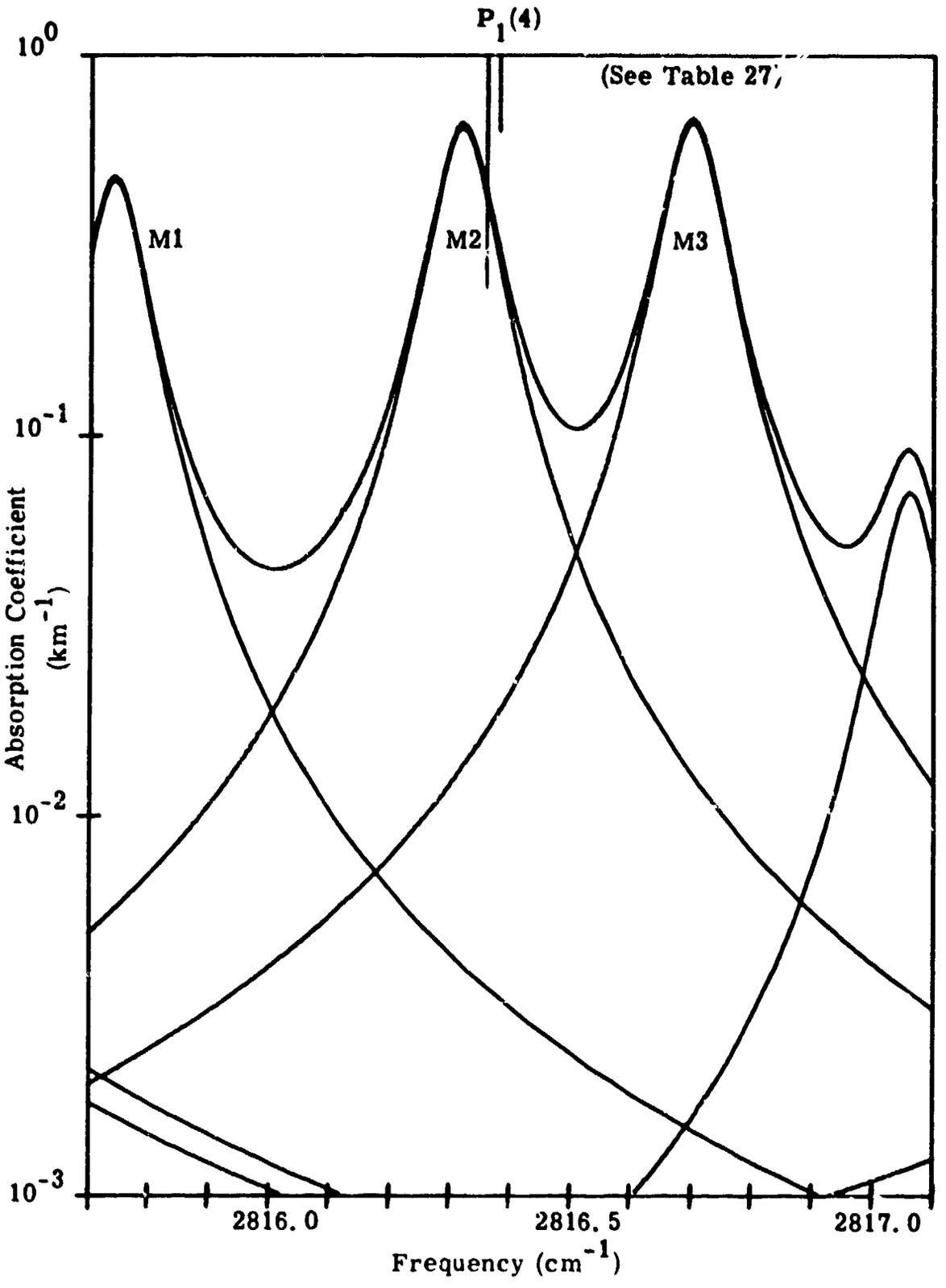

Figure 32. Methane Absorption of the $P_1(4)$ DF Line.

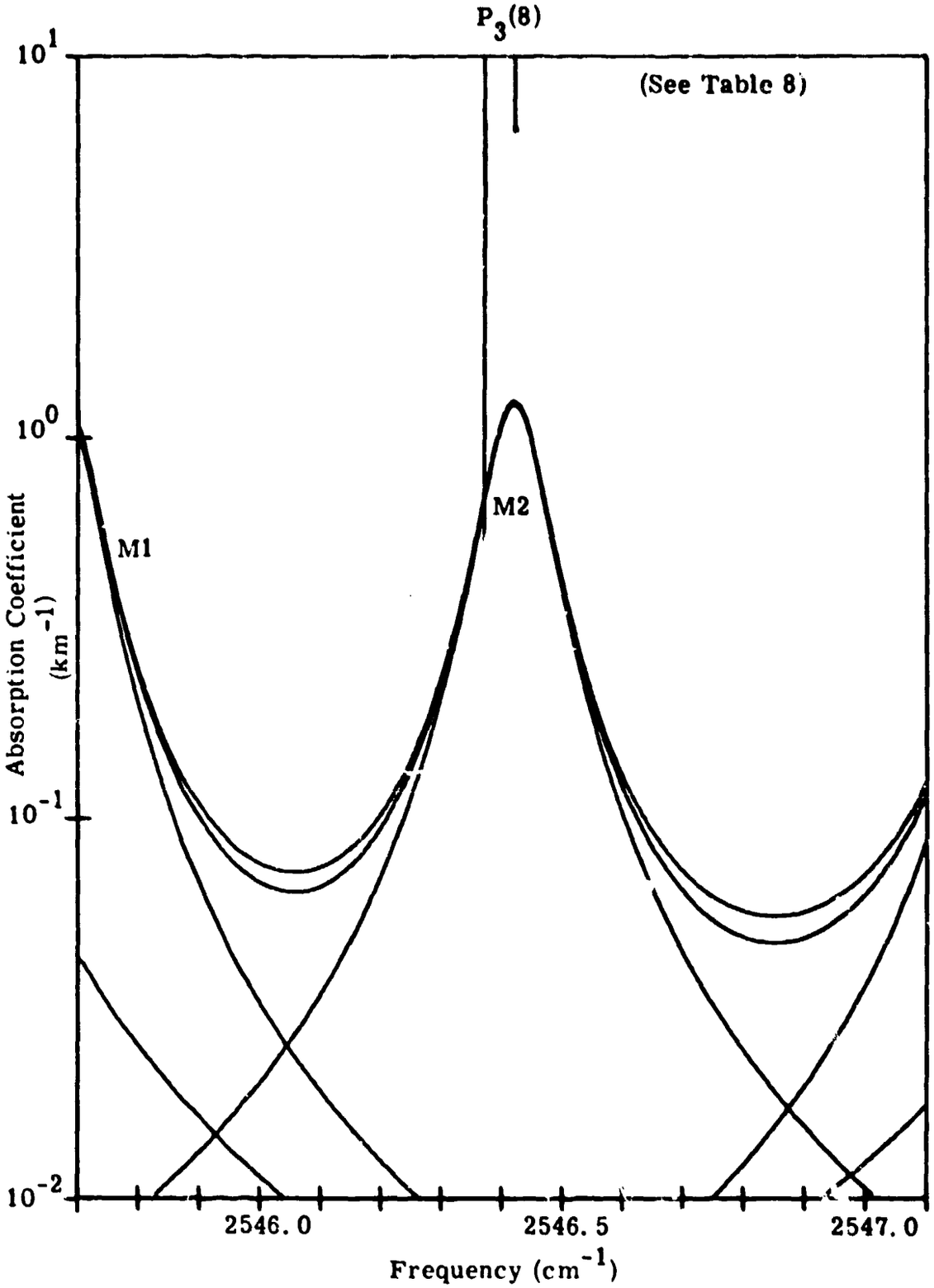

Figure 33. Methane Absorption of the $P_3(8)$ DF Line.

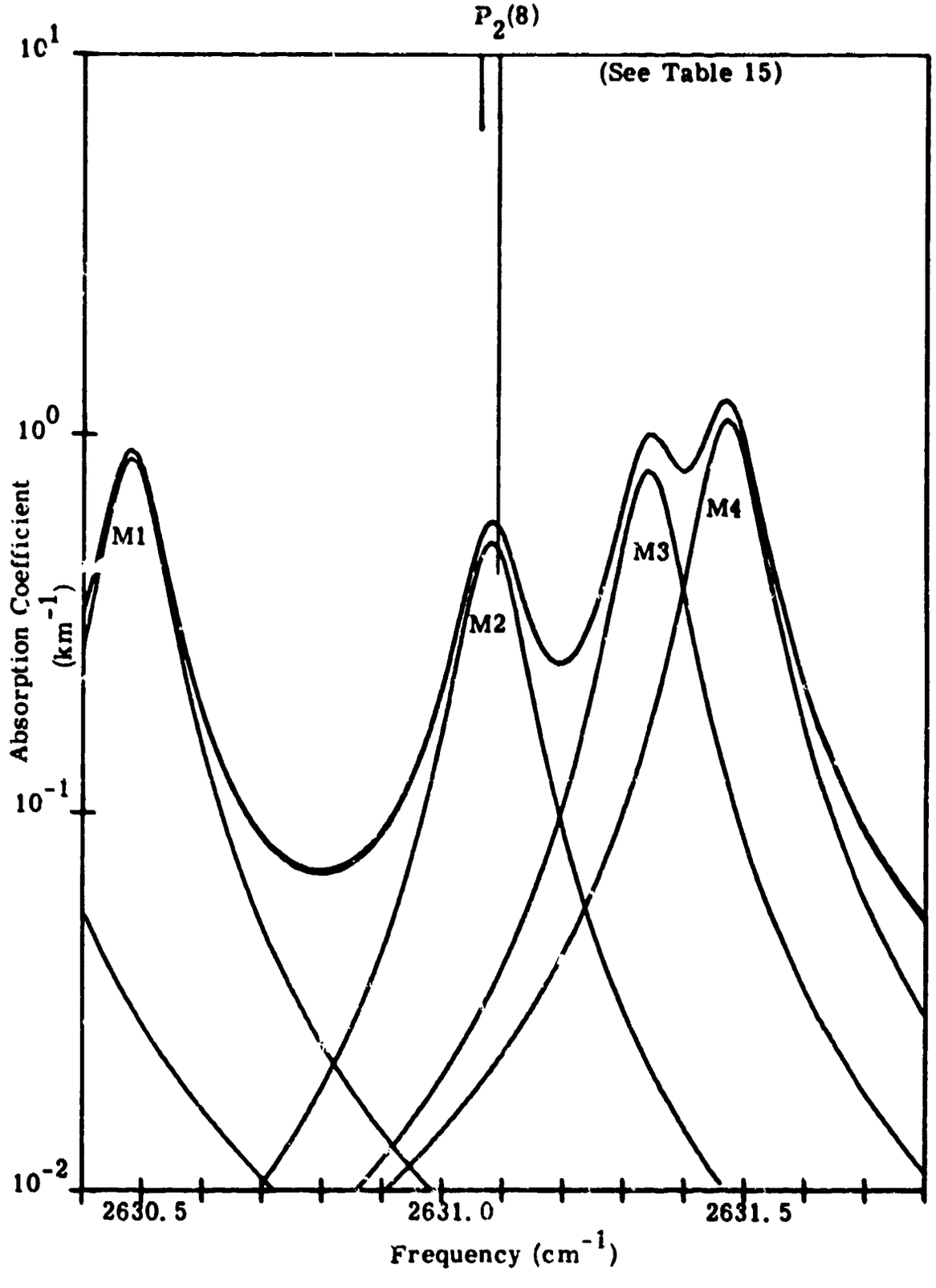

Figure 34. Methane Absorption of the $P_2(8)$ DF Line.

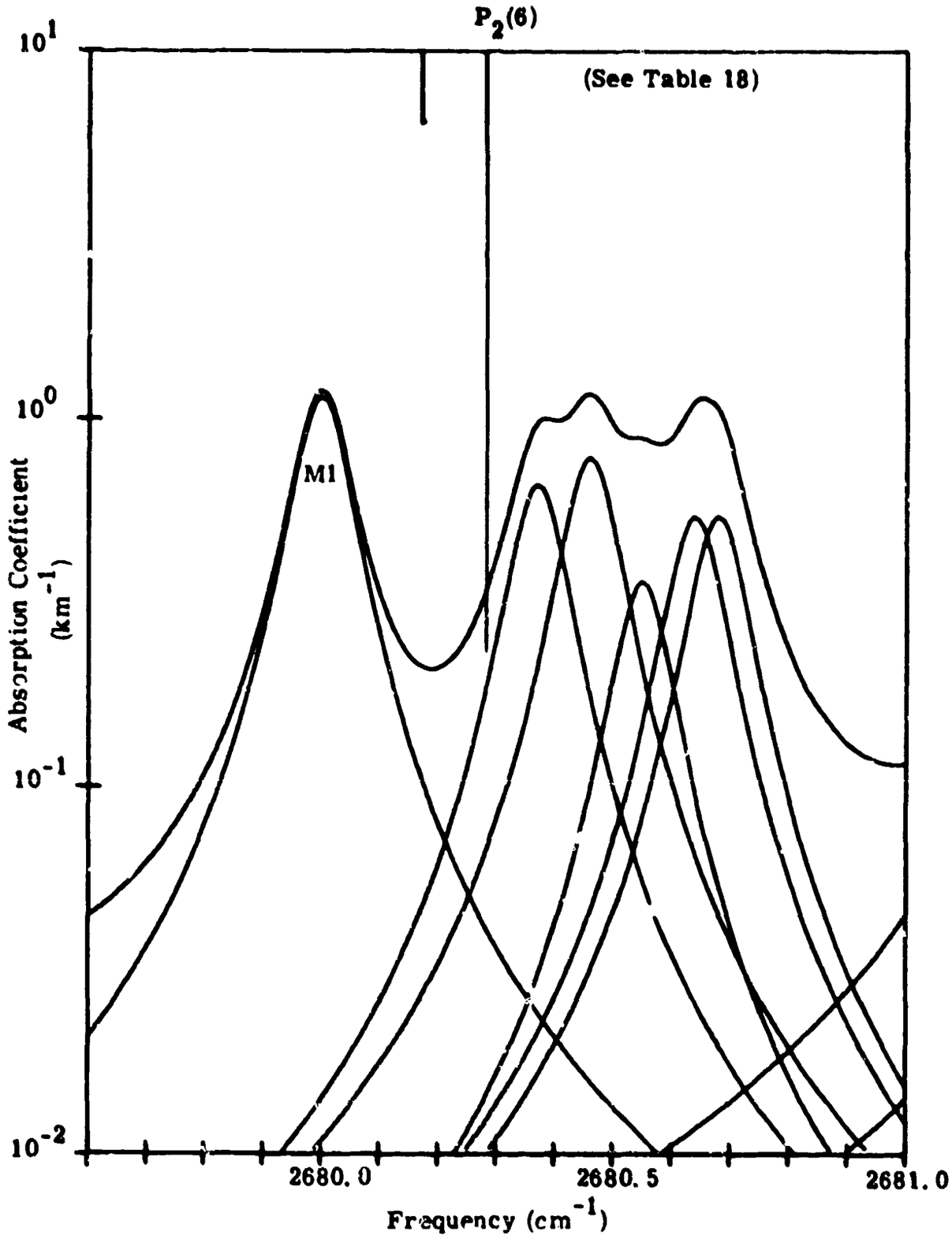

Figure 35. Methane Absorption of the $P_2(6)$ DF Line.

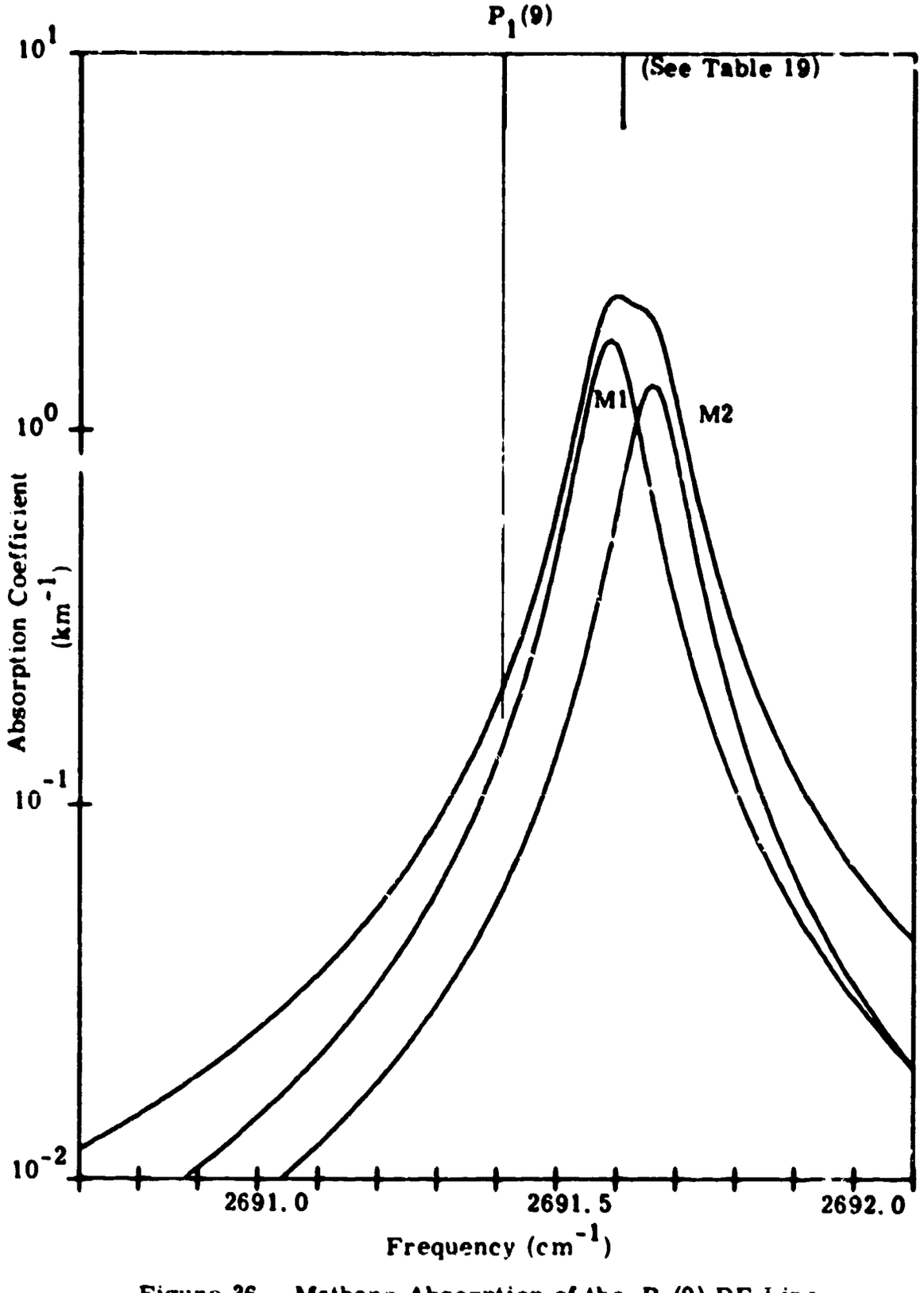

Figure 36. Methane Absorption of the $P_1(9)$ DF Line.

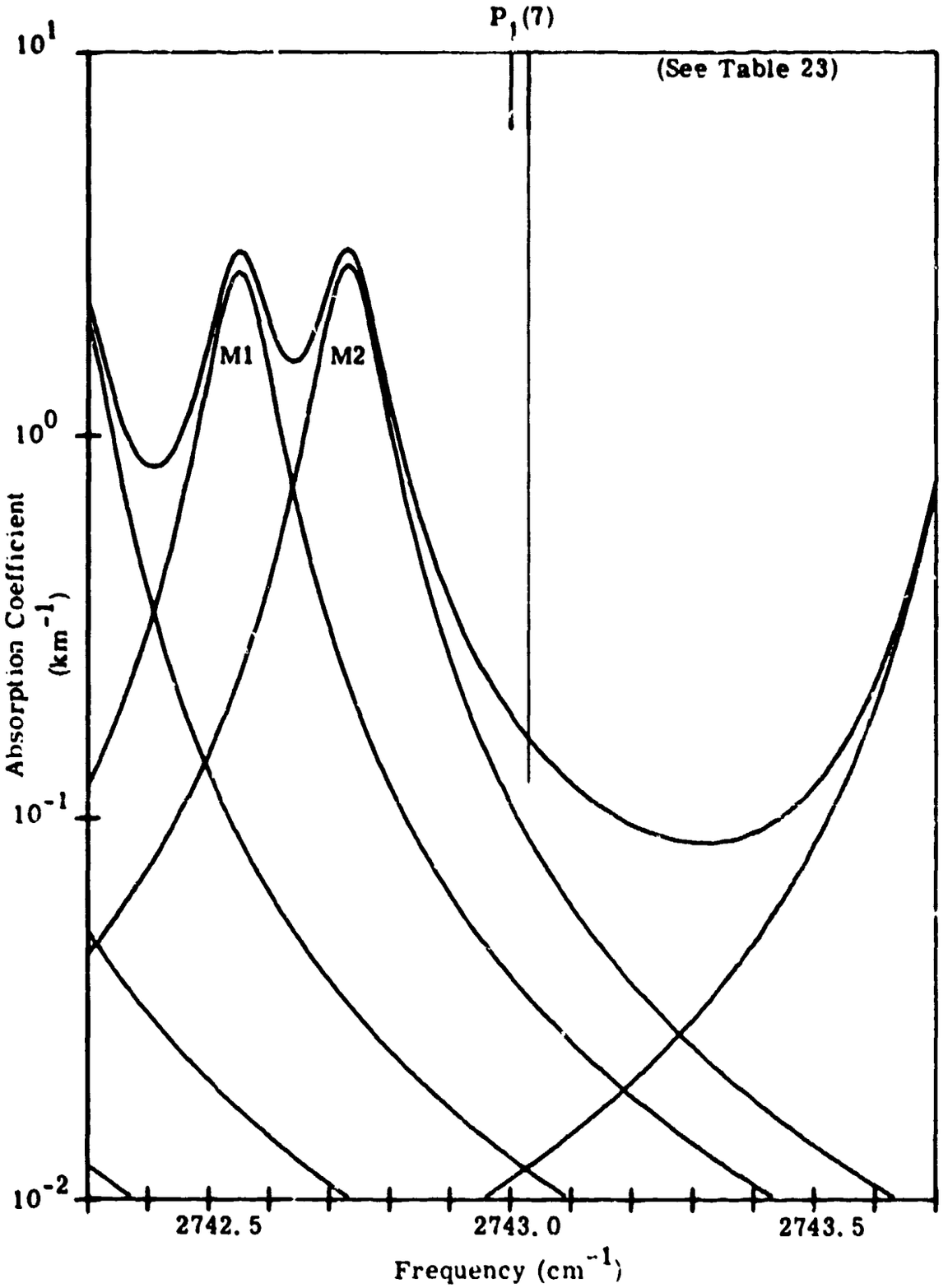

Figure 37. Methane Absorption of the $P_1(7)$ DF Line.

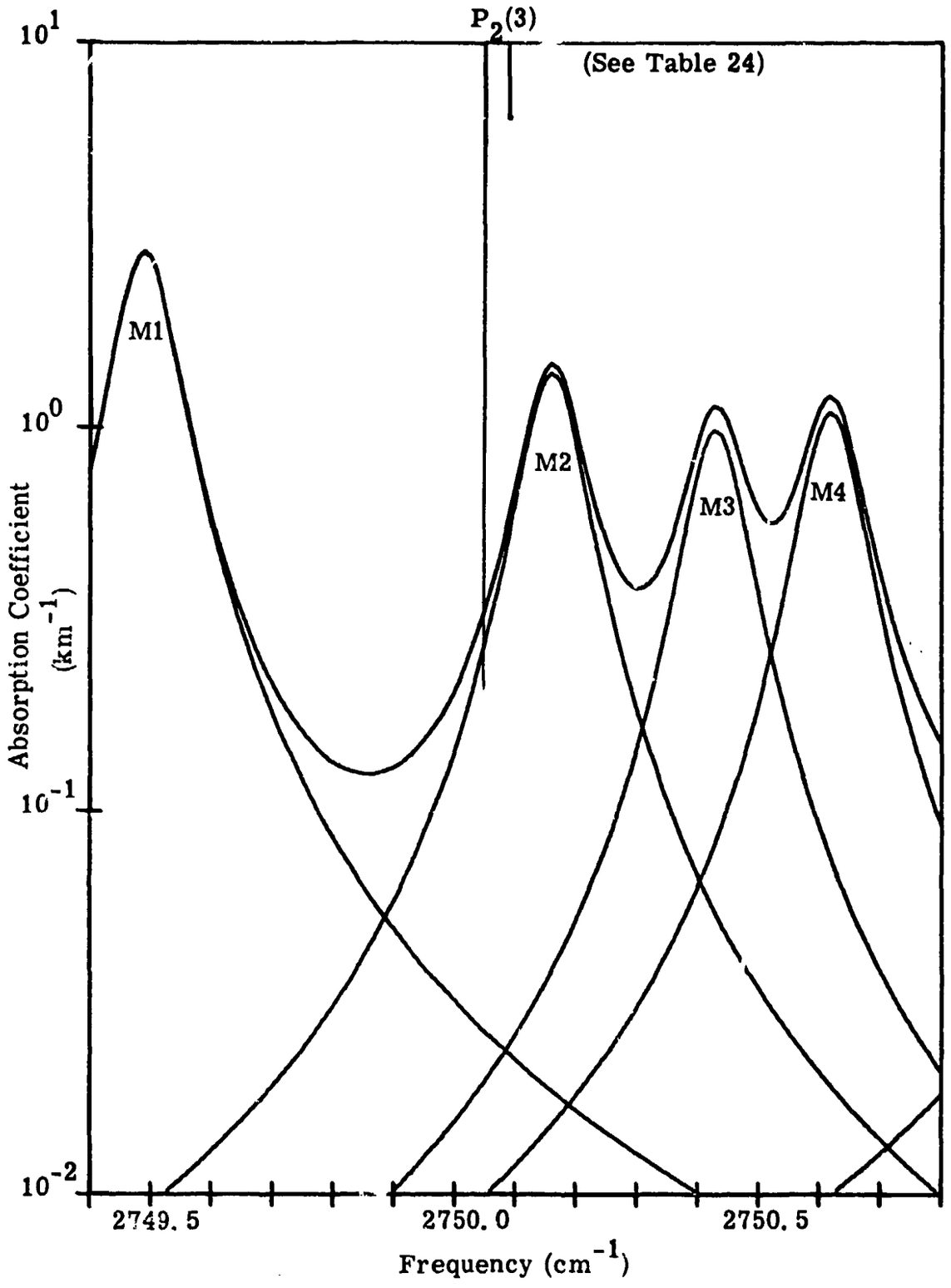

Figure 38. Methane Absorption of the $P_2(3)$ DF Line.

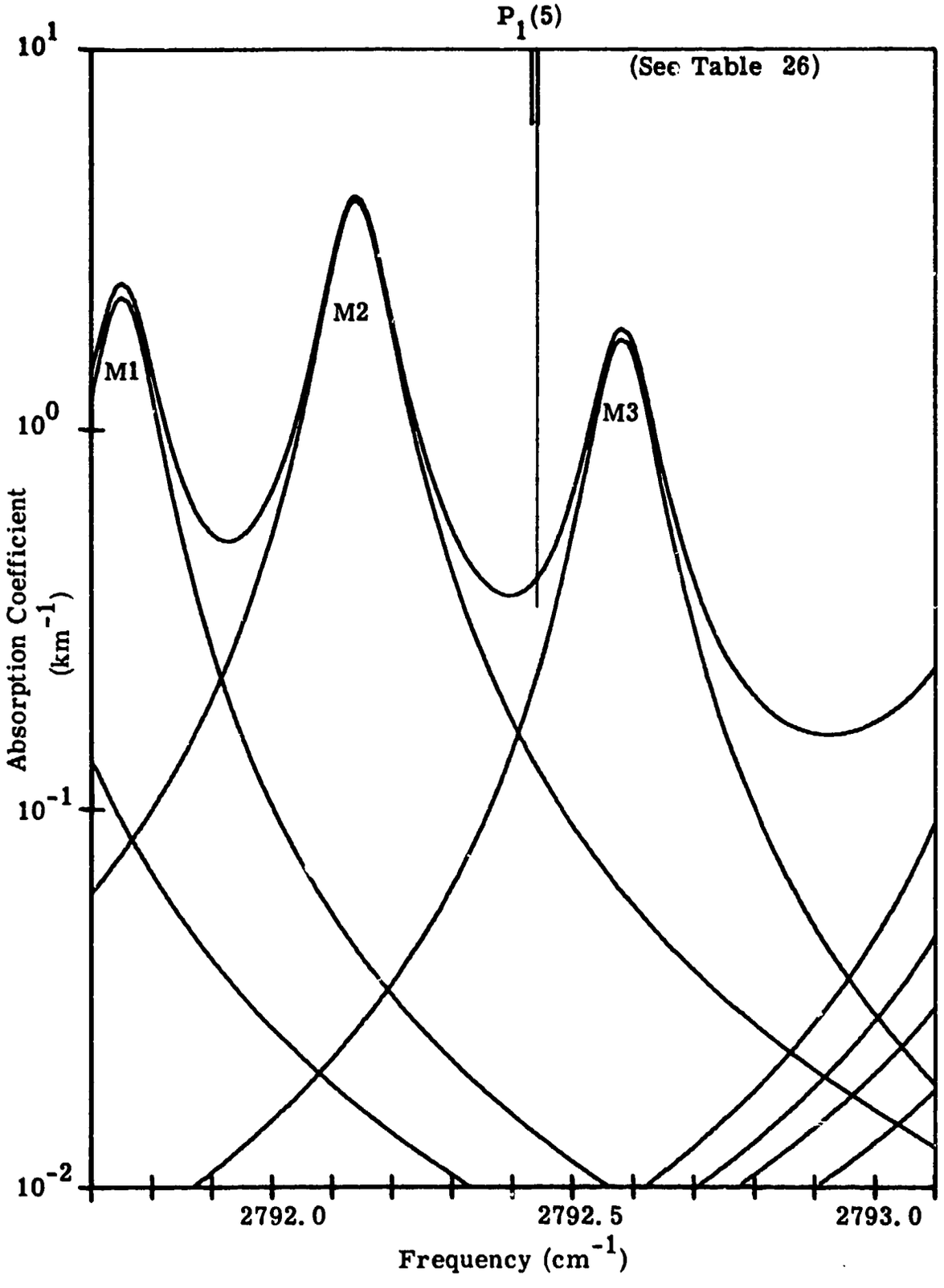

Figure 39. Methane Absorption of the $P_1(5)$ DF Line.

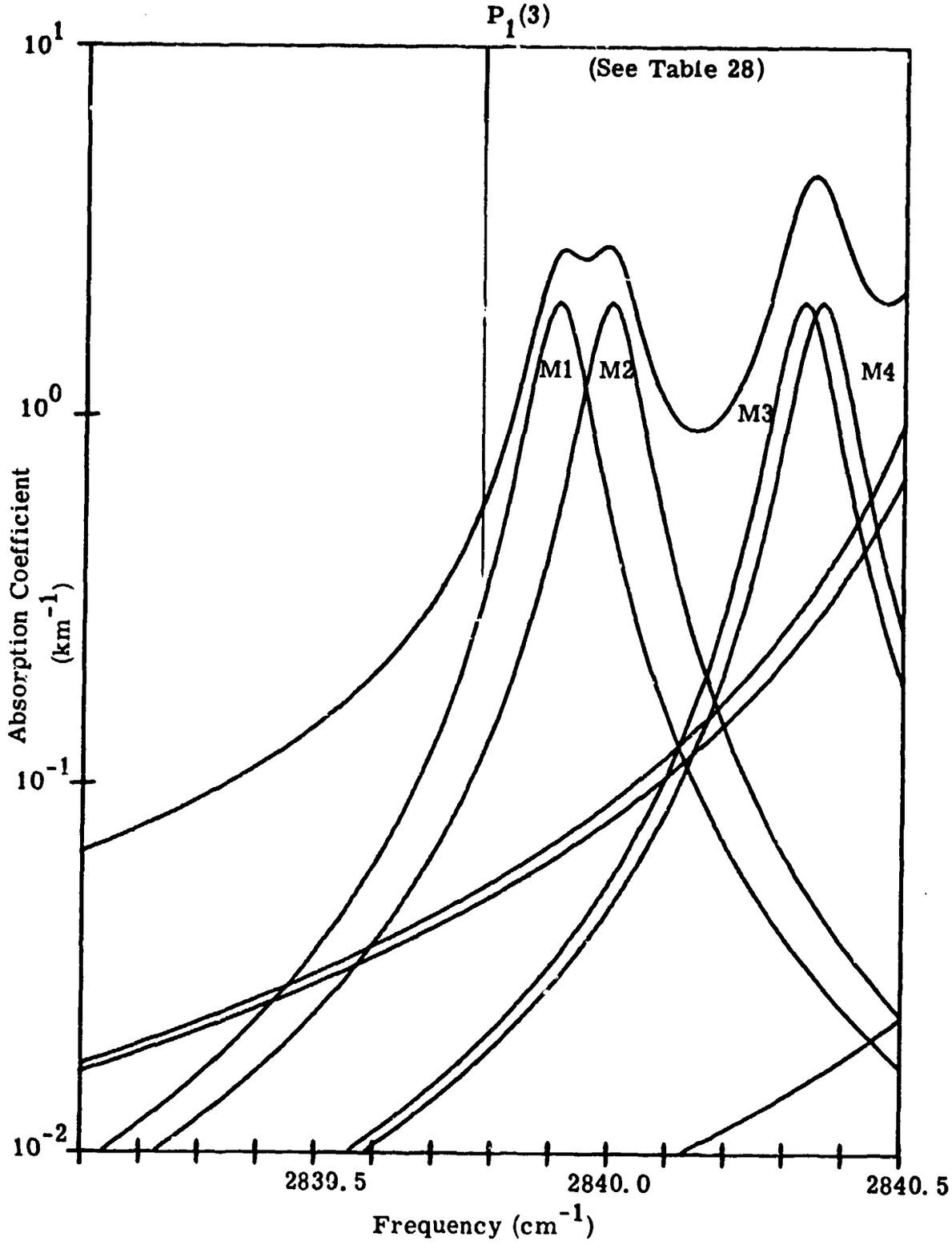

Figure 40. Methane Absorption of the $P_1(3)$ DF Line.

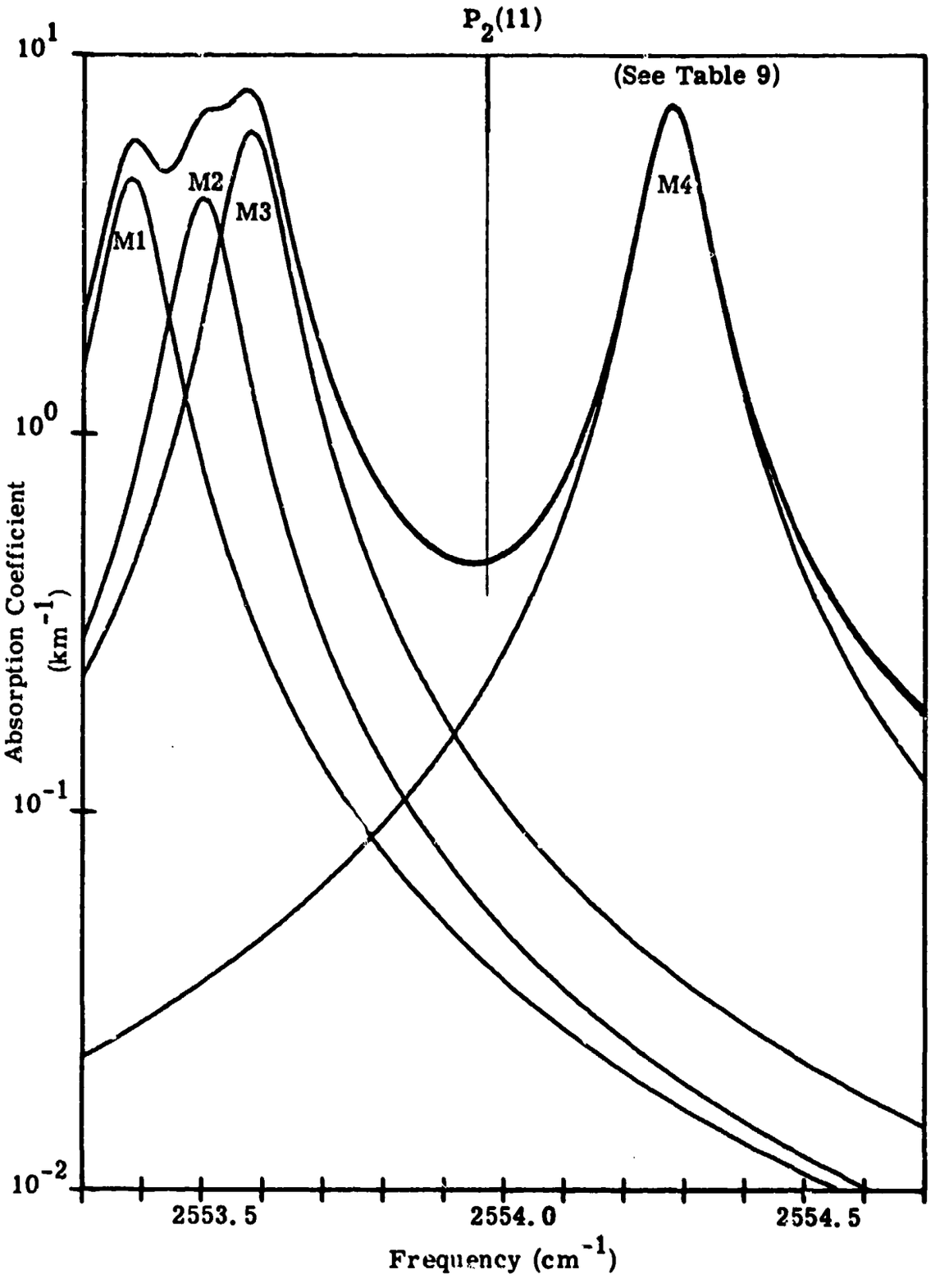

Figure 41. Methane Absorption of the $P_2(11)$ DF Line.

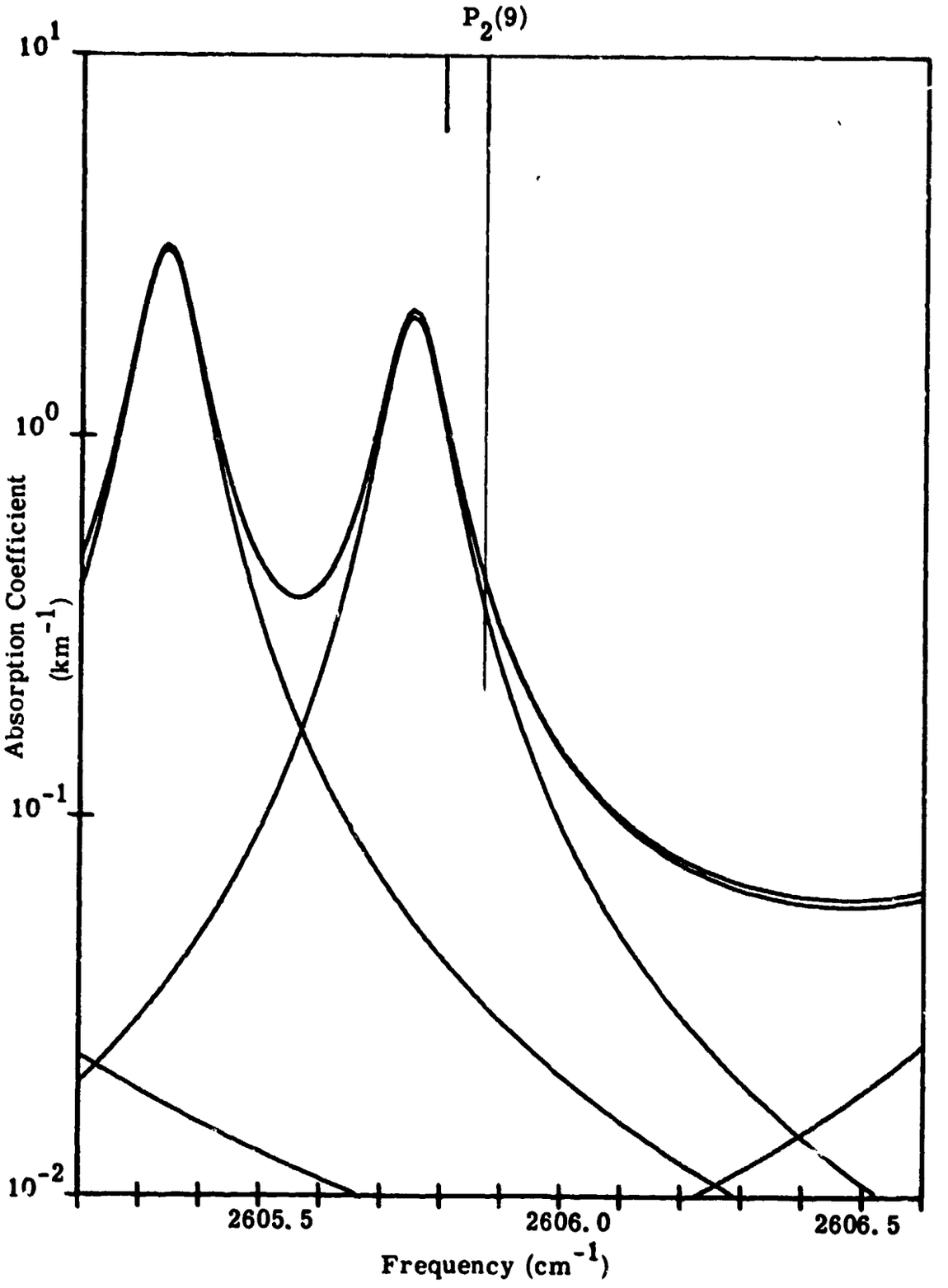

Figure 42. Methane Absorption of the $P_2(9)$ DF Line.

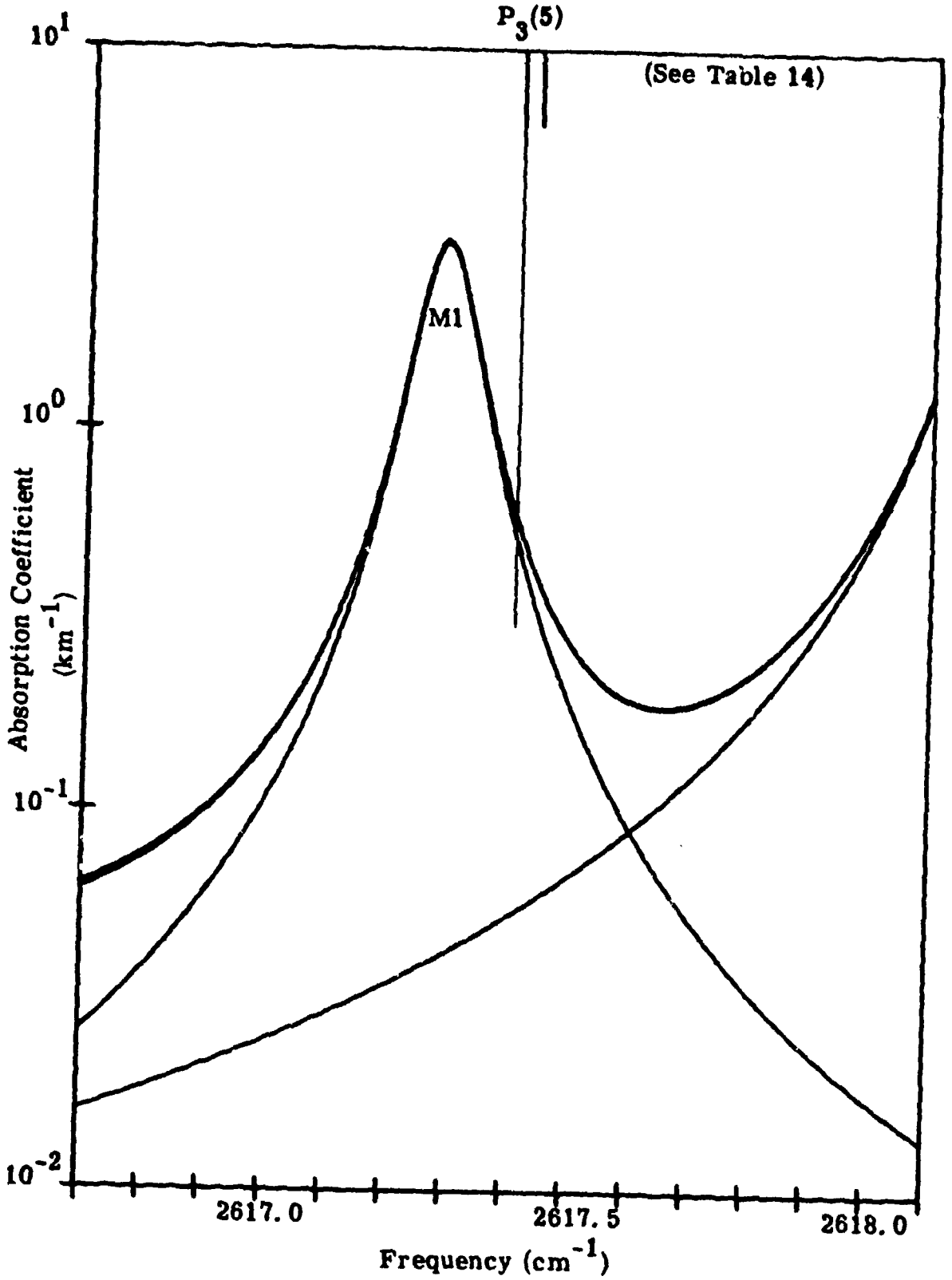

Figure 43. Methane Absorption of the $P_3(5)$ DF Line.

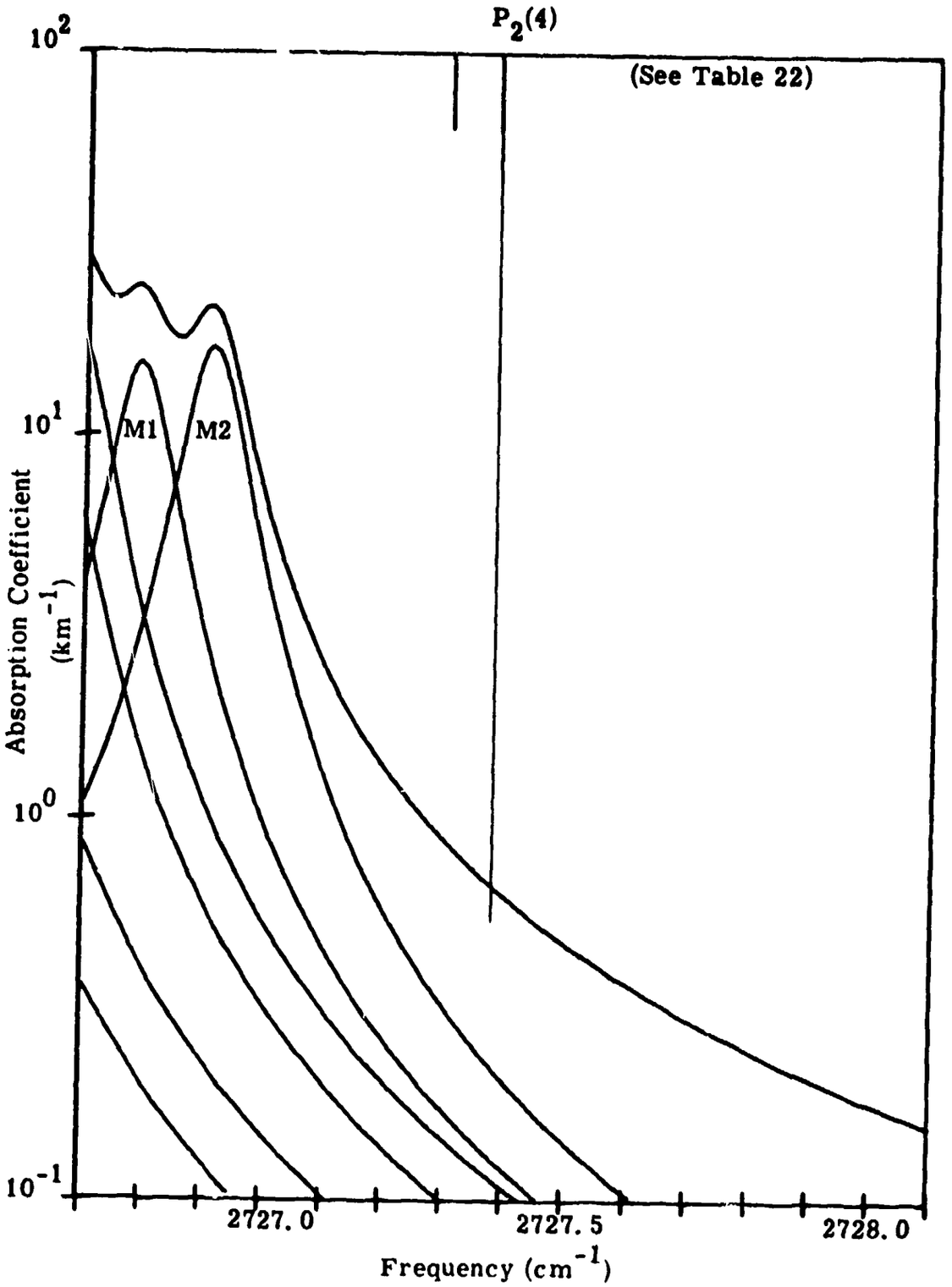

Figure 44. Methane Absorption of the $P_2(4)$ DF Line.

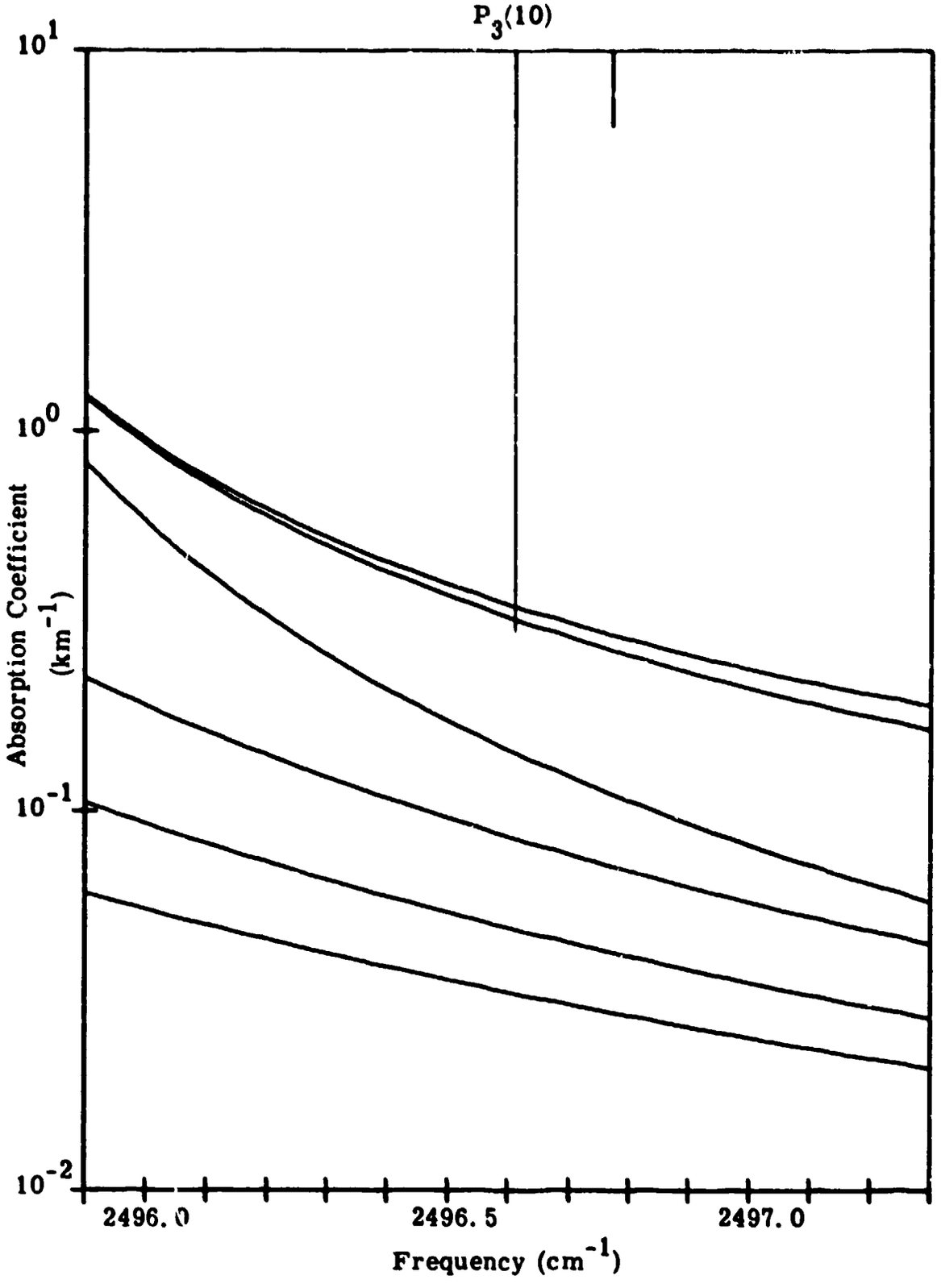

Figure 45. Methane Absorption of the $P_3(10)$ DF Line.

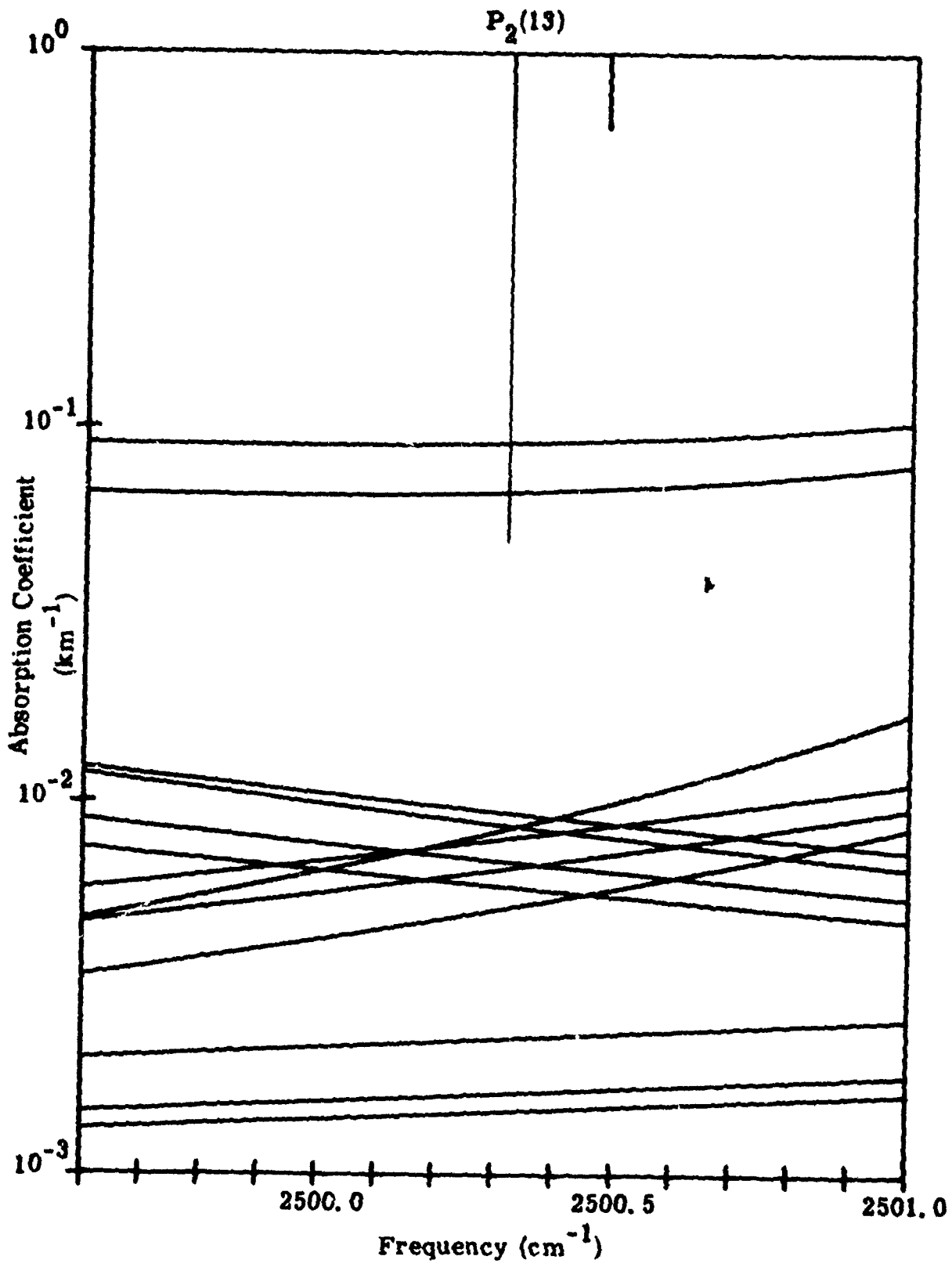

Figure 46. Methane Absorption of the $P_2(13)$ DF Line.

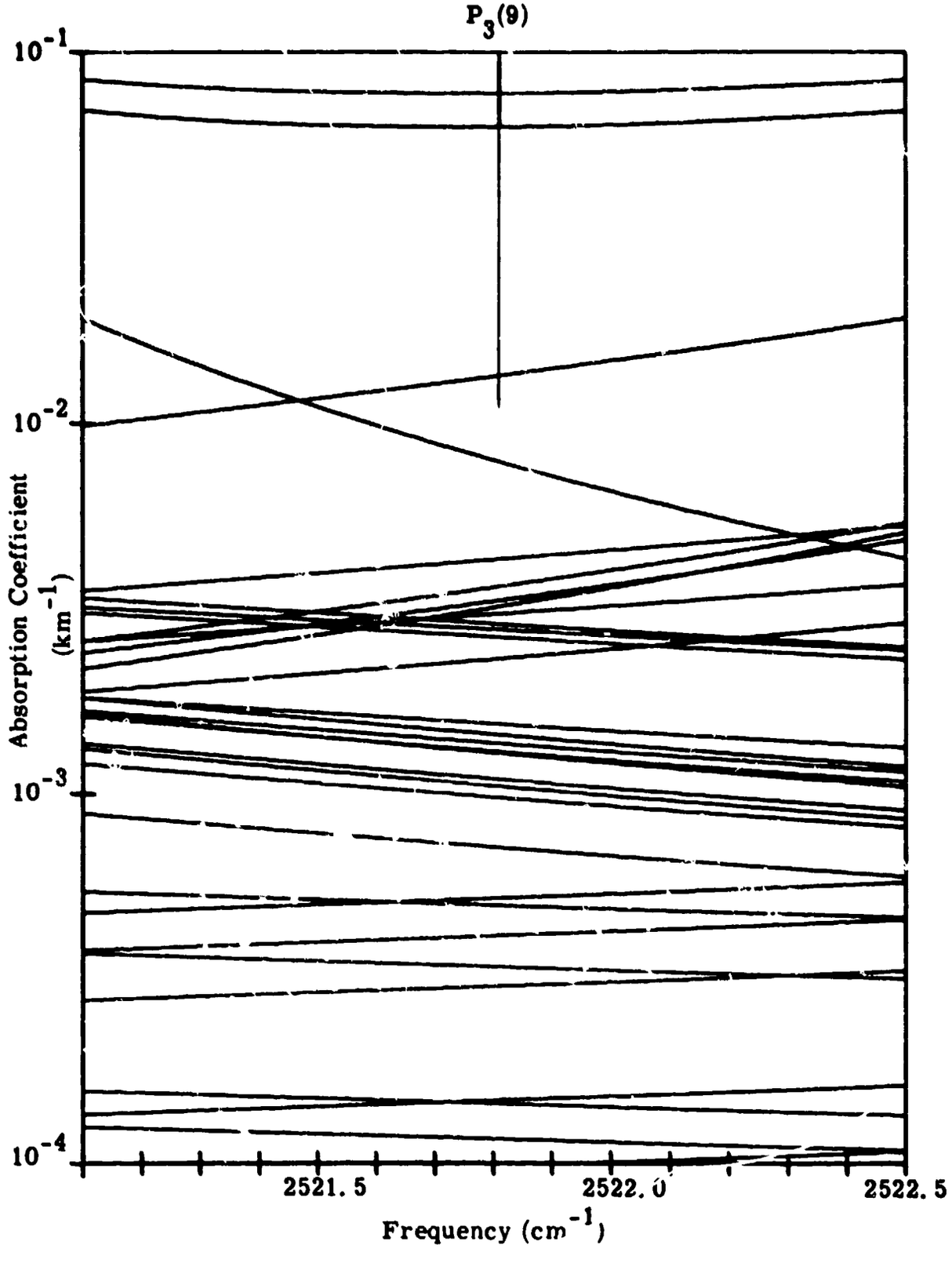

Figure 47. Methane Absorption of the $P_3(9)$ DF Line.

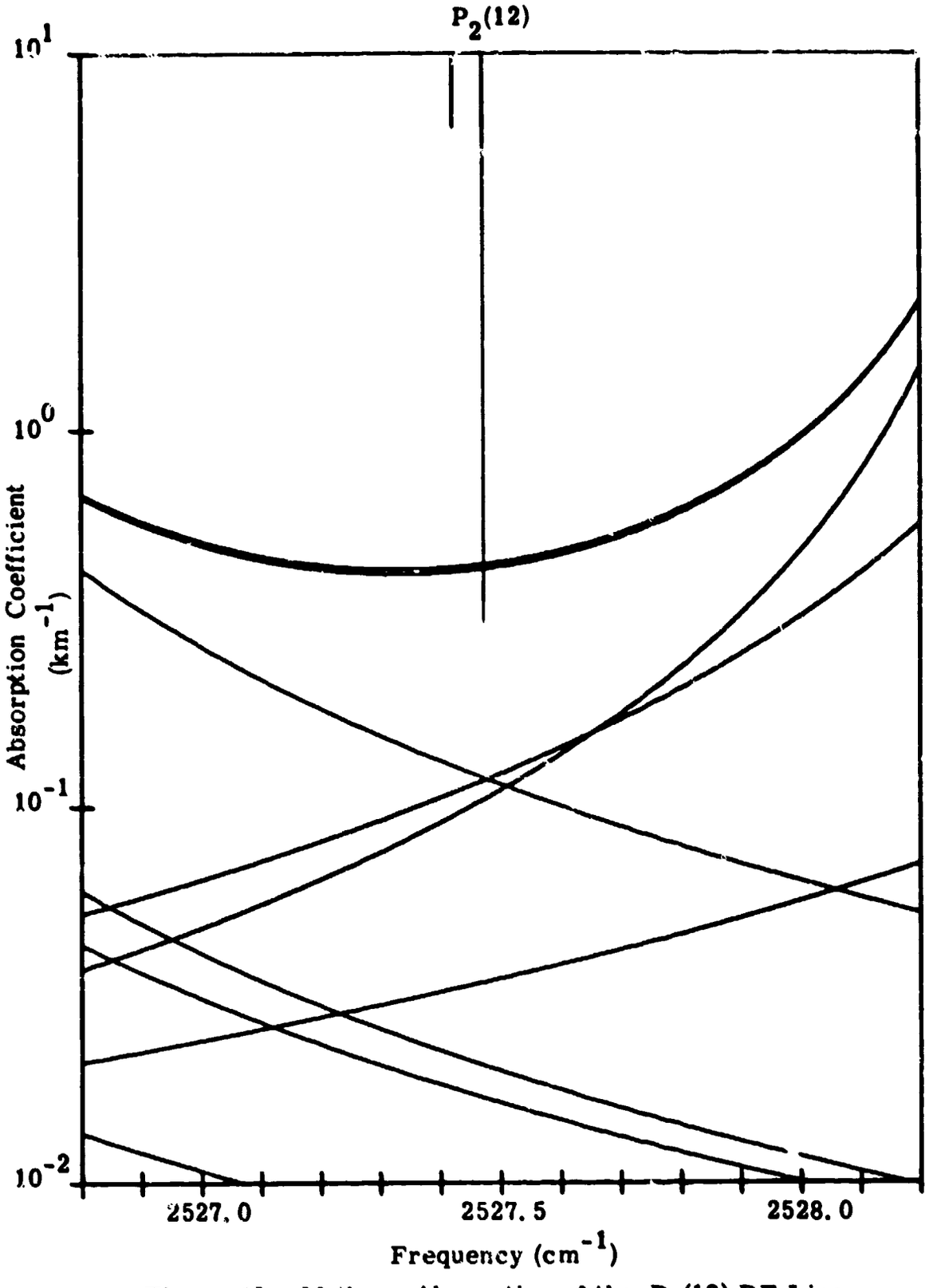

Figure 48. Methane Absorption of the $P_2(12)$ DF Line.

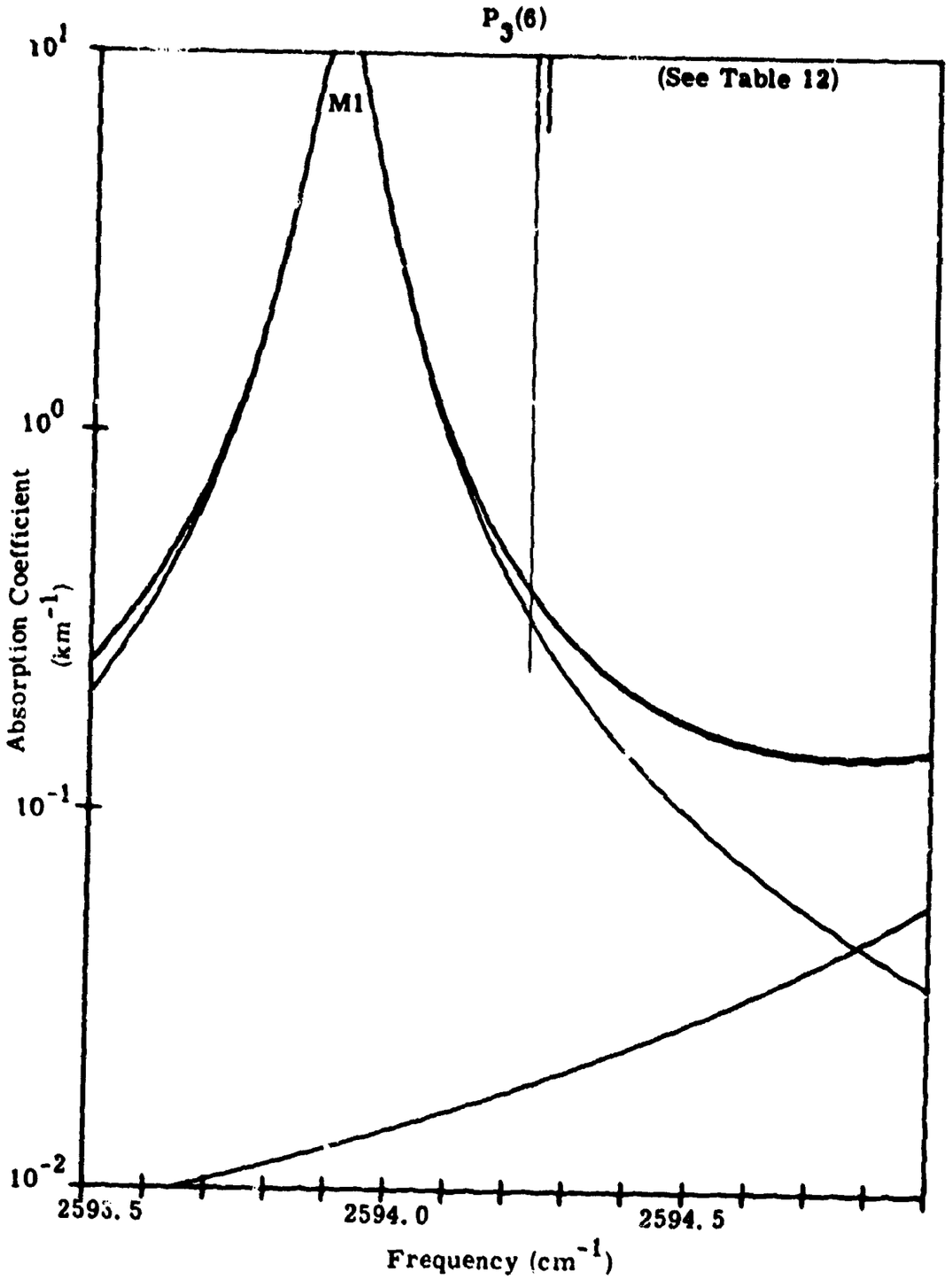

Figure 49. Methane Absorption of the $P_3(6)$ DF Line.

6. SPECIAL PROBLEMS IN THE MEASUREMENT OF HDO ABSORPTION COEFFICIENTS

HDO absorption at DF laser wavelengths is an example of absorption by relatively strong molecular transitions weakened by small natural abundance. One can therefore expect to be able to measure the important HDO absorptions in the laboratory, using enriched concentrations. The procedures for doing this are not straightforward, however, since the hydrogen and deuterium atoms convert very rapidly when both isotopes are present. Consequently, both H_2O and D_2O absorption always exist as a background to HDO. At most DF wavelengths, H_2O absorption is weak compared to that of HDO, whereas D_2O absorption is comparable or even greater than that of HDO. The H_2O : HDO : D_2O mixtures must therefore be chosen carefully for each wavelength to maximize the HDO absorption relative to the true background. This will usually require forming enriched HDO concentrations from mixtures of H_2O plus D_2O which will favor H_2O over D_2O.

The equation of equilibrium between the three modifications of water may be written as follows,

$$H_2O + D_2O \overset{K_e}{\rightleftharpoons} 2HDO$$

or, as an equality between particular concentrations,

$$[H_2O][D_2O]K_e = [HDO]^2$$

where the equilibrium constant K_e has been given [19] as follows

$K_e = 3.543$ $\quad T = 293^oK$, liquid phase

$K_e = 3.506$ $\quad T = 293^oK$, gas phase

The quantity of prime interest is the ratio of HDO molecules to D_2O molecules for given initial H_2O and D_2O conditions. This relation is shown

in Figure 50. To form a mixture having a hundred to one ratio of HDO to D_2O in equilibrium, for example, an initial mixture of $\sim$ 57 parts H_2O to 1 part D_2O would be required. In so driving the equilibrium in a given direction, however, the background caused by the favored modification is increased. The situation is complicated further by the relative loss of HDO for a given humidity, as either H_2O or D_2O is preferred. The weakening of HDO absorption as H_2O partial pressure is increased is illustrated for several DF lines in Figure 51. A nominal path of 480 meters and 50% relative humidity was chosen, as typical of normal operating conditions. It is clear that the HDO absorption weakens significantly as the ratio of HDO to D_2O increases. The background contributions are further open to question since the absorption coefficients of D_2O and H_2O are not well known in this spectral region.

The effect of background D_2O absorption is given in Table 30, using the short path D_2O background measurements of Spencer [20]. It can be seen in the table that even at HDO/D_2O ratios of 100, significant D_2O from background persists for several lines. $P_3(7)$ is always dominated by D_2O absorption, for example, but this is because the HDO contribution itself is not large at this wavelength.

The H_2O lines in this region are naturally weak, and no measurements exist. Consequently, both the H_2O and D_2O background to HDO measurements in this region must be considered inadequately known, at best.

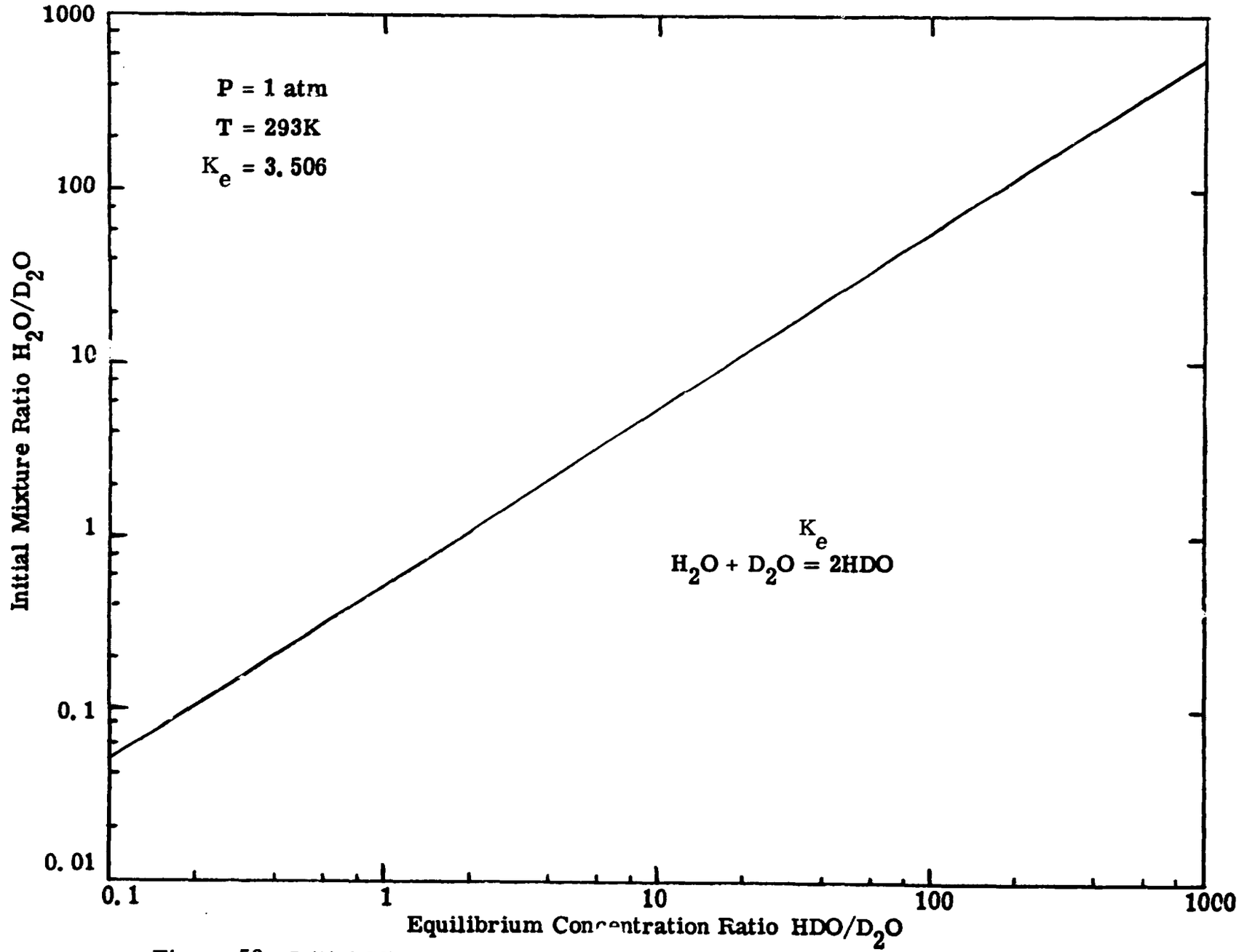

Figure 50. Initial Mixture Required to Yield Desired Equilibrium Concentration.

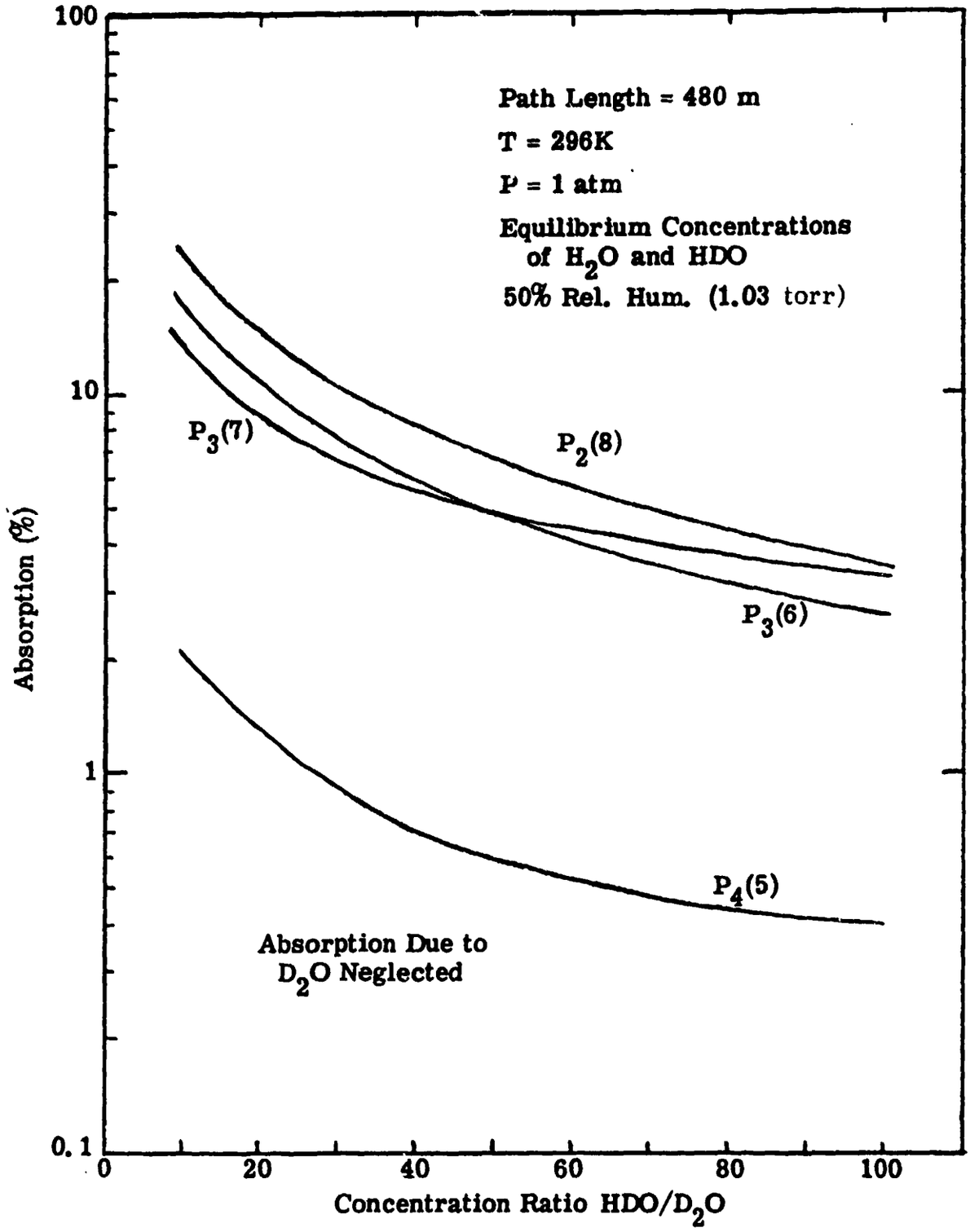

Figure 51. Percent Absorption Versus Relative HDO/D_2O Concentration for Selected DF Laser Wavelengths.

Table 30.

Ratio of Absorption Coefficients of D_2O and HDO for Various DF Laser Lines at Several Concentration Ratios of HDO to D_2O*

Laser Line		k_{D_2O}/k_{HDO}			
I. D.	Freq. (cm^{-1})	$\frac{[HDO]}{[D_2O]}=1$	=20	= 50	= 100
$P_2(8)$	2631.09	2.00	.100	.040	.020
$P_3(6)$	2594.23	1.96	.098	.039	.0196
$P_3(7)$	2570.51	"	"	"	"
$P_4(5)$	2532.50				
$P_1(12)$	2611.10	.667	.033	.013	.007
$P_3(4)$	2750.05	0	0	0	0
$P_2(4)$	2727.38	1.26	.062	.025	.013
$P_2(5)$	2703.98	5.06	.253	.101	.051
$P_2(6)$	2680.28	1.99	.100	.040	.020
$P_2(7)$	2655.97	2.20	.110	.044	.022
$P_2(9)$	2605.87	12.3	.614	.246	.123
$P_2(10)$	2580.16	38.3	1.92	.766	.383
$P_2(11)$	2553.97	2.00	.100	.040	.020
$P_3(8)$	2546.37	0	0	0	0
$P_3(9)$	2521.81	.524	.026	.010	.005
$P_3(10)$	2496.61	0	0	0	0
$P_3(11)$	2471.34	2.29	.114	.046	.023

*Calculations Based on Data Reported by Spencer, Ref. 20.

7. COMMENTS AND RECOMMENDATIONS FOR FUTURE MEASUREMENTS

The absorption coefficients presented in this report incorporate the current "best value" of line and continuum parameters. Therefore, these results are considered to be the most realistic attainable at present. However, the accepted input parameters are open to considerable suspicion for a number of reasons. The most basic of these is that the absorption coefficients themselves are very small. Such small absorption coefficients are very difficult to measure under controlled conditions, and the physical mechanisms which give rise to the absorption invoke higher order or previously uninteresting phenomena (pressure induced N_2 absorption, combination bands, isotopic absorption, etc.). A complete understanding of molecular absorption at DF wavelengths requires accurate theoretical modeling and an accurate data base.

The motivation for the present investigation has been to provide predictive calculations which would guide quick-response laboratory measurements of absorption coefficients at DF wavelengths, and which would guide interpretation of the data. The results presented here lead to the conclusion that measurements planning must consider two aspects of the DF molecular absorption problem. These are the selection of priorities for the choice of molecule and individual lines to investigate and the selection of the method of performing the measurements.

From the standpoint of the DF propagation problem, the major contributions, in order of decreasing contribution to absorption, are as follows:

H_2O Continuum
N_2 Continuum (2400 cm^{-1} - 2550 cm^{-1})
HDO Lines
N_2O Lines
CH_4 Lines
H_2O Lines

For very dry conditions, or at altitude, priorities will shift to a better understanding of the line absorption of the uniformly mixed gases. The species N_2O, CH_4 and H_2O are grouped together since each can be quite important at several specific wavelengths. H_2O occurs only at several DF wavelengths, but of these, H_2O often is the dominant absorber. There is more DF absorption by N_2O than by either CH_4 or H_2O, but the latter occur at more transparent wavelengths, and therefore are wavelengths of greatest interest and potential value.

(1) N_2 Continuum.

In the wavenumber region between 2400 cm^{-1} and 2550 cm^{-1}, N_2 continuum absorption is large. At larger wavenumbers, current predictions indicate that it will be small, but since this region is the one which is apparently best for DF propagation, this should be confirmed.

Accepted values for the N_2 continuum are probably accurate below 2500 cm^{-1}, but measurements on which they are based were made at unrealistic conditions. Pressures up to 20 atmospheres with short path lengths ($\sim$ 30 meters) were used to obtain sufficient absorption strength for accurate measurements. If the extrapolations to low pressures are not correct, or if spectral structure is unexpectedly present, important surprises can result for laser propagation. In any event, more accurate values should be obtained above 2550 cm^{-1}.

In addition to its importance to DF atmospheric propagation, N_2 continuum values should be known precisely since all measurements of H_2O foreign broadened continuum and N_2O-, HDO-, and CH_4-air mixtures will have an underlying N_2 continuum which must be accounted for in laboratory measurements or atmospheric simulations.

If long paths (1-2 km) are available, White cell measurements at several DF wavelengths should be performed at low pressures (1 atm - 2 atm). Above

2550 cm^{-1} however, more sensitive techniques should be used. Spectrophone measurements should be preferred over operating at increased pressures for the weakest values of $k(\nu)$. The use of several absorption techniques is always desirable for difficult measurements as a means of removing possible measurements error and artifact.

(2) H_2O Continuum.

The self and air broadened H_2O continua are the most important contributors to absorption throughout the DF region. Rapidly varying spectral structure is not expected, since distant line wings are the source of the absorption. (At 10.6 μm this is not necessarily true -- there is some evidence that dimer or polymer water may be responsible for the anomalously large self broadened H_2O continuum. Even so, some theories of the dimer formation indicate that structure may not be present [21].)

As discussed in Section 3, the Burch values of C_f^o and C_s^o are adopted here. However, one should remember that these values were not measured at this temperature. Because of the experimental difficulty in obtaining a sufficient number density of H_2O, values of C_s^o between 2400 cm^{-1} and 2650 cm^{-1} were extrapolated from measurements at 338°K, 384°K, and 428°K. Between 2650 and 2800 cm^{-1}, values were extrapolated from measurements at 384°K only. The ratio C_s^o/C_f^o was determined from mixtures of H_2O and N_2 at 428°K only. The value 0.12 was determined in this manner, and is suggested as the best value for 296°K as well. The total operating pressures ranged between 4.5 atm and 10 atm, with a 2 atm partial pressure of H_2O. Since sample conditions so drastically different than required for HEL applications were required to obtain the data, and since the quoted error flags are rather large, confirmation of the values by additional measurements is highly desirable.

The H_2O (broadened by N_2 and O_2) continuum is most important and difficult to measure since it is not possible to get the required number densities of H_2O at the desired temperature and pressures while maintaining a dilution of 1 part H_2O to $\sim$ 100 parts N_2 and O_2. The spectrophone appears to offer the best possibility of performing accurate measurements of such weak absorption, and thus the development of a spectrophone suited to this measurement should be pursued. Note that the accepted H_2O continuum parameters assume that O_2 broadening is the same as that of N_2.

Self broadened H_2O continuum measurements are also less difficult at ambient temperatures since number densities are small. If paths up to 2 km are available with White cells, this continuum contribution can be determined by careful measurement. The absorption is so weak, however, other techniques such as the spectrophone should be used for purposes of comparison, or in place of White cell measurements if paths of several kilometers and good signal-to-noise is not available.

(3) CH_4 Line Absorption Coefficients.

CH_4 absorption coefficients occur in the DF region as individual lines and as multiplets consisting of several lines within ~ 0.1 cm^{-1} spread. Invariably, these lines have not been observed directly, and the splittings have been predicted using low order approximations. Also, the individual strengths of splittings in tetrahedrally symmetric molecules are difficult to calculate accurately. Because of this uncertainty, and because of the rapid variation with wavelength, CH_4 absorption coefficients are the most suspect of the line contributors.

Because the self and foreign broadened CH_4 line widths are comparable, greatly enriched concentrations of methane can be used. Therefore, White cell measurements on samples with CH_4/air ratios ~ 0.1 to 0.01 are reasonable, and can be performed in a straightforward manner.

(4) HDO Line Absorption Coefficients.

HDO is the single most important line absorption coefficient in the DF laser region. Current strength and width values are in considerable doubt since they have not been measured directly, and their predictions have been based on H_2O strength and width calculations or measurements. HDO therefore ranks high as a molecule to be investigated experimentally.

As discussed in Section 6, special problems arise in attempting HDO measurements since HDO may be prepared straightforwardly only in the presence of D_2O and H_2O. Consequently, better knowledge of HDO line broadening by H_2O and D_2O, and of D_2O strengths should be obtained before careful measurements of HDO absorption coefficients can be performed.

(5) N_2O Line Absorption Coefficients.

N_2O is a strong absorber in the 3.8 - 4.0 μm region, and it is relatively transparent to DF atmospheric propagation only because its natural abundance is less than one part per million. Also, the N_2O line structure is regularly spaced, with line separations of ~ 1 cm^{-1}. Consequently, experimental data exist for lines in the dominant bands. Current N_2O parameters therefore are expected to be rather accurate compared to CH_4 and HDO, and measurement of N_2O absorption at DF wavelength is straightforward using conventional techniques.

Acknowledgement

The authors wish to acknowledge valuable discussions with Frederick G. Smith.

REFERENCES

1. Benedict, W. S., R. Herman, G. Moore and S. Silverman, 1956, "Strengths, Widths, and Shapes of Infrared Lines I," Canad. J. Phys., 34, 830.

2. Meredith, R. E., 1972, "A New Method for the Direct Measurement of Spectral Line Strengths and Widths," J. Quant. Spectrosc. Radiat. Transfer, 12, 455.

3. Benedict, W. S., R. Herman, G. E. Moore and S. Silverman, 1962, "The Strengths, Widths, and Shapes of Lines in the Vibration-Rotation Bands of CO," Astrophys. J., 135, 277.

4. Herget, W. F., W. E. Deeds, N. M. Gailar, R. J. Lovell and A. H. Nielsen, 1962, "Infrared Spectrum of Hydrogen Fluoride: Line Positions and Line Shapes, Part II," J. Opt. Soc. Amer., 52, 1113.

5. McClatchey, R. A., W. S. Benedict, S. A. Clough, D. E. Burch, R. F. Calfee, K. Fox, L. S. Rothman and J. A. Garing, 1973, AFCRL Atmospheric Absorption Line Parameters Compilation, AFCRL-TR-73-0096.

6. McClatchey, R. A., and J. E. A. Selby, 1972, Atmospheric Attenuation of HF and DF Laser Radiation, AFCRL-72-0312.

7. McClatchey, R. A., and J. E. A. Selby, 1974, Atmospheric Attenuation of Laser Radiation from 0.76 to 31.25 μm, AFCRL-TR-74-0003.

8. Benedict, W. S., and R. Herman, 1963, "The Calculation of Self Broadened Line Widths in Linear Molecules," J. Quant. Spectrosc. Radiat. Transfer, 3, 265.

9. Benedict, W. S., and L. D. Kaplan, 1959, "Calculation of Line Widths in H_2O-N_2 Collisions," J. Chem. Phys., 30, 388.

10. Meredith, R. E., and F. G. Smith, 1974, "Broadening of Hydrogen Fluoride Lines by H_2, D_2, and N_2," J. Chem. Phys., 60, 3388.

11. Burch, D. E., D. A. Gryvnak and J. D. Pembrook, 1970, "Investigation of Infrared Radiation by Atmospheric Gases," AFCRL-70-0373.

12. Burch, D. E., D. A. Gryvnak and J. D. Pembrook, 1971, "Investigation of the Absorption of Infrared Radiation by Atmospheric Gases: Water, Nitrogen, Nitrous Oxide," AFCRL-71-0124.

13. McCoy, J. H., D. B. Rensch and R. K. Long, 1969, "Water Vapor Continuum Absorption of Carbon Dioxide Laser Radiation Near 10 μm," Appl. Optics, 8, 1471.

14. Burch, D. E., E. B. Singleton and D. Williams, 1962, "Absorption Line Broadening in the Near Infrared," Applied Optics, 1, 359.

15. Benedict, W. S., and L. D. Kaplan, 1964, "Calculation of Line Widths in H_2O-H_2O and H_2O-O_2 Collisions," J. Quant. Spectrosc. Radiat. Transfer, 4, 453.

16. Long, R. K., F. S. Mills and G. L. Trusty, 1974, Calculated Absorption Coefficients for D. F. Laser Frequencies, RADC-TR-73-389.

17. Fox, K., 1974, Analysis of Vibration-Rotation Spectra of Methane, AFCRL-TR-73-0738.

18. Toth, R., Paper presented at the Symposium on Molecular Structure and Spectroscopy, June 1974, The Ohio State University. Also private communication.

19. Wagman, D. D., 1968, Selected Values of Chemical Thermodynamic Values, NBS Tech. Note 270-3.

20. Spencer, D., 1973, "Atmospheric Gas Absorption at DF Laser Wavelengths," Mitre Report M73-86, v. II.

21. Private communication from D. Ragovin, University of Arizona.

LIST OF SYMBOLS

B	ratio of self to foreign broadened half width: γ_s/γ_f
B(f←i)	Einstein coefficient for induced absorption
c	coefficient for temperature variation of C_s^o
C_f^o	empirical foreign continuum absorption coefficient
C_s^o	empirical self continuum absorption coefficient
E	initial energy level
F	factor quantifying α_j dependence of the electric dipole matrix element
$f(\nu-\nu_0)$	shapes or form factor of an absorption line
H	altitude
J	rotational quantum number
K	rotational quantum number
K_e	equilibrium constant
k	absorption coefficient
k_c	continuum absorption coefficient
k_{fw}	far wing absorption coefficient
k_{nw}	near wing absorption coefficient
k^P	peak value of absorption coefficient
L	path length
ℓ	superscript denoting lower levels
m	exponent for temperature variation of C_s^o
n_s	number density of absorbing molecule
P	total pressure
p_f	partial pressure of foreign molecule

LIST OF SYMBOLS

p_s	partial pressure of absorbing molecule
Q	partial function
r	value of $\frac{C_s^o}{C_f^o}$ when it is numerically equal to $\frac{\gamma_s}{\gamma_f}$
S	absorption line strength
S_o	absorption line strength per molecule per cm^3
T	temperature
u	superscript denoting upper levels
v	vibrational quantum number
α, β	line shape parameters
α_j	quantum numbers other than v, J
Γ	normalization constant for non-Lorentz lines
γ	half width at half height of absorption coefficient
γ_D	Doppler line half width
$\delta\nu$	frequency difference between laser and line center
η	non-Lorentz exponent
$\vec{\mu}$	electric dipole moment function
ν	frequency
ν_c	frequency beyond which a line is non-Lorentz
ν_0	center frequency of absorption line
τ	transmittance
$<f\|\vec{\mu}\|i>$	electric dipole matrix element connecting states i and f